ANOW RESPONSE RECORDED VIA ELECTROCOCHLEOGRAPHY IN NORMAL HEARING ADULTS

By

Hana Almohammad, MSc.

Submitted to the graduate degree program in Intercampus Programs in Communicative Disorders and the Graduate Faculty of the University of Kansas in partial fulfillment of the requirements for the degree of Doctor of Philosophy.

_____
John Ferraro, PhD, Chairperson

_____
Mark Chertoff, PhD, Committee Member

_____
Jonathan Brumberg, PhD, Committee Member

_____
Kostas Kokkinakis, PhD, Committee Member

_____
Francisco Diaz, PhD, Committee Member

Date Defended: December 8, 2016

The Dissertation Committee for Hana Almohammad certifies that this is the approved version of the following dissertation:

ANOW RESPONSE RECORDED VIA ELECTROCOCHLEOGRAPHY IN NORMAL HEARING ADULTS

_____

John Ferraro, PhD, Chairperson

Date approved: December 8th, 2016

ABSTRACT

Currently, there is no objective hearing measure used clinically that reliably assesses low frequency hearing thresholds (below a 1000 Hz or so). A new measure, the auditory nerve overlapped waveform response (ANOW), holds promise for providing more accurate assessment of low frequency hearing thresholds than currently used objective measures. However, ANOW recordings reported in the literature have been limited primarily to animal studies. This project aims to understand the nature of the ANOW response that is recorded non-invasively from humans. Three within session repeated recordings of the ANOW response using two low frequency TB stimuli (250 Hz and 500 Hz TBs) presented at 7 stimulus intensity levels were obtained from the tympanic membranes of normal hearing adult participants. ANOW's absolute amplitude, signal-to-noise ratio (SNR), and phase locking value (PLV) measures were used in the analysis. Results revealed significantly stronger phase locking to the stimulus for 250 Hz TB stimulus compared to 500 Hz TB stimulus. Statistically significant effect of the stimulus intensity on all three measures of the ANOW response was revealed for both TB stimuli. Test retest reliability of the ANOW's amplitude was the highest amongst the three measures, but was dependent on the stimulus intensity level. Unlike SNR measure, PLV measure is not dependent on the amplitude. The deviation from the standard approach of the PLV computation and manipulating the frequency of the TB stimulus may have biased PLV measures and affected test retest repeatability of PLV measures. Hence, developing a technique that would more accurately estimate phase synchronization between ANOW response and stimulus may reveal a new ANOW measure that is reliable across wide range of stimulus intensity levels.

KEYWORDS: ANOW, phase locking, electrocochleography, cochlear microphonics, low frequency hearing.

ACKNOWLEDGMETS

I would like to express my deep appreciation to my advisor Dr.John Ferraro for his continuous support, patience, and exceptional mentoring throughout my Ph.D study. I also express my sincere gratitude and deep appreciation to Dr.Mark Chertoff for advising me throughout my research and for the time he spent helping me setting up my experiment. I thank all the committee members (Dr.Jonathan Brumberg, Dr.Kostas Kokkinakis, and Dr.Francisco Diaz) for their help and advice throughout my study. I can't thank Dr.Franciso Diaz enough for the time he spent helping me analyzing my data, despite his busy schedule.

Dedication

To my amazing mother "Fatema", my father "Ahmad", my brothers "Omar, Hamza, Asem, and Ibrahim", and my little two angles "Naya and Tala" for their continuous support and encouragement.

TABLE OF CONTENTS

LIST OF TABLES

LIST OF FIGURES

CHAPTER 1

INTRODUCTION

The objective evaluation of hearing requires no behavioral response of the participant to indicate he/she can hear the acoustic stimulus. Such assessments are commonly used in populations where behavioral hearing tests may not be feasible (for example, infants and adults who may be unable to provide behavioral responses to sounds during conventional hearing tests). The currently used "objective" auditory measures are excellent in assessing hearing thresholds at frequencies equal to and higher than 1000 Hz or so (Aoyagi et al., 1999; Rogers et al., 2010; Schoonhoven et al., 1996; Sininger et al., 1997), but are less accurate and problematic in assessing low frequency sensitivity below 1 KHz or so (Burkard et al., 2007, pp. 441-481; Gorga et al., 1993; Sininger et al., 1997; Spoor et al., 1976).

One commonly used objective measure of hearing is the auditory brainstem response (ABR), which belongs to a group of measures called the auditory evoked potentials (AEPs). AEPs are changes in the random ongoing spontaneous brain electrical activity (Electroencephalogram responses (EEGs)) that occur in response to auditory stimulation. AEPs arise from one or more sources within the peripheral/central auditory nervous systems and have a major role in the diagnosis, assessment, and monitoring of many audiological, otological, and neurological disorders (Du et al., 2011; Møller, 2010). In general, the ABR often is used to evaluate the integrity of the auditory system from the level of the cochlea up through the lower brainstem.

Amplification of low frequency vowels as well as other high frequency speech and environmental sounds is an important consideration when fitting hard of hearing infants with

hearing aids (American Speech-Language-Hearing Association, 2007). Accurate fitting requires accurate evaluation of hearing. Hence, there is a need for a nonbehavioral measure that can accurately quantify low frequency hearing thresholds in newborns/infants. Objective approaches for assessing hearing function are also needed for adults who may be unable to perform behavioral testing, and/or to verify the results of subjective hearing tests. Since behavioral measures of hearing are time consuming and may not be obtainable recordable from infants, ABR measures are recommended to estimate hearing thresholds in this population (According to the guidelines of the American speech-language hearing association ((ASHA)), 2004). However, ABR measures are less accurate in estimating low frequency hearing status compared to high frequency hearing thresholds. Several reasons account for this well-known finding. First, ABR measures are onset neural responses, where synchronized neural responses occur to only the onset of the sound stimulus and do not last as long as the stimulus. Onset synchrony is poor for low frequency acoustic stimuli and improves as the frequency of the stimulus increases (E Laukli et al., 1988). To get enough neural synchrony to produce recordable ABR responses, sound stimuli have to be very brief with very short rise/fall and plateau times (preferably as brief as a 100 microsecond click). However, click stimuli excite only the high frequency end of the cochlea and the nerve fibers that innervate this region (Coats, 1978). To evoke an onset synchronized neural response from the low frequency end of the cochlea, relatively brief, frequency-specific tone bursts and tone pips are used. Unfortunately, these signals do not produce neural responses which are well synchronized since they involve a wider spread of stimulation along the cochlea. Hence, low frequency tone pips and tone bursts do not produce accurate early ABR peaks of cochlear origin (originating from the cochlear nerve as it is leaving the cochlea). Moreover, correction factors are applied whenever frequency specific ABR is done to estimate hearing

thresholds (Stapells, 2000). Those correction factors are high when low frequency tone bursts and tone pips are used, which causes additional uncertainty.

Another limitation of ABR measures is that only wave V, which is thought to have a midbrain origin, is considered for threshold estimation (Katz et al., 2014, p. 188). This leaves us with no objective measure that has a direct cochlear origin and can accurately quantify low frequency cochlear neural thresholds in the difficult-to-test populations described above.

The Auditory Nerve Overlapped Waveform response

Recent research done on animals draws the attention to a new "objective" measure, the auditory nerve overlapped waveform response (ANOW), which holds promise for providing more accurate assessment of low frequency hearing thresholds than currently used objective measures (Lichtenhan et al., 2014). ANOW has mostly been recorded invasively from the round window in animals (Henry, 1997; Jeffery T Lichtenhan et al., 2013; Lichtenhan et al., 2014), but more recently in humans (Choudhury et al., 2012). ANOW is a sustained neural response that lasts as long as the auditory stimulus and reflects the phase locking activity of the cochlear nerve in the periphery (which is an important mechanism for coding sustained auditory stimuli such as vowels). Currently, there is no objective measure of auditory function used clinically that assesses the phase locking activity of the cochlear nerve. In fact, all current measures basically record the onset/offset neural response to auditory stimuli, and not the sustained neural response which lasts as long as the auditory stimulus. Being able to record the sustained neural response will have many clinical applications, such as accurately assessing the perception of sustained speech sounds (vowels) in infants and customizing hearing aid fitting accordingly. Also, these measures have potential use in differentiating between peripheral/central auditory processing dysfunction.

ANOW occurs when auditory nerve neurophonic (ANN) (see chapter 5 of literature review for more about the ANN response) to tones presented separately at opposite polarities are averaged together (i.e., summed together). This summation results in a neural response that appears twice twice for each acoustic stimulus cycle in the response waveform (Kenneth R Henry, 1995; Jeffery T Lichtenhan et al., 2013; Lichtenhan et al., 2014). This pattern occurs because the auditory nerve fires preferentially at one direction of basilar membrane movement, which results in preferential neural response at one phase of the tone (Kenneth R Henry, 1995; Jeffery T Lichtenhan et al., 2013; Lichtenhan et al., 2014). ANOW has major energy at double the tone frequency and a negligible energy at the tone frequency. It shows adaptation (amplitudes that start high and reduce over time), nonlinear growth and phase shift as a function of stimulus intensity (Lichtenhan et al., 2014).

Preliminary research in our laboratory has shown that ANOW is recordable from normal hearing adults at low frequencies, using Electrocochleography (ECochG), a noninvasive technique which is routinely used in the audiology clinic. Tone bursts, of relatively long plateaus, that are presented in an alternating polarity were used to evoke the phase locked neural response from the auditory nerve. An electrode in contact with the lateral surface of the tympanic membrane was used to record the response. The response was then analyzed using the fast Fourier transform (FFT) analysis, which revealed a response of twice the frequency of the original auditory signal.

Research Objective, Questions, and Hypothesis

Aims, Research Questions and Hypotheses

The main goal of this project is to investigate the robustness and the nature of the ANOW response that is recorded noninvasively from normal hearing adult participants. More specifically, this research aims to gain normative data from normally hearing adult participants and to measure the test retest reliability of the ANOW response. To achieve these aims, the mean hearing threshold of the ANOW was objectively determined and the recordings were repeated to investigate the test-retest variability of the response. Both the phase synchrony between the stimulus and the response and the amplitude of the response were used to test for reliability..

Based on the small amount of literature on the subject, we hypothesize that the test retest reliability of the ANOW response that is recorded noninvasively from normal hearing adult participants will exceed 0.8. We also hypothesize that the ANOW norms developed in this study will form the basis for developing an effective low frequency monitoring technique. The research questions include the following:

- Are the three repeated measures of the ANOW response that were recorded noninvasively from normal hearing adult participants, in the same test session, highly correlated?
- Are the ANOW response measures that were recorded noninvasively in different test sessions highly correlated?
- Is the ANOW response well synchronized with the evoking tone burst stimulus?
- Which measurement parameter of the ANOW response, the amplitude or the phase synchrony, is more reliable in tracking the ANOW response?

- What is the effect of the stimulus intensity on the test retest reliability of the ANOW response?
- What is the effect of the stimulus intensity on the synchronization between the stimulus and the response?
- What is the effect of the stimulus intensity on the amplitude of the ANOW?

Answering these research questions provides essential information about threshold and reliability of the ANOW response that is recorded noninvasively, using ECochG, from normally hearing adult participants. The outcomes of this study are essential to achieve the ultimate goal of gaining more knowledge about the nature of the ANOW that is recorded noninvasively from humans. The long term goal of this study is to develop a clinically viable tool that will provide a more accurate assessment of low frequency hearing in difficult-to-test populations.

CHAPTER 2

METHODS

Preliminary work

The stimulus parameters of the noninvasive ECochG technique were refined to capture the ANOW response in normal hearing adult participants. Three tone bursts (TBs) (250 Hz, 500 Hz, and 1000 Hz) of relatively long durations (2 ms rise/fall times and 10 ms plateau for the 500 Hz and 1000 Hz TBs, 4 ms rise fall times and 16 ms plateau for the 250 Hz,) were used to evoke the ANOW. As expected, FFT analysis of the recorded response showed major energy at double the frequency of the stimulus. Using low frequency tone bursts, the ANOW response was detected in all participants. However, the response was detected in only 3 out of the 5 recruited participants when the 1000 Hz tone burst was used. This finding indicates that the ANOW response best occurs at frequencies below a 1000 Hz or so, which is consistent with Lichtenhan et al., (2014) findings. Moreover, the ANOW response recorded to low frequency TBs demonstrates significantly lower thresholds and higher amplitudes when compared to that recorded to TBs of higher frequency (see table 1). This finding shows that the ANOW response recorded to low frequency TBs is more robust than responses evoked by high frequency TBs, and is consistent with the literature (Kenneth R. Henry, 1995; Henry, 1997; Lichtenhan et al., 2014). In addition, ANOW recorded to the three stimulus frequencies showed nonlinear growth in amplitude as stimulus level increased, which is also consistent with the literature (Kenneth R. Henry, 1995; Henry, 1997; Lichtenhan et al., 2014).

Table 1: Shows descriptive statistics of ANOW thresholds at the three test tone frequencies.

Frequency	***250***	***500***	***1000***
Mean	50	46	80
Median	50	50	80
Mode	40	50	NA
Standard Deviation	10	11.40175	10

Overall, the preliminary research done in our laboratory showed that the ANOW response is recordable via ECochG from normal hearing adult participants, at the three testing TB stimuli. Furthermore ANOW recorded to low frequency TBs is more robust than responses recorded to 1000 Hz TB, which is evident in the significantly lower thresholds and higher amplitudes. ANOW thresholds recorded to low frequency TBs were traced down to moderate stimulus intensity levels.

Participants

This study was approved by the Human Subjects Committee at the University of Kansas Medical Center. Appendix A shows the consent form that was signed by the participants. Ten normal hearing adults within the age range of 18 to 40 years were recruited. All participants

included in this study had no history of otologic disorders, ear surgeries, neurologic disorders, noise exposure, acoustic trauma, or ototoxic drug usage. Informed consents were obtained prior to their participation.

Otoscopic examination and audiological screening were performed. All participants had normal otoscopic examination of the ear canal and the tympanic membrane (TM), normal pure tone auditory (PTA) thresholds of 15 dB or less across the frequency range of 250 Hz to 8000 Hz, normal click ABR thresholds, as well as normal click evoked ECochG.

Participant Preparation

Participants were seated comfortably in a recliner. Two electrode sites on the forehead were cleansed with an alcohol pad and mildly abraded with electrode gel. Disposable surface electrodes with an adhesive backing were placed over these sites. Otoscopic examination of the ear canal and TM was then performed to insure that both structures were normal and healthy in appearance. Commercially-available TM electrodes (Sanibel^{TM}) were used for ECochG recording. Prior to insertion, the tip of the "tymptrode" was lightly coated with conductive gel to insure good electrical contact with the TM. As the electrode is inserted, the participant is asked to report when he/she feels it touching the TM. Contact also is verified via EEG monitoring on the video screen of the recording instrument. Once the participant reported that the electrode is touching the TM and the EEG verified this condition, a small, rubber-foam ear tip was compressed and placed into the entrance of the ear canal. The outer end of the ear tip is connected via a sound delivery tube to the acoustic transducer (tubal insert earphone

Disposable, surface electrodes were attached to the upper (Fz) and lower (Fpz) forehead. Electrode configuration was Fz (+) – to – TM (-), with ground at Fpz.

Acoustic Stimuli

Stimuli were provided by an ER-3 tubal insert earphone connected to the ear via a sound tube and rubber ear tip. Responses were averaged from 1000 repetitions of tone bursts (TBs) (2 ms rise/fall times, 28 ms plateau for the 500 Hz tone and 4 ms rise/fall times, 24 ms plateau for the 250 Hz tone) presented in an alternating polarity and shaped by a Blackman window. Separate responses were recorded to 250 Hz and 500 Hz TBs beginning at 90 dB nHL. A stimulus repetition rate of 11.3/sec was used at all frequencies Recordings with the sound tube crimped were first taken at 90 dB nHL to estimate electrical artifact, if any. No significant electrical artifact interference was detected. Thresholds (at each frequency) were then obtained starting at 80 dB nHL and decreasing in 5 to 10 dB steps. Online response filtration with 100 Hz high pass cutoff and 3000 Hz low pass cutoff was applied. 100,000 response gain was also applied. Keeping the same test setting, recording procedures were repeated two additional times for a total of three runs of the experimental condition in the same session. Five to ten minute breaks were given between runs. Two participants were brought back to repeat the experiment in different day and test sessions.

Calibration

Physical calibration of stimuli was conducted prior to testing to ensure that the intensity of the stimuli remained constant during testing and that the sound pressure level at the ear drum is within safe ranges. The acoustic output was delivered to an ER7C microphone which was attached to an oscilloscope. Two TBs (250 Hz and 500 Hz) were calibrated. Stimuli were presented at various dial levels. Peak amplitude levels in volts were measured at each dial level. Next, the recorded levels were converted to pressure levels in Pascal (Pa) using the conversion equation taken from the specification of the used mic (50 milli Volts per 1 Pa). Pa pressure levels were then

converted to peak sound pressure levels (p-SPL) using the following equation: $dBSPL=20\log_{10}$(Pa level/0.00002 Pa). All stimuli levels were within the maximum permissible noise levels using transient tones to avoid any harm to the participant. Using several dial tone levels, we were able to test the linearity of the dial tone level in p-SPL. A fixed change in the dial level corresponded to fixed change in the measured peak to peak volts and p-SPL, confirming the linearity of the change in the dial tone level.

The reference 0 dB nHL also was measured by recording the minimum hearing threshold of 10 normal hearing ears for each stimulus, using the same system that was used in the actual experiment. The average of the 10 hearing thresholds was then calculated to find the 0 dBnHL level for each stimulus.

Statistical Analysis

All statistical analyses were conducted using IBM SPSS Statistics 23 and MATLAB R2015a softwares. FFT analysis was conducted to convert the time domain representation of responses into the frequency domain representation. The power spectrum was then obtained by multiplying the FFT by its complex conjugate. The result is a display of the magnitude of signal's energy in squared microvolts (μV^2) over its frequency content. The magnitude of the spectrum corresponding to double the frequency of the evoking stimulus was considered as the response of interest corresponding to ANOW's absolute amplitude in (μV^2).

The mean background noise was calculated as the mean of the spectrum magnitude over 6 bins around the response (3 on each side of the signal, starting 2 bins away from the peak of the signal). Both ANOW's absolute amplitude and ANOW's amplitude normalized by the mean background noise (by calculating the ratio of ANOW's absolute amplitude in (μV^2) to the mean background noise in (μV^2)) were used as dependent variables in the analysis of the response.

Thresholds represent the lowest stimulus levels at which the absolute amplitude of the ANOW is significantly larger than the mean background noise at least 50% of time (i.e., in at least two out of the three repeated recordings at each level). Three criteria were used to determine the significance of the ANOW response: at least one standard deviation larger than noise, two standard deviations larger than noise, and three standard deviations larger than noise. Detection per cents of the ANOW response were also computed. Responses of all runs and all participants were tested for significant absolute amplitudes based on the three criteria discussed earlier (amplitudes at least 1 SD, 2 SD, and 3 SD higher than mean background noise). For each stimulus frequency and stimulus intensity, the ratio of number of runs of significant amplitudes to the total number of runs (at that specific level and stimulus) were computed and multiplied by 100% to find the detection percent of the ANOW.

Phase locking analysis

Another dependent variable used in the analysis is the Phase Locking Value (PLV), which looks at the variability of latencies of phase difference between trials of two signals. PLV is originally introduced as a method to detect phase synchrony between two narrowband signals recorded from two EEG recording sites (Lachaux et al., 1999). Given two series of narrow band signals, the PLV method computes the phase difference of the two signals' components for each latency. Three steps are used to compute PLV, starting with band pass filtering the two signals at the frequency range of interest, computing the analytic signals using Hilbert Transform and the relative phase, and computing the instantaneous PLV (appendix B explains method in more details and include the equation used) (Aydore et al., 2013). PLV represents the trial to trial phase differences (or relative phases) variability between the two signals. Small variability of phase differences across trials produces a PLV close to 1 (perfect synchronization between

signals), whereas high variability of phase differences produce a PLV close to zero (no synchronization) (Aydore et al., 2013). In practice, the absolute PLV value is not usually of interest. Instead, we are interested in investigating whether an experimental condition induced a change in the PLV value; usually a comparison between PLVs pre and post stimulus presentation, for example Hanslmayr et al. (2007) and Melloni et al. (2007).

To compute PLVs between stimuli and the evoked responses we used two simulated TBs that mimic the two original TB stimuli used in this experiment. Simulated TBs were created using the MATLAB software. The frequency of each simulated TB was then doubled before applying the Blackman window to the stimulus. Time series of amplitudes for stimuli and for their corresponding responses were used to compute PLVs. No offline filtration was applied to responses. However, responses are already online filtered between 100 Hz and 3000 Hz. This is different from (Aydore et al., 2013) work in that we are measuring the synchrony between a single frequency signal and a narrow band signal as opposed to using two EEG narrow band signals filtered to same frequency range of interest. However, filtering responses to have a frequency content similar to that of the tone (i.e., single frequency) could result in a false perfect synchrony because we simply could be creating another single frequency signal similar to our stimulus.

The PLV was also computed between simulated TBs and a random noise signal created using the MATLAB software (noise-TB PLV). Two probability density functions of noise-TB PLVs were created for the two TB stimuli. Similar probability density functions were also created of PLVs corresponding to ANOW responses at each stimulus frequency (response-TB PLVs). The probability density function is defined as:

$$f(x,\mu,\sigma) = \frac{1}{\sigma\sqrt{2\pi}} e^{-\frac{1}{2}\left(\frac{x-\mu}{\sigma}\right)^2}$$

Where: e=2.7182 (Euler's number), x: PLV data points, σ: standard deviation of PLV data, μ: mean of PLV data.

Noise and response PLV probability distributions were then plotted against each other and compared, for each TB stimulus.

Reliability measures

Two measures were used to test the test-retest reliability of the ANOW: Intra-class correlation coefficient (ICC) and coefficient of variation (CV). Both within and between participants' designs were used to investigate within session test retest-reliability.

ICC is a statistical measure of observations between clusters relative to the total variability in the outcome (across all observations and all clusters). The ICC also measures the correlation between two measures of the same participant (Bartko, 1966). The general formula is given by:

$$\text{ICC} = \frac{\sigma^2_{\alpha 0}}{\sigma^2_{\alpha 0} + \sigma^2_{\epsilon}}$$

For the within participants' design, ICC values were computed for each stimulus intensity level and each stimulus frequency using the three repeated recordings of the ANOW. Participants are clusters. I.e., for each stimulus frequency and each stimulus intensity, the three repeated recordings of the ANOW for each participant represent a cluster. Within and between clusters' variances were used to compute the ICC. In the between participants' design, ICC values were computed for each participant and each stimulus frequency. Clusters are stimulus intensity

levels. I.e., for each participant and each stimulus frequency, the three repeated recordings at each stimulus intensity level represent a cluster. Within and between clusters' variances were used to compute the ICC.

A linear mixed model was used at each stimulus frequency and each stimulus intensity level to model ANOW's dependent variables (absolute amplitude, SNR, and PLV), treating participant as a random effect:

$$A = \alpha_0 + \alpha_i L + \epsilon$$

Where: $\alpha_0 \sim N(\mu_{\alpha 0}, \sigma^2_{\alpha 0})$, $\epsilon \sim N(0, \sigma^2_{\epsilon})$, A: the dependent variable, L: single fixed independent variable (stimulus intensity), $\sigma^2_{\alpha 0}$: between participants variance, ϵ: variability of repeated runs, σ^2_{ϵ}: between repeated runs variance or within participants variance, for the within participants design. For between participants design: $\sigma^2_{\alpha 0}$: between stimulus levels variance, ϵ: variability of repeated runs, σ^2_{ϵ}: between repeated runs variance or within stimulus levels variance, and L: single fixed independent variable (in this case participant).

ICC values >0.7 indicate highly correlated repeated observations with strong agreement; ICCs between 0.5 to 0.6 indicates moderate agreement between repeated observations; 0.3 to 0.4 indicate fair agreement between repeated observations, and <0.2 indicate poor agreement between repeated observations (Bartko, 1966).

The coefficient of variation (CV) is the ratio of the standard deviation to the mean of a set of data points. CV provides better description of the dispersion of observations than the SD alone, given that data may vary greatly in their means and measurement units. CV is unit-less, which allows a fair comparison of dispersions of data with originally different units. The larger the CV the more dispersed the data (Reed et al., 2002). Coefficient of variation (CV) of the three repeated

recordings of ANOW's absolute amplitudes and of signal to noise ratios (SNRs) was computed at each stimulus intensity for each TB stimulus in each participant. Box plots of CV values across different stimulus intensity levels for both 250 Hz and 500 Hz TB stimuli were also created. Box plots are highly informative because they show measure of central tendency (median) and measures of variability (interquartile range and range of data). Figure (1) shows a diagram of the box plot.

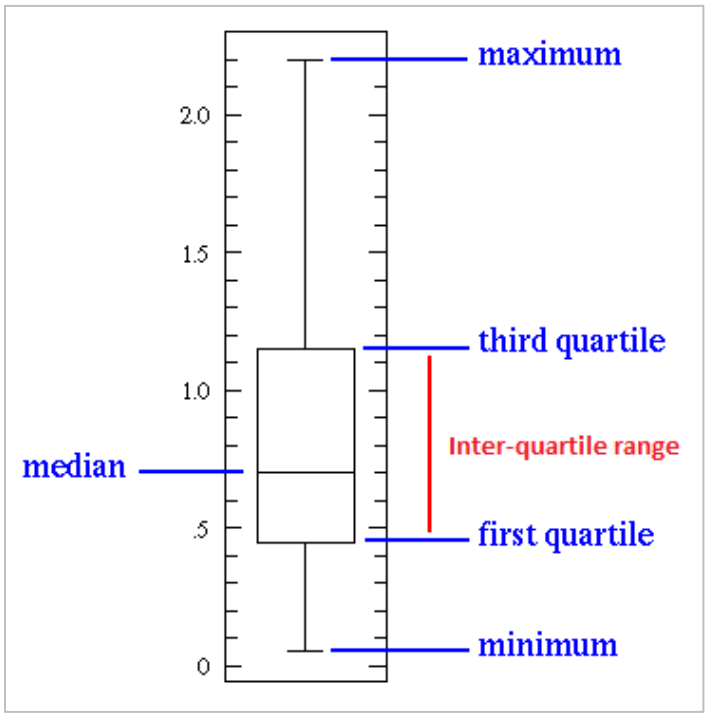

Figure 1: An explanatory diagram of the box plot.

Coefficient of variation (CV) of the three repeated recordings of ANOW's absolute amplitudes, SNRs, and PLVs within the same session were computed across different stimulus intensities, stimulus frequencies, and participants. CVs were also calculated for between sessions' repetitions of the ANOW response.

CHAPTER 3

RESULTS

Raw data of absolute ANOW's amplitudes, mean background noise, and SNRs corresponding to within-session and between sessions repeated measures for 250 Hz and 500 Hz tone burst stimuli presented at multiple intensity levels are reported in appendices C and D. Figures 2&3 show examples of waveform responses recorded in our lab for the two TB stimuli at high and low stimulus intensity levels. Visual inspection of waveforms in figures 2&3 show cyclic kind of periodic pattern, mainly at higher stimulus intensity levels. Low stimulus intensity levels correspond to noisier and less periodic waveforms (see waveforms at 30 dB nHL and 40 dB nHL in figures 2&3). Visually analyzing response waveforms' envelopes, by counting cycles per second (Hz), at higher stimulus intensity levels reveals responses that have double the frequency of the original stimulus. Tables 2, 3, and 4 summarize individual and mean hearing thresholds as well as detection percentages of the ANOW response using the two test stimuli presented at multiple intensity levels. Mean hearing thresholds (in dB nHL) based on 1SD, 2SD, and 3SD criteria are 30.77 ± 11.88, 34.62 ± 16.64, and 38.33 ± 16.97, respectively, for 250 Hz TB and 25.38 ± 6.6, 26.92 ± 7.51, and 38.33 ± 10.3, respectively, for the 500 Hz TB. Table (2) also shows hearing thresholds corrected based on the 0 dB nHL recorded from the test sample (-12.14 dB for the 250 Hz TB and -18.57 dB for the 500 Hz TB) as well as thresholds in peak sound pressure level (p-SPL). Mean hearing thresholds in p-SPL based on 1SD, 2SD, and 3SD criteria are 80.00 ± 10.02, 83.21 ± 14.17, and 86.37 ± 14.65, respectively, for the 250 Hz TB, and 74.82± 5.78, 76.22± 6.71, 86.36 ± 8.97, respectively, for the 500 Hz TB.

Detection percentages of the ANOW response are displayed in table (4). High detection percentages (>90%) are detected at stimulus intensities above 90 p-SPL for both stimuli, when 1

SD significance criteria is applied. Applying the 3 SD significance criteria, detection percentages were lower 90% across all stimulus intensity levels. In general, as the stimulus intensity decreases detection percentages decrease.

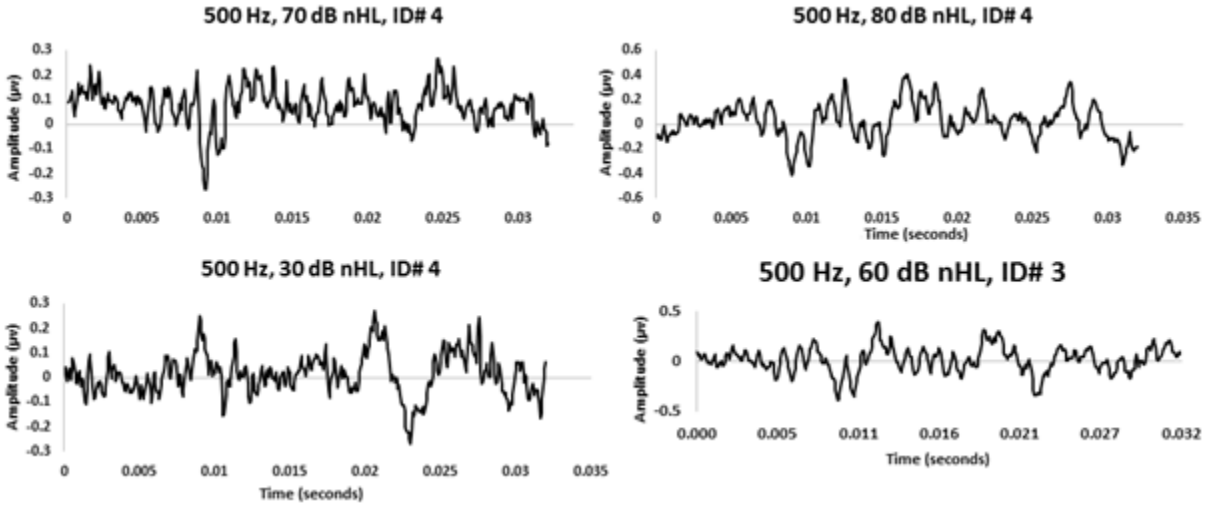

Figure 2: Examples of waveform responses recorded in our lab using the 500 Hz TB stimulus. Responses were recorded from two participants at 4 different stimulus intensity levels.

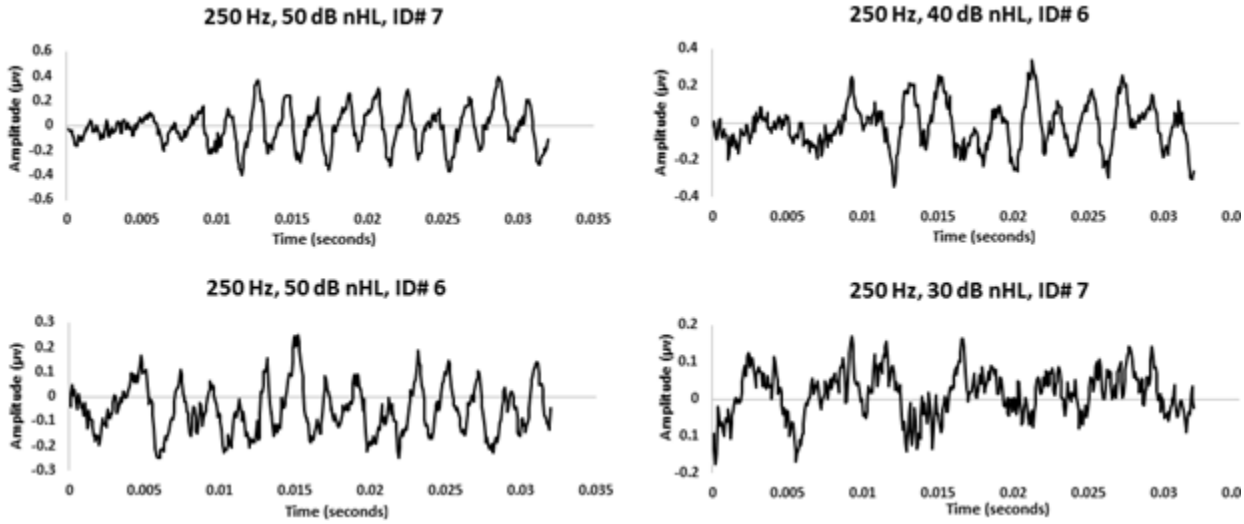

Figure 3: Examples of waveform responses recorded in our lab using the 250 Hz TB stimulus. Responses were recorded from two participants at 4 different stimulus intensity levels.

Table 2: Individual hearing thresholds of the ANOW response based on the three significance criteria, for both 250 Hz and 500 Hz TB stimuli. The table also shows individual thresholds of the repeated recordings of the ANOW response in second session for participants 2 and 6.

ID#	250 Hz						500 Hz					
	1 SD		2 SD		3 SD		1 SD		2 SD		3 SD	
	dB nHL	p-SPL	dB nHL	p-SPL	dB nHL	p-SPL	dB nHL	p-SPL	dB nHL	p-SPL	dB nHL	p-SPL
1	40	86.82	40	86.82	40	86.82	40	88.42	40	88.42	40	88.42
2	20	71.07	30	79.58	40	86.82	20	70.22	20	70.22	20	70.22
3	20	71.07	20	71.07	20	71.07	30	78.52	30	78.52	40	88.42
4	40	86.82	40	86.82	NR	NR	20	70.22	20	70.22	NR	NR
5	30	79.58	50	95.82	60	105.82	20	70.22	40	88.42	40	88.42
6	30	79.58	30	79.58	40	86.82	30	78.52	30	78.52	40	88.42
7	20	71.07	20	71.07	30	79.58	30	78.52	30	78.52	40	88.42
8	20	71.07	20	71.07	20	71.07	20	70.22	20	70.22	40	88.42
9	40	86.82	40	86.82	40	86.82	20	70.22	20	70.22	30	78.52
10	20	71.07	20	71.07	30	79.58	30	78.52	30	78.52	30	78.52
11	30	79.58	30	79.58	30	79.58	20	70.22	20	70.22	50	95.42
12	30	79.58	30	79.58	30	79.58	30	78.52	30	78.52	30	78.52
13	60	105.82	80	122.84	80	122.84	20	70.22	20	70.22	60	104.58
2 repeated	30	79.58	40	86.82	40	86.82	20	70.22	20	70.22	20	70.22
6 repeated	30	79.58	30	79.58	30	79.58	20	70.22	20	70.22	40	88.42

Table 3: Mean hearing thresholds and standard deviations (SDs) of the ANOW response based on the three significance criteria for the 250 Hz and 500 Hz TB stimuli. Thresholds are displayed in dial dB nHL, corrected dial dB nHL based on the 0 dB nHL measured in our lab, and peak sound pressure level (p-SPL).

	250 Hz			500 Hz		
Threshold significance criterion	1 SD	2 SD	3 SD	1 SD	2 SD	3 SD
Mean (dial dB nHL)	30.77	34.62	38.33	25.38	26.92	38.33
SD (dial dB nHL)	11.88	16.64	16.97	6.60	7.51	10.30
Corrected mean (based on our 0 dB nHL)	42.91	46.76	50.48	43.96	45.49	56.90
Corrected SD (based on our 0 dB nHL)	11.88	16.64	16.97	6.60	7.51	10.30
Mean (peak SPL)	80.00	83.21	86.37	74.82	76.22	86.36
SD (peak SPL)	10.02	14.17	14.65	5.78	6.71	8.97

Table 4: Detection percentages of the ANOW response based on the 3 significance criteria.

	Stimulus Intensity		Total number of runs	> 1 SD		> 2 SD		> 3 SD	
	(dB nHL)	p-SPL		Detected	Detection percent	Detected	Detection percent	Detected	Detection percent
500 Hz	80	121.85	38	35	92%	35	92%	34	89%
	70	113.36	39	39	100%	35	90%	33	85%
	60	104.58	39	37	95%	35	90%	29	74%
	50	95.42	39	35	90%	33	85%	27	69%
	40	88.42	39	29	74%	28	72%	28	72%
	30	78.52	39	25	64%	20	51%	14	36%
	20	70.22	39	20	51%	14	36%	9	23%
250 Hz	80	122.84	37	34	92%	32	86%	32	86%
	70	115.58	39	39	100%	35	90%	33	85%
	60	105.82	39	37	95%	34	87%	33	85%
	50	95.82	39	36	92%	33	85%	30	77%
	40	86.82	39	32	82%	29	74%	25	64%
	30	79.58	39	27	69%	21	54%	16	41%
	20	71.07	38	17	45%	14	37%	8	21%

Before fitting a statistical model to ANOW's measurement parameters, data were tested for homoscedasticity assumption (the assumption of uniform distribution of the variance around the regression line for all values of the predictor variable). The homoscedasticity assumption was violated for all measurement parameters (PLV, amplitude, and SNR). To correct for the issue of heteroscedasticity, the inverse variance of each measurement parameter for each stimulus level and each stimulus frequency was computed. A linear mixed effects model was used to model ANOW's measurement parameters (absolute amplitude, SNR, and PLV) using the random subject effect and fixed effect experimental factors of stimulus frequency, stimulus intensity level, and the interaction of stimulus intensity level and stimulus frequency. Inverse variance weighted least squares were applied to the statistical model to correct for the non-uniform distribution of the residuals (to achieve the assumption of homoscedasticity). A *P* value of 0.05

was used to test the statistical significance of effects. Statistically significant maximizing effect of stimulus intensity level on the absolute amplitude of the ANOW response ($F(1, 526.003) = 137.735$, $P<0.001$), the SNR ($F(1, 526.015 = 171.938$, $P<0.001$), and the PLV ($F(1, 526.079) = 108.193$, $P<0.01$) was revealed. Statistically significant effect of the stimulus frequency on both the absolute amplitude ($F(1, 526.010) = 52.441$, $P<0.001$) and the PLV ($F(1, 526.081)= 14.783$, $P<0.001$) was revealed. Moreover, a significant interaction effect of stimulus intensity level and stimulus frequency on both absolute amplitude ($F(1, 526.004)= 121.420$, $P<0.001$) and PLV ($F(1, 526.110)= 7.189$, $P<0.01$) was revealed. No statistically significant effect of the frequency ($P=0.366$) and the interaction of stimulus intensity level and stimulus frequency ($P=0.070$) on the SNR was found. Model parameter estimates were used to predict measurement parameters of the ANOW response and to draw regression lines. The significance of the regression coefficient of the interaction between stimulus intensity level and stimulus frequency determines the significance of the difference between the slopes of lines, while the significance of the regression coefficient of the frequency (taking 500 Hz TB as the reference frequency) determines the significance of the difference between the two y-axis intercepts of the two lines. Following is the model equation used to draw regression lines:

$$M = \beta_0 + \beta_1 F + \beta_2 L + \beta_3 F*L + \epsilon$$

Where: M: the predicted measurement parameter (absolute amplitude, PLV, or SNR), $F\begin{cases}1 \; if \; Frequency = 500\\0 \; if \; frequency = 250\end{cases}$, L: stimulus intensity level, β_0: y-intercept, β_1: regression coefficient of the frequency, β_2: regression coefficient of the stimulus intensity level (determines the slope of regression line for 250 Hz), β_3: Regression coefficient of the interaction between stimulus intensity level and stimulus frequency, ϵ: error.

Figure (4) shows regression lines based on predicted measurement parameters. Regression lines for each parameter estimate and for both stimulus frequencies were plotted on the same figure. Figure (4) shows that the relationship between the stimulus intensity level and absolute amplitude, SNR, and PLV is linear for both 250 Hz and 500 Hz TB stimuli. Positive slopes of regression lines show that as the stimulus intensity increases we expect the three measurement parameters to increase. However, the rate of the change in both absolute amplitude and PLV of the ANOW response with stimulus intensity differs significantly between the two stimulus frequencies. 250 Hz TB shows higher rates of increase in amplitude and PLV of the ANOW response compared to 500 Hz TB stimulus. No statistically significant change in the rate of increase of the SNR with stimulus intensity was found between the two stimulus frequencies (P=0.070). This is evident in the similar slopes of regression lines for the two TB stimuli. Overall, 250 Hz TB evoked significantly higher PLV values compared to the 500 Hz TB, indicating stronger phase locking between 250 Hz TB and ANOW response compared to 500 Hz TB. Regression lines also suggest higher absolute amplitudes of the ANOW response for the 250 Hz TB compared to the 500 Hz TB, at least at higher range of stimulus intensity levels.

Table 5: Regression model parameters, their 95% confidence intervals, and p-values corresponding to the absolute amplitude of the ANOW response.

Estimates of Absolute Amplitude of the ANOW response							
Parameter	Estimate	Std. Error	Degrees of Freedom	t	P	95% Confidence Interval	
						Lower Bound	Upper Bound
Intercept (β_0)	-.337251	.043970	527.060	-7.67	.000	-.423630	-.250873
Frequency (β_1)	.319760	.044156	526.010	7.24	.000	.233017	.406503
Level (β_2)	.021628	.001843	526.003	11.74	.000	.018008	.025248
Interaction (β_3)	-.020390	.001850	526.004	-11.02	.000	-.024026	-.016755

Table 6: Regression model parameters, their 95% confidence intervals, and p-values corresponding to the SNR of the ANOW response.

Estimates of the SNR							
Parameter	Estimate	Std. Error	df	t	Sig.	95% Confidence Interval	
						Lower Bound	Upper Bound
Intercept (β_0)	-3.765290	.731317	193.510	-5.15	.000	-5.207665	-2.322915
Frequency (β_1)	.811977	.898077	526.025	.90	.366	-.952281	2.576235
Level (β_2)	.314456	.023981	526.015	13.1	.000	.267345	.361567
Interaction (β_3)	-.058133	.031968	526.015	-1.82	.070	-.120934	.004668

Table 7: Regression model parameters, their 95% confidence intervals, and p-values corresponding to the PLV of the ANOW response.

Estimates of the PLV							
Parameter	Estimate	Standard Error	Degrees of Freedom	t	P	95% Confidence Interval	
						Lower Bound	Upper Bound
Intercept (β_0)	0.0726983	0.0178465	301.7904170	4.07	0.000059	0.037580	0.107818
Frequency (β_1)	-0.0726980	0.0189076	526.0814314	-3.85	0.000135	-0.109842	-0.035554
Level (β_2)	0.0037864	0.0003640	526.0789085	10.40	0.000000	0.003071	0.004502
Interaction (β_3)	-0.0011369	0.0004240	526.1102600	-2.68	0.007566	-0.001970	-0.000304

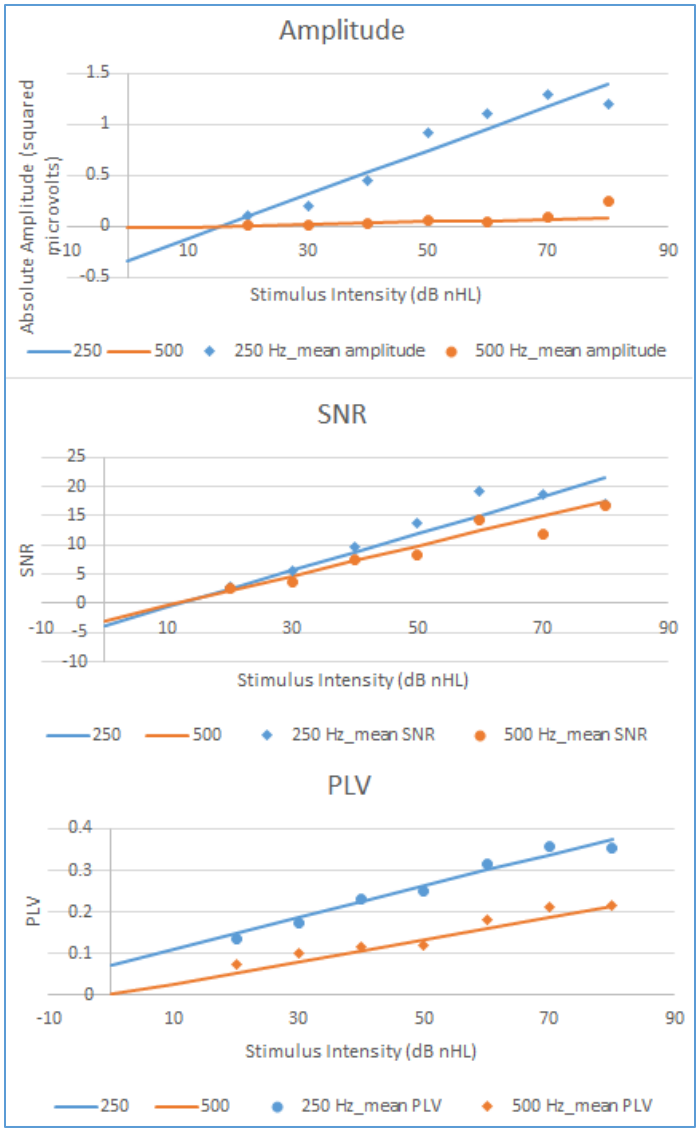

Figure 1: Regression lines based on predicted measurement parameters. Regression lines for each parameter estimate and for both stimulus frequencies were plotted on the same figure.

Within-session test retest reliability analysis

Intra-class correlation coefficient (ICC)

Intra-class correlation coefficient (ICC) between the three repeated recordings of the ANOW responses in the same session were calculated using absolute amplitudes of the ANOW (amplitude ICCs) and signal-to-noise ratios (SNR ICCs) (see figures 5-6 and tables 8-11). High

degrees of reliability were found between the three repeated recordings of absolute amplitudes corresponding to both TB stimuli at presentation levels higher than 40 dB nHL (86.82 p-SPL for 250 Hz, and 88.42 p-SPL). Single measure ICCs were higher than 0.8 with relatively narrow 95% confidence intervals and significant P values (<0.001). Poor to moderate degrees of reliability were found between the three repeated recordings of absolute amplitudes of the response corresponding to 500 Hz TB presented at intensities lower than 50 dB nHL (95.42 p-SPL). Amplitude ICCs corresponding to 250 Hz TB presented at stimulus intensities below 50 dB nHL (95.82 p-SPL) ranged from approximately 0.5 at 20 dB nHL (71.07 p-SPL) ($F(11,24)= 4.074$, $P<0.05$) to more than 0.7 at 30 dB nHL (79.58 p-SPL) ($ICC=0.765$,$F(12,26)= 10.781$, $P<0.05$) and 40 dB nHL (86.82 p-SPL) ($ICC=0.846$,$F(12,26)= 17.514$, $P<0.05$), indicating moderate to strong agreement between the three repeated recordings of the absolute amplitude.. Amplitude ICC values recorded to both stimuli showed an increase with the stimulus intensity level, with steeper slope of increase corresponding to the 500 Hz TB compared to 250 Hz TB. Moreover, Stimulus presentation levels lower than 50 dB nHL (95.82 p-SPL for 250 Hz TB and 95.42 p-SPL for 500 Hz TB) were associated with wider confidence intervals, indicating higher levels of uncertainty of ICCs, and some statistically insignificant P-values (higher than 0.05 at 20 dB nHL (70.22 p-SPL) and 30 dB nHL (78.52 p-SPL) using the 500 Hz TB) compared to higher stimulus presentation levels.

Overlaying amplitude ICC plots of both TB stimuli against each other (figure 5) shows that 250 Hz TB results in higher ICC values at low intensity levels (20 dB nHL (around 70 p-SPL), 30 dB nHL (around 79 p-SPL), and 40 dB nHL (around 87 to 88 p-SPL)), with statistically significant difference at 30 dB nHL (around 79 p-SPL) evident by the non-overlapping 95% confidence intervals. The two curves rise as the intensity level increases and the difference between the two

curves narrows until they cross at around 50 dB nHL (around 95 p-SPL) level and stay close to each other at higher intensity levels with ICC values >0.7.

Poor to fair degrees of test retest reliability were found between the three repeated measures of SNRs corresponding to 500 Hz TB at stimulus intensity levels below 50 dB nHL (95.42 p-SPL). Single measure ICC values ranges from 0.043 at 20 dB nHL (70.22 p-SPL) ($F(12,26)= 1.134$, $P>0.05$), to 0.269 at 40 dB nHL (88.42 p-SPL) ($F(12,26)= 2.106$, $P>0.05$). Moderate to high degrees of test retest reliability were found at intensity levels above 40 dB nHL (88.42 p-SPL) using the 500 Hz TB stimulus, with significant P values (<0.05) and relatively narrower confidence intervals compared to lower intensity levels.

Fair degrees of reliability were found between the three repeated measures of SNRs corresponding to 250 Hz TB at stimulus 20 dB nHL (71.07 p-SPL) ($ICC=0.392$, $F(11,24)= 2.933$, $P<0.05$), 30 dB nHL (79.58 p-SPL) ($ICC=0.280$, $F(12,26)= 2.168$, $P<0.05$), and 70 dB nHL (115.58 p-SPL) ($ICC=0.197$, $F(12,26)= 1.735$, $P<0.05$). Moderate degrees of reliability were found at 40 dB nHL (86.82 p-SPL) ($ICC=0.625$, $F(12,26)=5.994$, $P<0.05$), 60 dB nHL (105.82 p-SPL) ($ICC=0.547$, $F(12,26)= 4.629$, $P<0.05$), and 80 dB nHL (122.84 p-SPL) ($ICC=0.561$, $F(11,24)= 4.827$, $P<0.05$). ICC value at 50 dB nHL (95.82 p-SPL) indicates a high degree of reliability when using SNRs of within session repeated recordings of the ANOW response using 250 Hz TB ($ICC=0.856$, $F(12,26)= 18.815$, $P<0.05$).

To make sure that the violation of the homoscedasticity assumption did not bias ICCs, data were also transformed into the logarithmic scale form. ICCs were also computed using the logarithms (to base 10) of data (figure 5). The Koenker test for heteroscedasticity (Koenker et al., 1982; Pryce et al., 2002) was done to test for the significance of the heteroscedasticity in data. Appendix (E) show Koenker test's results using both no logarithmic scale as well as logarithmic

scale of data. Transforming data into logarithmic scale successfully removed heteroscedasticity in our data (P-values >0.05). The same conclusions maybe drawn from ICCs of both logarithmic and no logarithmic forms of data. However, transforming data into logarithmic scale resulted in smaller 95% confidence intervals mainly at high intensity levels and for absolute amplitudes. Moreover, ICCs of absolute amplitudes for 250 Hz TB at 20 dB nHL and 30 dB nHL were reduced from around 0.5 and 0.75 to 0.4 and 0.6, respectively. This indicates fair to moderate within session test retest reliability of the ANOW's absolute amplitude for 250 Hz TB.

Overall, SNR ICC values comprise wider confidence intervals, indicating higher levels of uncertainty compared to amplitude ICC values. Moreover, SNR ICC increases with stimulus intensity level for the 500 Hz TB, indicating within session test retest reliability of SNR that improves with stimulus intensity level. However, SNR ICCs for the 250 Hz TB did not show the same trend of increase with stimulus intensity; ICCs at 40 dB nHL, 50 dB nHL, and 60 dB nHL are highest amongst all (0.6 to 0.8, indicating moderate to high test retest reliability), while ICCs at other levels are lower than 0.5 (fair test retest reliability).

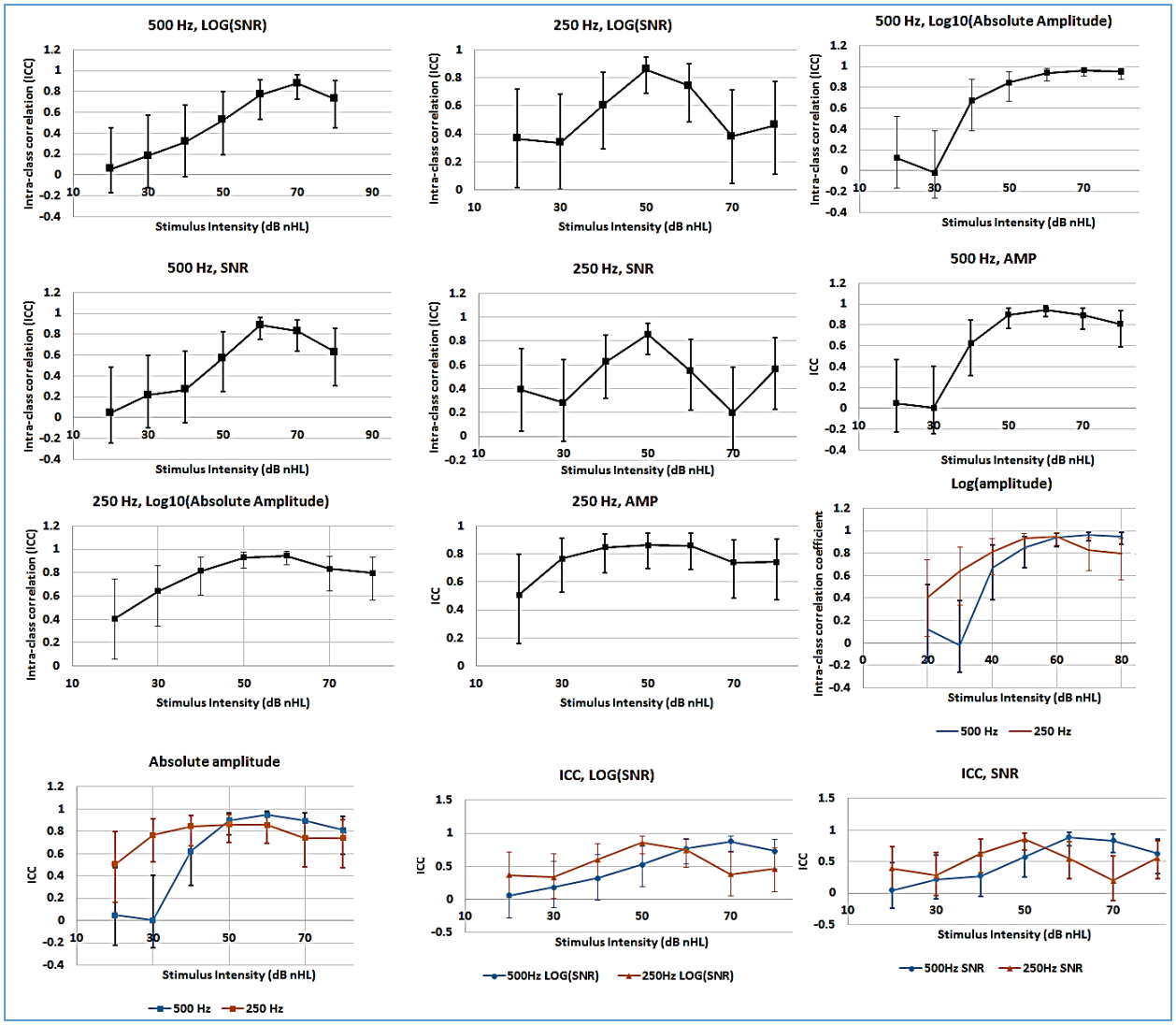

Figure 5: Intra-class correlation coefficient (ICC) of repeated recordings of the ANOW response across different stimulus intensities computed using absolute amplitudes in (μv^2), signal-to-noise ratios, logarithms of absolute amplitudes, and logarithms of PLVs corresponding to 500 Hz and 250 Hz TB stimuli. Error bars are upper and lower limits of 95% confidence intervals.

Table 8: ICC values at different stimulus intensity levels and frequencies, using signal-to-noise ratios. N: total number of triplet repeated recordings used to compute each ICC value. P: the statistical significance value.

SNR							
Stimulus Intensity		**Stimulus Frequency (Hz)**	**N**	**ICC**	**95% Confidence Interval**		**P-Value**
dB nHL	**p-SPL**				**Lower Bound**	**Upper Bound**	
20	70.22	500	11	0.043	-0.24	0.487	0.086
30	78.52	500	13	0.216	-0.097	0.599	0.096
40	88.42	500	13	0.269	-0.054	0.639	0.054
50	95.42	500	13	0.572	0.252	0.824	0
60	104.58	500	13	0.887	0.748	0.96	0
70	113.36	500	13	0.83	0.637	0.939	0
80	121.85	500	12	0.628	0.309	0.859	0
20	71.07	250	12	0.392	0.043	0.735	0.013
30	79.58	250	13	0.28	-0.045	0.647	0.048
40	86.82	250	13	0.625	0.319	0.85	0
50	95.82	250	13	0.856	0.686	0.949	0
60	105.82	250	13	0.547	0.222	0.811	0.001
70	115.58	250	13	0.197	-0.113	0.583	0.116
80	122.84	250	12	0.561	0.224	0.827	0.001

Table 9: ICC values at different stimulus intensity levels and frequencies, using absolute amplitudes. N: total number of triplets repeated recordings used to compute each ICC value. P: the statistical significance value.

Absolute Amplitude							
Stimulus Intensity		**Stimulus Frequency (Hz)**	**N**	**ICC**	**95% Confidence Interval**		**P-Value**
dB nHL	**p-SPL**				**Lower Bound**	**Upper Bound**	
20	70.22	500	12	0.049	-0.226	0.47	1.155
30	78.52	500	13	0.004	-0.247	0.404	0.467

40	88.42	500	13	0.623	0.316	0.849	0
50	95.42	500	13	0.898	0.77	0.964	0
60	104.58	500	13	0.948	0.877	0.982	0
70	113.36	500	13	0.893	0.759	0.963	0
80	121.85	500	12	0.81	0.591	0.934	0
20	71.07	250	12	0.506	0.161	0.799	0.002
30	79.58	250	13	0.765	0.526	0.913	0
40	86.82	250	13	0.846	0.668	0.945	0
50	95.82	250	13	0.861	0.697	0.951	0
60	105.82	250	13	0.858	0.69	0.949	0
70	115.58	250	13	0.738	0.482	0.901	0
80	122.84	250	12	0.741	0.473	0.907	0

ICC values for each participant and each TB stimulus were computed using absolute amplitudes (amplitude ICCs) and SNRs (SNR ICCs) of within session repeated recordings of all intensity levels (figure 6 and tables 10-11). High degrees of test retest reliability were revealed using absolute amplitudes for both TB stimuli and all participants, except participant 1 (ICC=0.358, $P<0.05$, indicating fair reliability) and participant 11 (ICC=0.05, $P>0.05$, indicating poor reliability using 500 Hz TB stimulus). Between participants SNR ICC values indicates a fluctuation between fair and moderate degrees of test retest reliability, for the most part, with some ICC values >0.7 indicating high degree of test retest reliability for few participants. Overall, amplitude ICC values were higher than SNR ICC values across participants and for both TB stimuli. However, their confidence intervals overlap and it is hard to judge if the difference is statistically significant.

Table 10: Amplitude ICC values across participants using 250 Hz and 500 Hz TB stimuli. For each participant, repeated amplitude responses at all stimulus levels were used to compute ICC for each participant.

Participant ID#	Frequency (Hz)	ICC	Lower Bound of 95% CI	Upper Bound of 95% CI	F Value	N	P
1	500	0.358	-0.06	0.788	2.677	8	0.049
2	500	0.746	0.405	0.936	9.8	8	0.000
3	500	0.771	0.419	0.951	11.082	7	0.000
4	500	0.82	0.638	0.929	14.697	8	0.000
5	500	0.937	0.799	0.988	45.314	7	0.000
6	500	0.903	0.709	0.981	29.046	7	0.000
7	500	0.863	0.633	0.968	19.907	8	0.000
8	500	0.888	0.691	0.974	24.841	8	0.000
9	500	0.961	0.845	0.993	108.834	7	0.000
10	500	0.793	0.463	0.956	13.379	7	0.000
11	500	0.05	-0.153	0.589	1.27	6	0.348
12	500	0.955	0.854	0.991	65.15	7	0.000
13	500	0.963	0.878	0.993	79.02	7	0.000
1	250	0.78	0.436	0.953	11.633	7	0.000
2	250	0.735	0.356	0.941	9.3	7	0.000
3	250	0.831	0.538	0.965	15.75	7	0.000
4	250	0.69	0.285	0.93	7.689	7	0.001
5	250	0.764	0.406	0.949	10.693	7	0.000
6	250	0.691	0.286	0.93	7.711	7	0.001
7	250	0.676	0.263	0.926	7.255	7	0.001
8	250	0.939	0.789	0.99	47.504	6	0.000
9	250	0.883	0.658	0.976	23.688	7	0.000
10	250	0.695	0.293	0.931	7.849	7	0.001
11	250	0.953	0.833	0.993	62.086	6	0.000
12	250	0.979	0.928	0.996	139.072	7	0.000
13	250	0.742	0.369	0.943	9.643	7	0.000

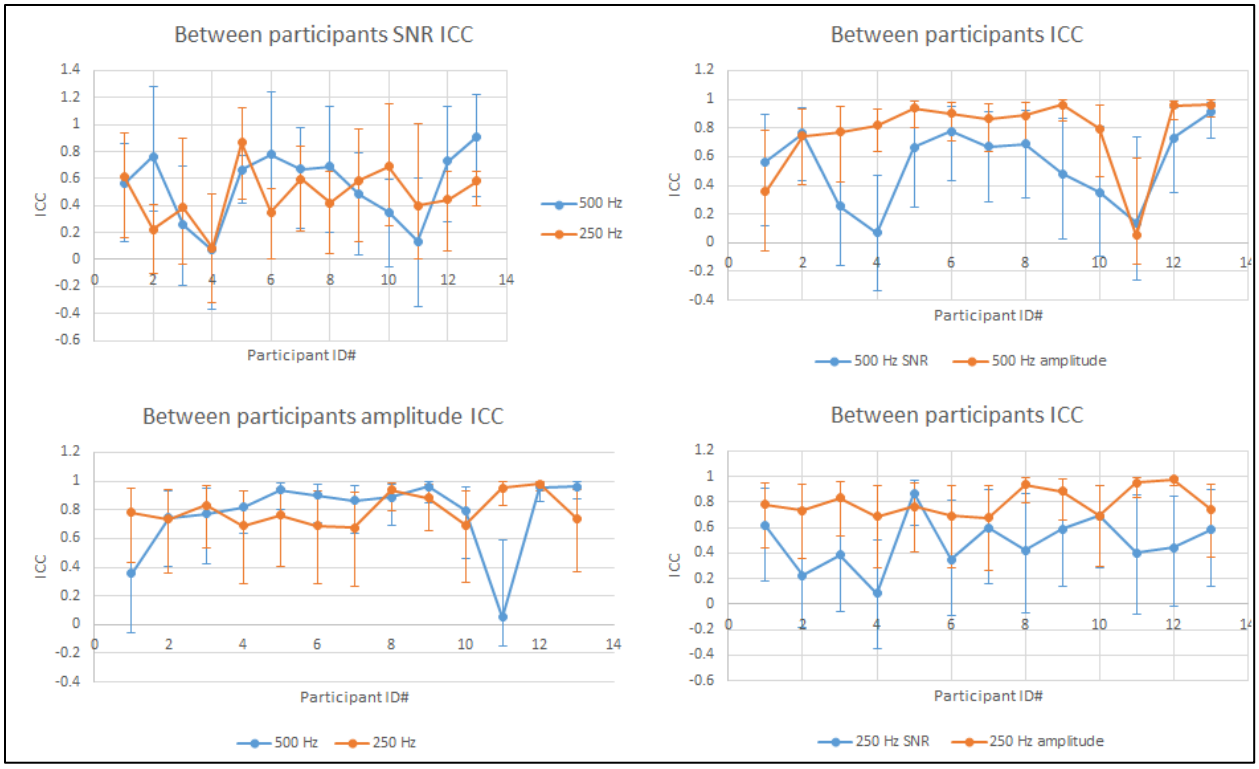

Figure 6: Between participants ICC values using amplitudes and SNRs of within session repeated recordings of the ANOW response. Repeated amplitude and SNR responses at all stimulus levels were used to compute ICC for each participant. Error bars are upper and lower limits of 95% confidence intervals.

Table 11: SNR ICC values across participants using 250 Hz and 500 Hz TB stimuli. For each participant, repeated amplitude responses at all stimulus levels were used to compute ICC for each participant.

Participant ID#	Frequency (Hz)	ICC	Lower Bound of 95% Confidence Interval	Upper Bound of 95% Confidence Interval	F value	N	P value
1	500	0.564	0.116	0.892	4.881	6	0.007
2	500	0.763	0.435	0.941	10.663	7	0.000
3	500	0.256	-0.162	0.765	2.034	6	0.128
4	500	0.07	-0.333	0.469	0.804	7	0.596
5	500	0.665	0.248	0.923	6.964	6	0.001
6	500	0.778	0.432	0.952	11.495	6	0.000
7	500	0.672	0.288	0.913	7.134	7	0.001
8	500	0.688	0.313	0.918	7.62	7	0.000
9	500	0.482	0.026	0.864	3.787	6	0.019
10	500	0.351	-0.091	0.811	2.622	6	0.064
11	500	0.137	-0.261	0.742	1.475	5	0.268
12	500	0.729	0.346	0.94	9.07	6	0.000
13	500	0.91	0.725	0.982	31.172	6	0.000

1	250	0.614	0.178	0.908	5.77	6	0.003
2	250	0.225	-0.184	0.748	1.871	6	0.157
3	250	0.387	-0.062	0.827	2.892	6	0.048
4	250	0.085	-0.352	0.504	0.764	6	0.610
5	250	0.867	0.619	0.973	20.58	6	0.000
6	250	0.35	-0.092	0.811	2.619	6	0.065
7	250	0.598	0.157	0.903	5.454	6	0.004
8	250	0.422	-0.064	0.868	3.188	5	0.046
9	250	0.587	0.143	0.9	5.26	6	0.005
10	250	0.691	0.286	0.93	7.708	6	0.001
11	250	0.399	-0.083	0.861	2.994	5	0.056
12	250	0.442	-0.012	0.849	3.376	6	0.028
13	250	0.582	0.138	0.898	5.182	6	0.005

Coefficient of Variation (CV)

Coefficient of variation (CV) of the three repeated recordings of ANOW's absolute amplitudes and of signal to noise ratios (SNRs) were computed at each stimulus intensity for each TB stimulus in each participant. Figures (7 & 8) show box plots of CV values across different stimulus intensity levels for both 250 Hz and 500 Hz TB stimuli. Amplitude CV medians are similar at the lower range of intensity levels (below 50 dB nHL for the 250 Hz TB and below 40 dB nHL for the 500 Hz TB) and decreases with stimulus intensity to less than 0.2, except for 80 dB nHL for the 250 Hz TB where the median increases to around 0.4. The interquartile range decreases with stimulus intensity for the 250 Hz TB, except for 80 dB nHL, indicating lower variability of CV values with stimulus intensity. Overall, Interquartile ranges range between 0.2 to 0.4 at stimulus intensities above 40 dB nHl and between around 0.4 to around 0.6 at lower intensity ranges for both stimuli. This indicates that SDs corresponding to within session repeated recordings of the ANOW response range between 20% to 40% of their means at intensity levels above 40 dB nHL to 50 dB nHL and between 40% to 60% of the means at lower intensity levels in most participants. Overall, it might be concluded that the within session test retest reliability of the ANOW response improves with stimulus intensity for both TB stimuli.

Box plots of CV values corresponding to SNRs of within session repeated recordings of the ANOW show overall wider interquartile ranges for both stimuli and medians that decreases with stimulus intensity for the 500 Hz TB. Medians of CVs corresponding to 250 Hz TB show a decrease from 20 dB nHL to 50 dB nHL followed by an increase with intensity from 50 dB nHL to 80 dB nHL. Hence, it appears that the absolute amplitude measure of the ANOW shows better within session repeatability compared to the SNR measure.

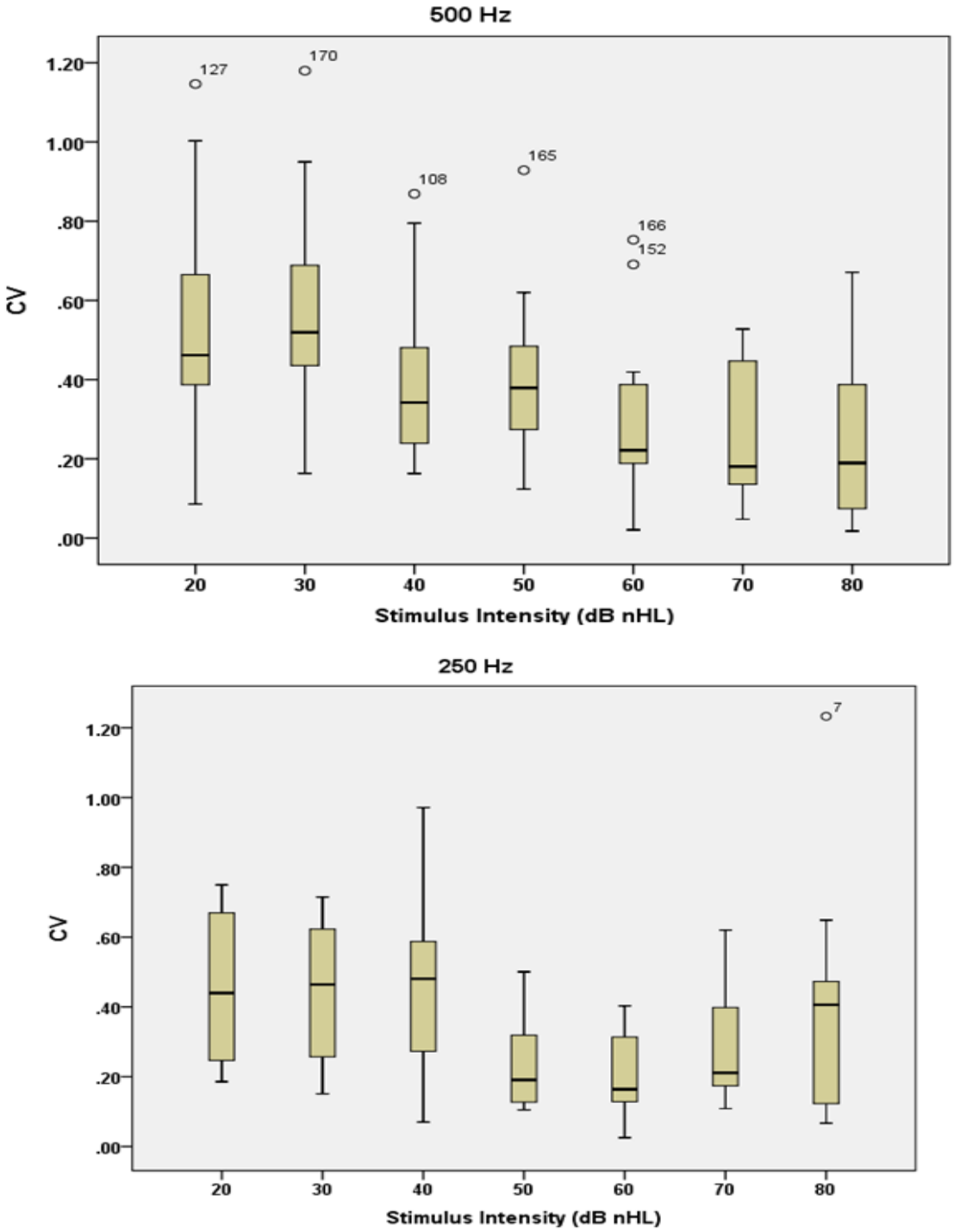

Figure 7: Box plots of CV values corresponding to absolute amplitudes of within session repeated recordings of the ANOW response across different stimulus intensity levels in dB nHL, for both 250 Hz and 500 Hz TB stimuli.

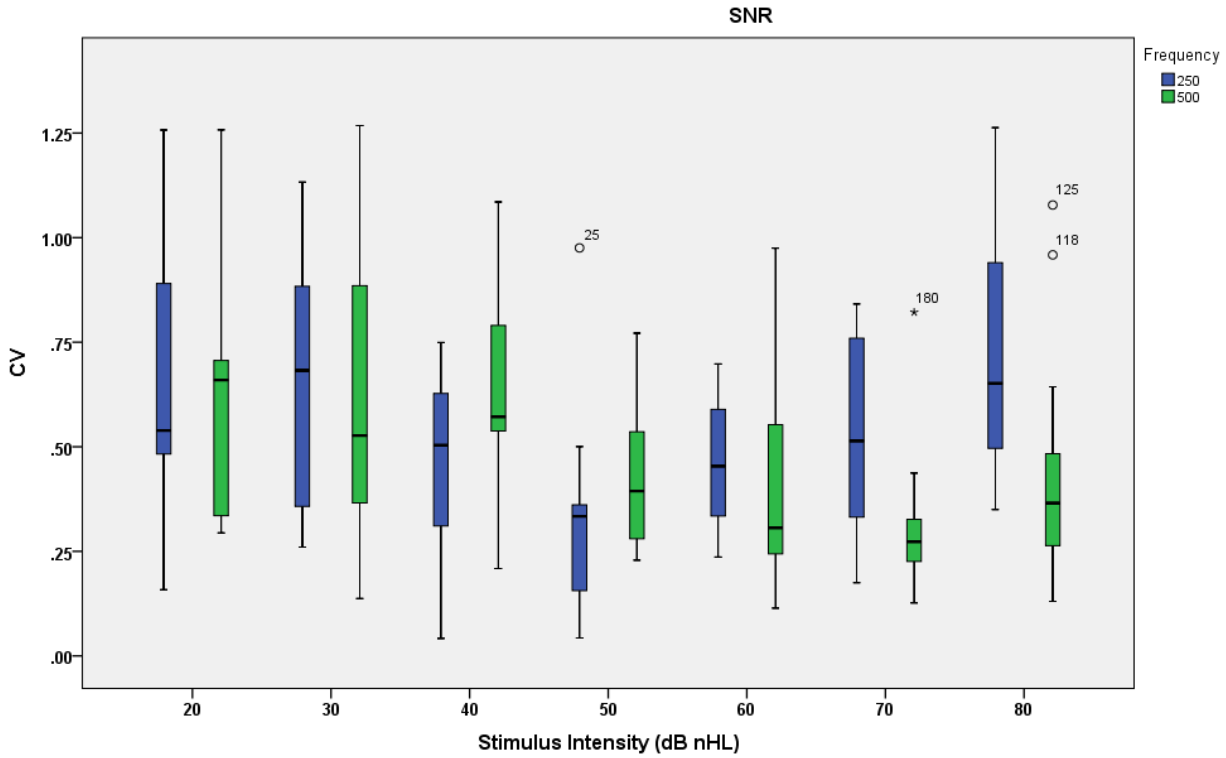

Figure 8: Box plots of CV values corresponding to SNRs of within session repeated recordings of the ANOW response across different stimulus intensity levels in dB nHL, for both 250 Hz and 500 Hz TB stimuli.

Phase Locking Value (PLV)

Data points of waveform responses (Absolute amplitudes in (μv^2) across time points) of the ANOW response and of a simulated TB signal that mimics the evoking TB stimulus but has double its frequency were used to compute the phase locking value (PLV) at each stimulus presentation level in dB nHL. No filtration was applied to either of the stimulus and the response. Overall, PLV values were below 0.7. In practice, the absolute PLV value is not usually of interest. Instead, we are interested in investigating whether an experimental condition induced a change in the PLV value; usually a comparison between PLVs pre and post stimulus presentation, for example Hanslmayr et al. (2007) and Melloni et al. (2007).

PLV values of the response and the evoking tone (response-tone PLV) were compared to PLV values of random noise (created using the MATLAB software) band-pass filtered from 100 to 3000 Hz and the same tone (noise-tone PLV). Figures (9-11) show probability density function distributions of noise-tone PLV plotted against the probability density function distributions of the response-tone PLV. It is clear in the figures that the mean of the response-tone PLV is higher than the noise-tone PLV mean, suggesting a phase locking (or synchronization) between the response and the tone higher than random chance at least for the 250 Hz TB stimulus. Probability density functions of noise-tone PLVs overlap with response-tone PLVs for both TB stimuli. However, 250 Hz TB curve comprised smaller overlap area with the noise curve compared to 500 Hz TB. The mean of the 250 Hz response-tone PLV probability density function is higher than three standard deviations of the mean noise, while the mean of the 500 Hz response-tone PLV probability density function is higher than two standard deviations of the mean noise. Probability density functions suggest stronger phase locking between 250 Hz TB and the ANOW response compared to 500 Hz TB. They also suggest mean response PLV higher than random chance, at least for 250 Hz TB.

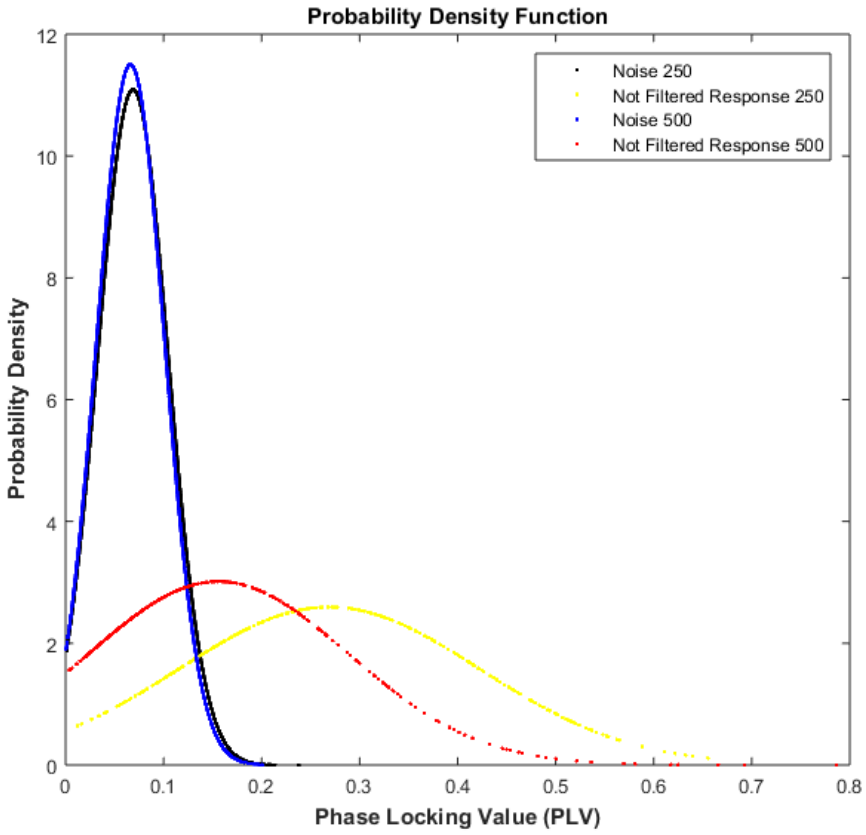

Figure 9: Probability density function of noise-tone PLV values and response-tone PLV values corresponding to 250 Hz and 500 Hz TB stimuli. Both noise and response are band pass filtered between 100 Hz and 3000 Hz. Blue curve: probability distribution of noise-tone PLV values for 500 Hz TB, Red curve: probability distribution of response-tone PLV values for 500 Hz TB, Black curve: probability distribution of noise-tone PLV values for 250 Hz TB, and Yellow curve: probability distribution of response-tone PLV values for 250 Hz TB.

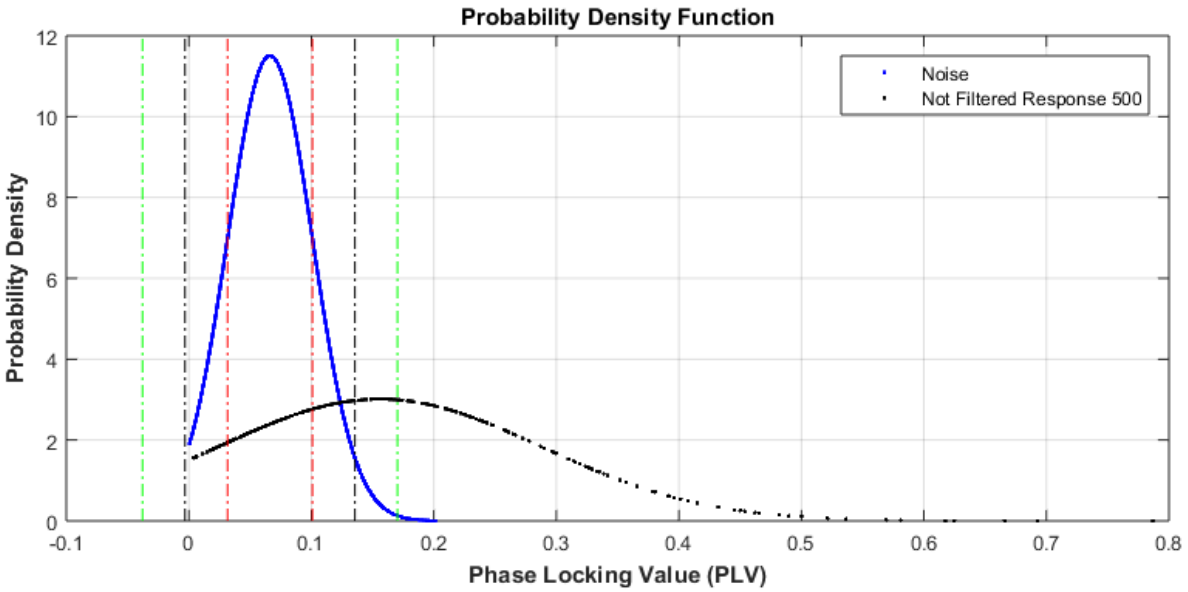

Figure 10: Probability density function of noise-tone PLV values and response-tone PLV values corresponding to 500 Hz TB stimulus. Both noise and response are band pass filtered between 100 Hz and 3000 Hz. Black curve: probability distribution of noise-tone PLV values for 500 Hz TB, and Yellow curve: probability distribution of response-tone PLV values for 500 Hz TB. Red dotted vertical lines: 1 SD limits around the mean noise, black dotted vertical lines: 2 SD limits around the mean noise, and green dotted vertical lines: 3 SD limits around the mean noise.

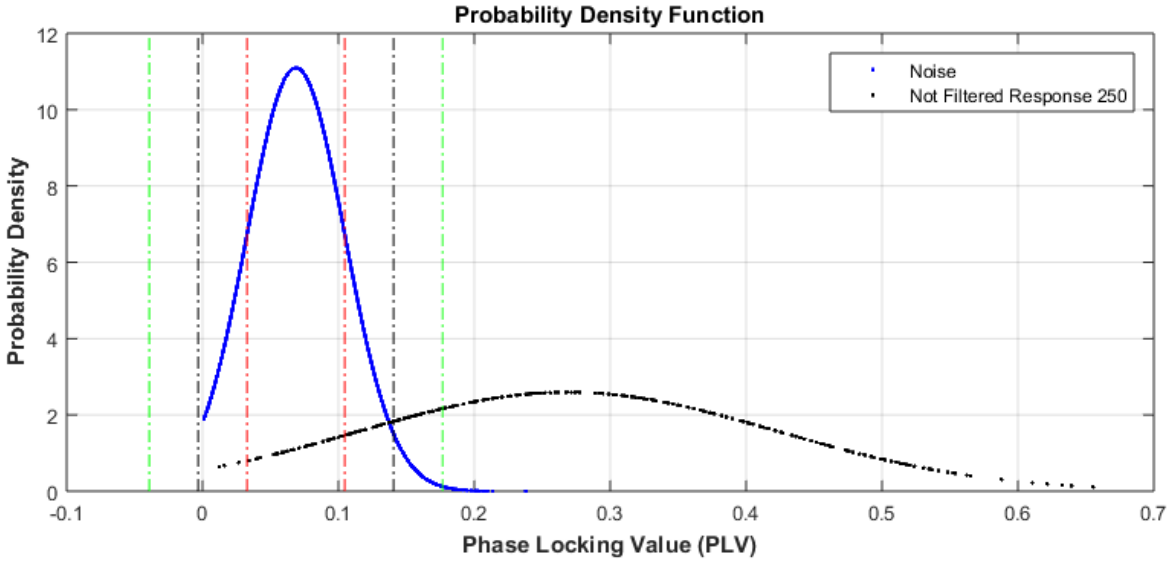

Figure 11: Probability density function of noise-tone PLV values and response-tone PLV values corresponding to 2500 Hz TB stimulus. Both noise and response are band pass filtered between 100 Hz and 3000 Hz. Black curve: probability distribution of noise-tone PLV values for 250 Hz TB, and Yellow curve: probability distribution of response-tone PLV values for 250 Hz TB. Red dotted vertical lines: 1 SD limits around the mean noise, black dotted vertical lines: 2 SD limits around the mean noise, and green dotted vertical lines: 3 SD limits around the mean noise.

ICC analysis using PLV

Intra-class correlation coefficient (ICC) was used to test the test-retest reliability of PLVs corresponding to the 3 repeated recordings of the ANOW at each stimulus presentation intensity, in the same session. Overall, fair to moderate degrees of test retest reliability were found between PLVs corresponding to the three repeated recordings of the ANOW response using both TB stimuli across most of intensity presentation levels in dB nHL, with ICC values fluctuating from around 0.4 to around 0.6 and significant statistical P value (<0.05), except for 40 dB nHL (86.82 p-SPL) using 250 Hz TB (ICC = 0.748, P<0.05, indicating high test retest reliability), 20 dB nHL (70.22 p-SPL) (ICC=0.022, P>0.05, indicating poor test retest reliability) using 500 Hz TB stimulus, 30 dB nHL (78.52 p-SPL) (ICC=0.86, P<0.05, indicating high test retest reliability) using 500 Hz TB stimulus, and 60 dB nHL (104.58 p-SPL) (ICC=0.73, P<0.05, indicating high test retest reliability) using 500 Hz TB stimulus (figure 12 and table 12).

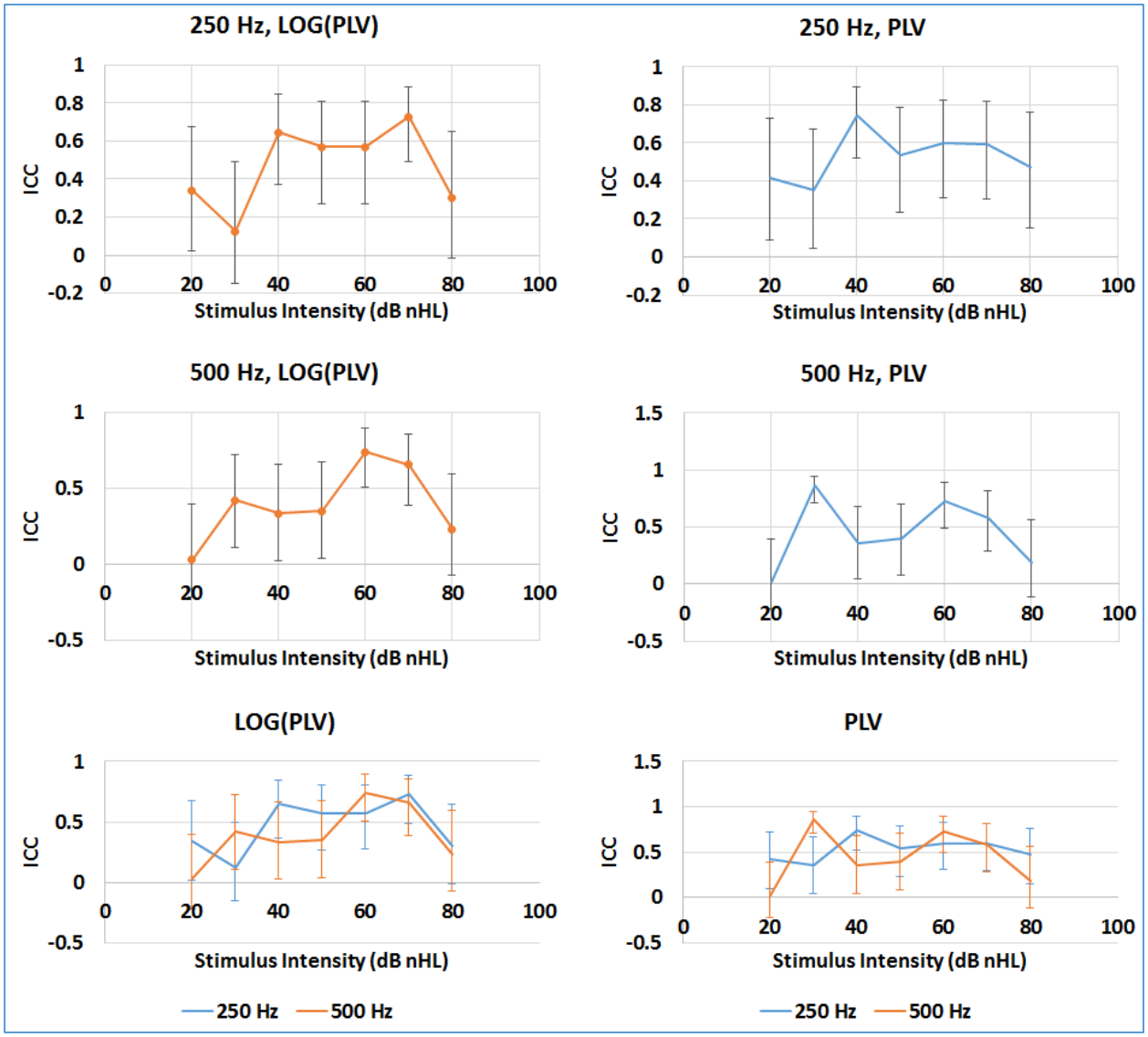

Figure 12: ICC values computed using PLVs and logarithms of PLVs across different stimulus intensities for both 250 Hz and 500 Hz TB stimuli. Error bars are 95% confidence intervals.

Overall, PLV ICC values show less dependence on the change in stimulus Intensity level than amplitude ICC values and SNR values. Amplitude ICC values are higher than both SNR and PLV ICC values across all stimulus intensities for 250 Hz TB and at levels higher than 30 dB nHL (78.52 p-SPL) for 500 Hz TB. PLV ICC value is statistically significantly higher than both amplitude and SNR ICCs at 30 dB nHL (78.52 p-SPL) for 500 Hz TB stimulus (evident in the non-overlapping 95% confidence intervals of PLV ICC and intervals of both amplitude and SNR

ICCs). This is not the case for 20 dB nHL (70.22 p-SPL). However, all three ICCs are low and not statistically significant at 20 dB nHL (70.22 p-SPL) ($P<0.05$) (figure 13).

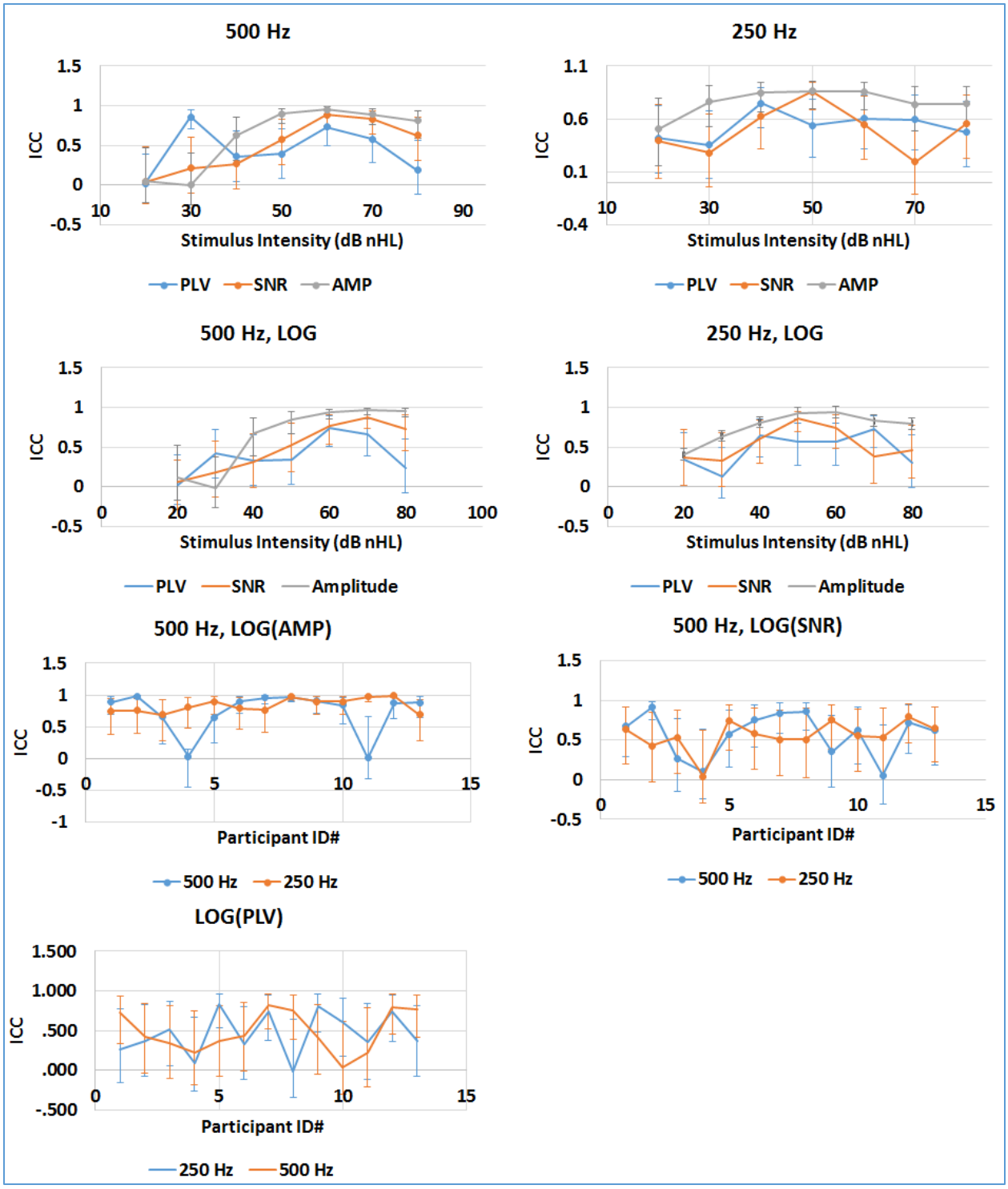

Figure 13: ICC values corresponding to within session repeated recordings of the ANOW response across stimulus intensity levels and across participants. Original and logarithmic scale of absolute amplitudes, SNRs, and PLVs were used to compute ICCs for both 250 Hz and 500 Hz TB stimuli.

Table 12: PLV ICC values across stimulus intensities for both 250 Hz and 500 Hz TB stimuli, with 95% confidence intervals, corresponding F value, statistical significance P value, and total number of participants included in the analysis.

	Stimulus Intensity		ICC	95% confidence Interval		F	N	p
	(dB nHL)	p-SPL		Lower Bound	Upper Bound			
250 Hz	20	71.07	0.417	0.092	0.727	3.145	13	0.005
	30	79.58	0.355	0.042	0.675	2.649	13	0.012
	40	86.82	0.748	0.519	0.897	9.898	13	0.000
	50	95.82	0.539	0.236	0.79	4.503	13	0.000
	60	105.82	0.602	0.313	0.825	5.538	13	0.000
	70	115.58	0.594	0.303	0.821	5.39	13	0.000
	80	122.84	0.474	0.152	0.761	3.705	13	0.002
500 Hz	20	70.22	0.022	-0.221	0.39	1.067	13	0.422
	30	78.52	0.86	0.708	0.945	19.37	13	0.000
	40	88.42	0.359	0.047	0.678	2.68	13	0.011
	50	95.42	0.394	0.081	0.702	2.953	13	0.006
	60	104.58	0.73	0.492	0.889	9.129	13	0.000
	70	113.36	0.581	0.287	0.814	5.161	13	0.000
	80	121.85	0.188	-0.11	0.561	1.694	13	0.118

CV analysis using PLV

CV values were computed using PLV values of within session repeated recordings of the ANOW response for both TB stimuli. Table (13) shows CV values computed of PLVs corresponding to within session repeated recordings of the ANOW response at each stimulus intensity, for each TB stimulus, and in each participant. Box plots of PLV CVs (figure 14) across stimulus intensity levels between 20 dB nHL to 70 dB nHL show a decrease of medians with stimulus intensity increase from around 0.5 to around 0.1 for the 250 Hz TB stimulus and from 0.5 to 0.3 for the 500 Hz TB stimulus. Overall interquartile ranges, third quartile percentiles, and maximum CV values show a

decrease with stimulus intensity for both TB stimuli. However, the trend is stronger for the 250 Hz TB compared to the 500 Hz TB, except at 80 dB nHL for the 250 Hz TB that shows a wide interquartile range and high maximum CV value. This may suggest that the within session test retest repeatability of the ANOW response improves with stimulus intensity for both stimuli with decreasing SD to mean ratios of PLV values corresponding to within session repeated recordings of the ANOW response at higher stimulus intensity levels.

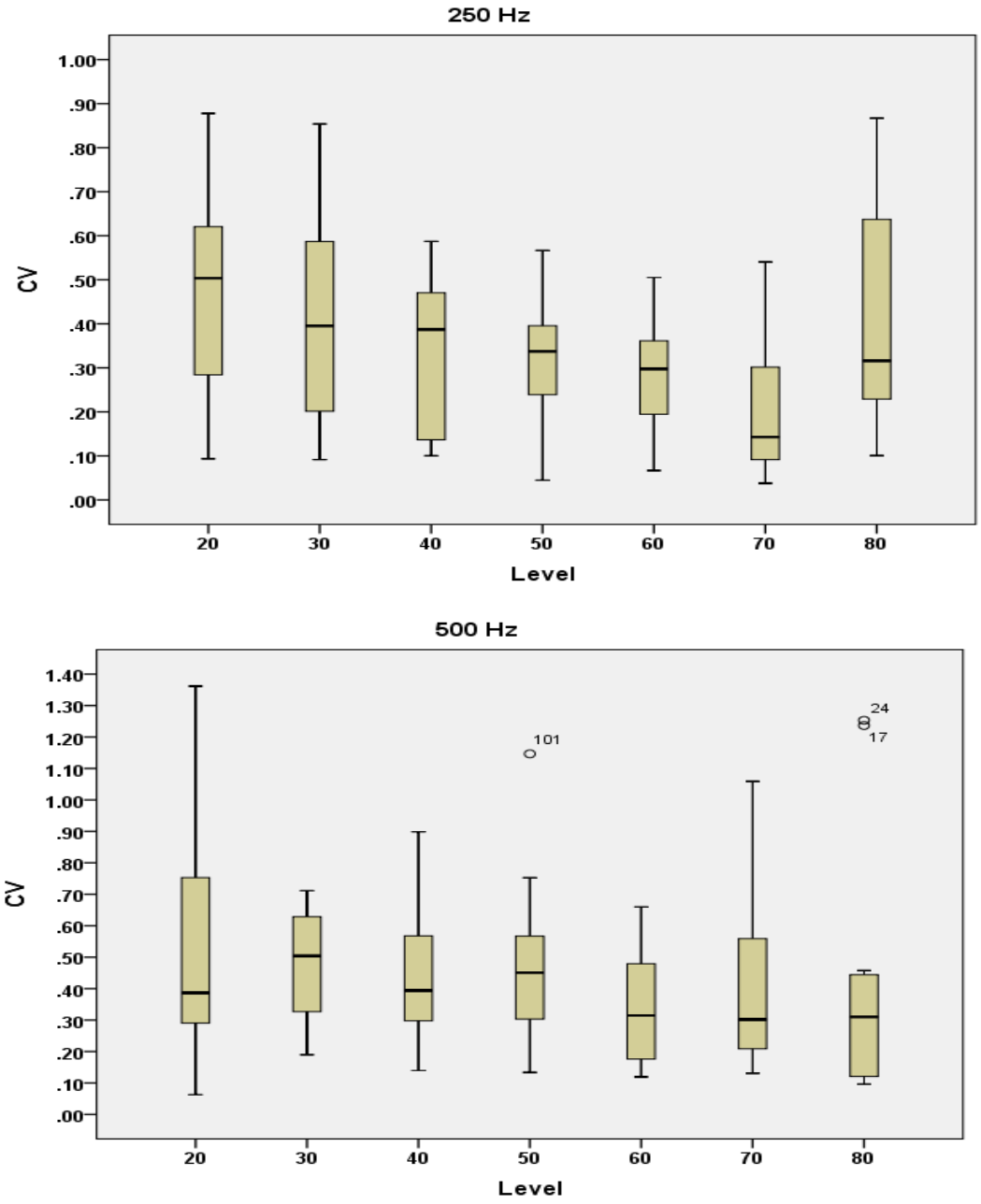

Figure 14: Box plots of CV values computed of PLVs corresponding to within session repeated recordings of the ANOW response. Box plots are plotted across different stimulus intensity levels.

Table 13: CV values computed of PLVs corresponding to within session repeated recordings of the ANOW response at each stimulus intensity, for each TB stimulus, and in each participant.

		Stimulus Intensity (dB nHL)						
Participant ID#	Frequency (Hz)	20	30	40	50	60	70	80
1	250	0.88	0.25	0.10	0.39	0.43	0.35	0.87
2	250	0.57	0.10	0.59	0.31	0.24	0.54	0.82
3	250	0.63	0.62	0.39	0.24	0.30	0.30	0.53
4	250	0.62	0.85	0.47	0.34	0.50	0.45	0.41
5	250	0.47	0.20	0.21	0.36	0.31	0.20	0.10
6	250	0.28	0.51	0.53	0.43	0.51	0.27	0.34
7	250	0.09	0.13	0.39	0.33	0.07	0.14	0.19
8	250	0.10	0.09	0.27	0.23	0.27	0.13	-
9	250	0.30	0.40	0.45	0.40	0.11	0.12	0.19
10	250	0.20	0.23	0.14	0.08	0.19	0.06	0.29
11	250	0.14	0.68	0.48	0.57	0.34	0.04	0.75
12	250	0.70	0.41	0.12	0.04	0.10	0.09	0.28
13	250	0.55	0.59	0.13	0.44	0.36	0.06	0.27
1	500	1.13	0.71	0.57	0.35	0.15	0.23	0.31
2	500	0.83	0.65	0.30	0.18	0.48	0.44	0.44
3	500	0.75	0.63	0.36	0.57	0.56	0.21	0.46
4	500	1.36	0.90	0.51	0.48	0.54	1.06	1.24
5	500	0.36	0.48	0.41	0.75	0.66	0.21	0.12
6	500	0.29	0.32	0.71	0.13	0.19	0.56	0.41
7	500	0.32	0.60	0.33	0.45	0.36	0.30	0.29
8	500	0.44	0.51	0.14	0.66	0.15	0.18	0.10
9	500	0.08	0.40	0.90	0.45	0.12	0.39	0.10
10	500	0.06	0.50	0.50	1.15	0.18	0.83	0.43
11	500	0.22	0.33	0.22	0.56	0.37	0.92	1.25
12	500	0.59	0.67	0.18	0.30	0.31	0.13	0.10
13	500	0.39	0.33	0.39	0.30	0.28	0.21	0.30

Between sessions analysis

Recordings of the ANOW response were repeated in a second session for two participants (participants 2 and 6). Appendix (F) show raw data of absolute amplitudes and SNRs corresponding to the two test sessions for both participants. Figures (15-17) show mean measures (amplitudes, SNR, and PLV) and 95% confidence intervals corresponding to the two test sessions for both participants and both 250 Hz and 500 Hz TB stimuli. Overall, both participants showed noticeable difference between absolute amplitudes corresponding to the two sessions for

both stimuli (figure 15). Participant 6 showed higher mean amplitude in session 2 compared to session 1 for both stimuli at intensity levels higher than 40 dB nHL, while participant 2 showed generally lower mean amplitude in session 2 compared to session 1 at stimulus levels above 40 dB nHL for the 500 Hz TB. The difference in ANOW's amplitude between the two sessions generally increases with stimulus intensity.

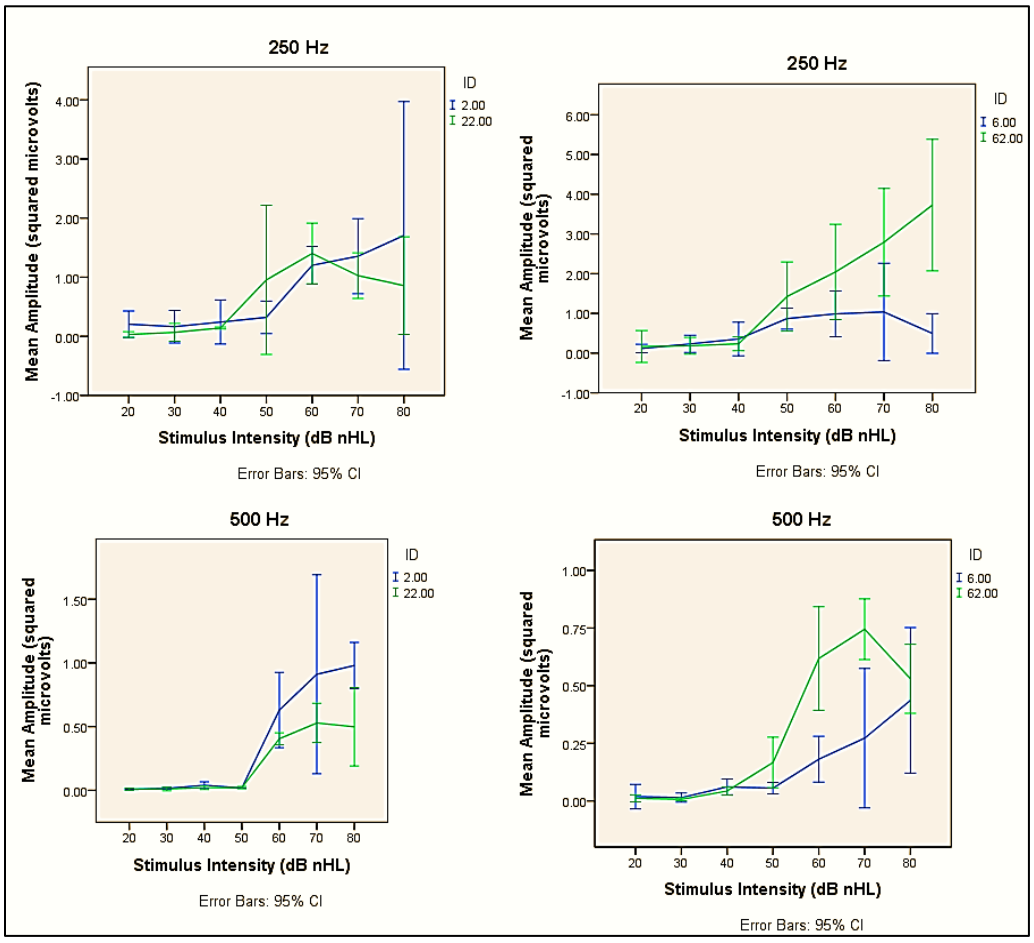

Figure 15: Between sessions mean absolute amplitudes across different stimulus intensity levels (dB nHL), for each participant and each stimulus frequency. 2: responses of participant 2 in session 1, 22: responses of participant 2 in session 2, 6: responses of participant 6 in session 1, and 62: responses of participant 6 in session 2.

The difference of between sessions mean SNR responses as well as mean PLV responses across stimulus intensity levels were smaller and more variant than that of between sessions' mean absolute amplitudes across same intensity levels. Figures (16-17) show curves of mean SNR responses and mean PLV response of the two sessions for each participant and each stimulus

frequency. The curves go close to each other and cross at multiple points suggesting less variability between the two sessions using SNRs and PLVs than amplitudes.

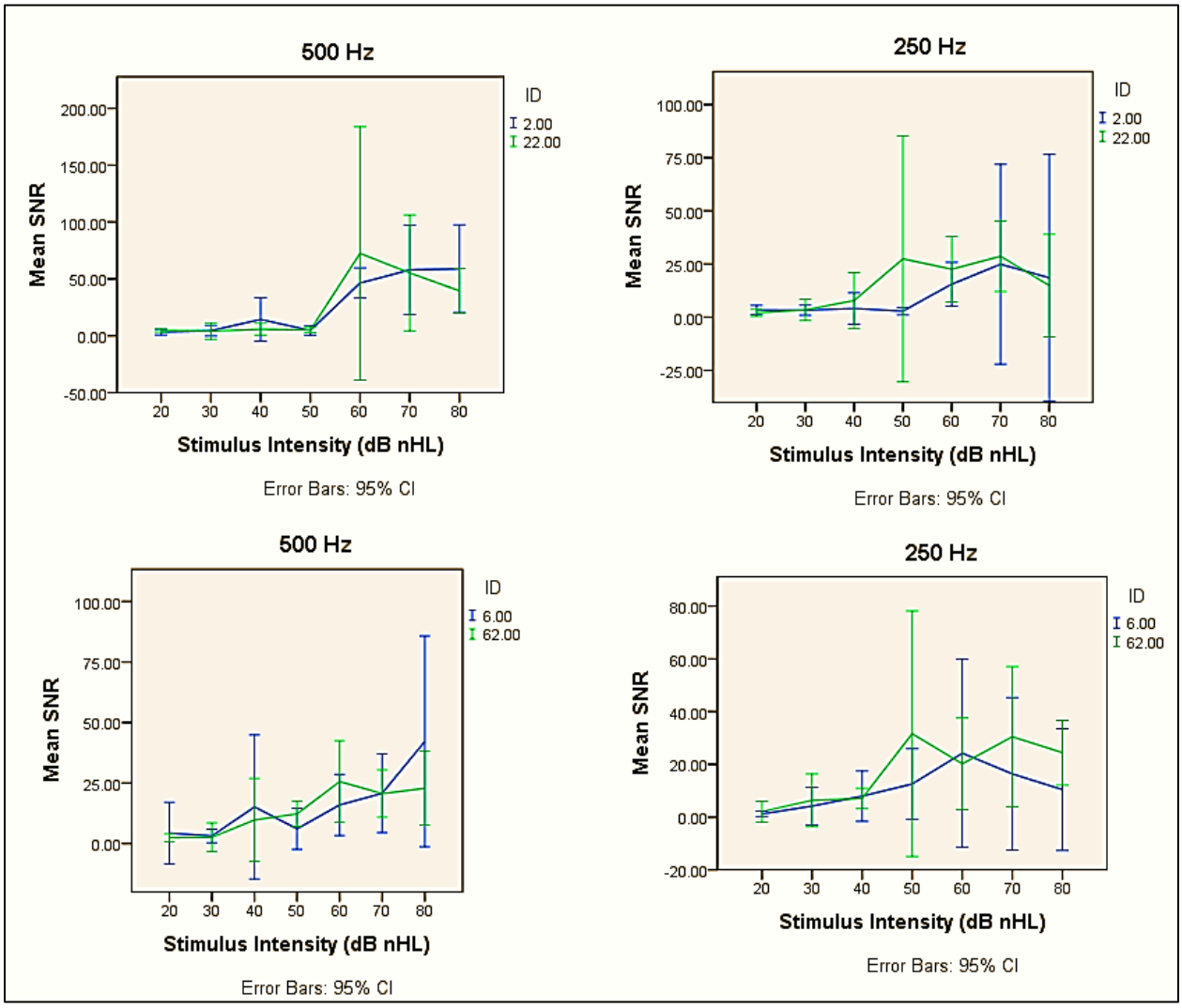

Figure 16: Between sessions mean SNRs across different stimulus intensity levels (dB nHL), for each participant and each stimulus frequency. 2: responses of participant 2 in session 1, 22: responses of participant 2 in session 2, 6: responses of participant 6 in session 1, and 62: responses of participant 6 in session 2.

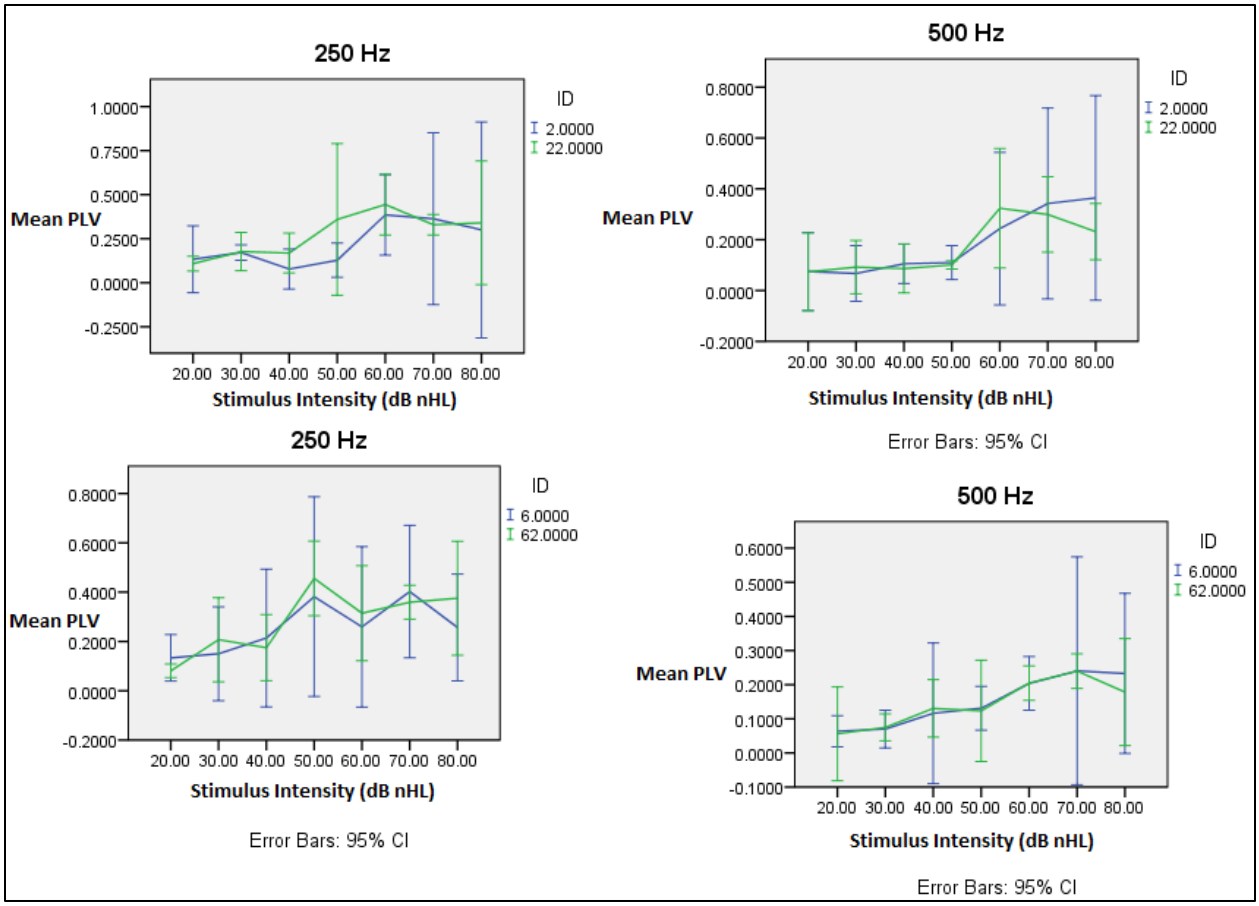

Figure 17: mean PLVs across different stimulus intensity levels of between sessions for participants 2 and 6. 2: responses of participant 2 in session 1, 22: responses of participant 2 in session 2, 6: responses of participant 6 in session 1, and 62: responses of participant 6 in session 2. Error bars are 95% confidence intervals.

Between sessions reliability analysis

CV values were also computed between inter-sessions repeated measures of the ANOW response at different stimulus intensity levels for 250 Hz and 500 Hz TB stimuli (figure 18). Repeated recordings of the ANOW response of the two sessions were combined for each stimulus frequency and in each participant (a total of 6 responses at each level). CV values were then computed by taking the ratio of the SD of the combined response to their mean. The result is a CV value at each stimulus intensity for each TB stimulus in each participant. CV values were computed using the three measurement parameters of the ANOW response (absolute amplitude,

SNR, and PLV of the ANOW response). Overall, PLV measure shows lowest CV values across different intensity levels for both TB stimuli in participant 6, ranging from 0.4 to 0.2 for the 250 Hz TB and from 0.6 to 0.4 for the 500 Hz TB. For participant 2, on the other hand, the absolute amplitude measure shows lowest CV values across different stimulus intensity levels, except at levels below 40 dB nHL for the 250 Hz TB where CV values corresponding to PLV measure were lower.

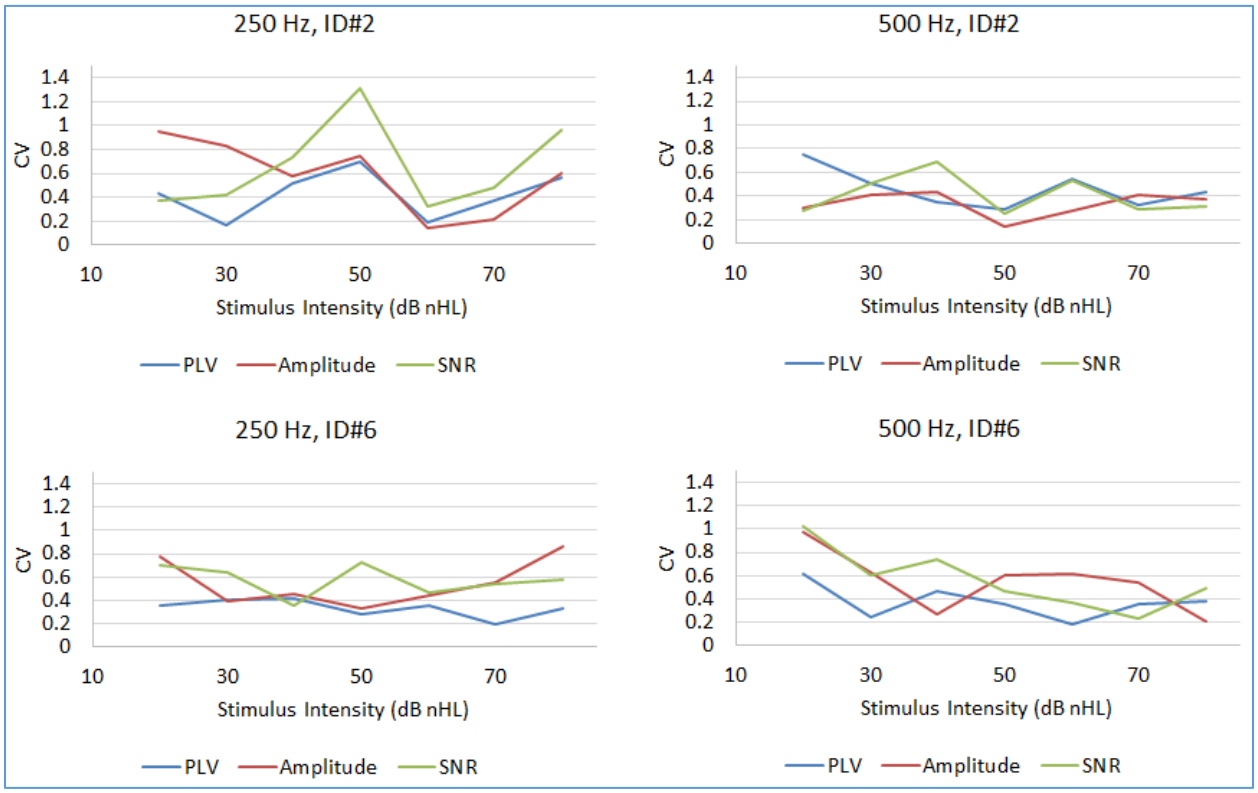

Figure 18: CV values corresponding to measurement parameters of between sessions' repeated recordings of the ANOW response for each TB stimulus and in each participant.

CHAPTER 4

DISCUSSION

Effect of stimulus intensity on the ANOW response

This study examines the effects of the stimulus intensity level on the measurement parameters of the ANOW response. Our results show that the three ANOW measurement parameters (absolute amplitude, SNR, and PLV) increase with stimulus intensity for both 250 Hz and 500 Hz TB stimuli. Both absolute amplitude and PLV of the response show higher rates of increase for the 250 Hz TB compared to the 500 Hz TB. This finding is evident in the slopes of regression lines presented in figure (4). The SNR, on the other hand, shows similar rate of change with stimulus intensity for both TB stimuli. This result is evident in similar slopes of regression lines for both TBs. The difference in slopes of regression between the two TB stimuli is determined by the significance of the interaction effect between stimulus intensity and stimulus frequency. P value of the interaction effect between stimulus level and stimulus intensity for the SNR is slightly higher than 0.05 (P=0.07). Hence, there is a chance that a significant interaction effect between stimulus intensity and stimulus frequency is present but was not detected by our fitted model.

Our results also suggest that a statistically significant difference may be present between means of absolute amplitudes of higher stimulus intensity range and lower stimulus intensity range, at least for the 250 Hz TB. Moreover, PLV corresponding to 250 Hz TB are significantly higher than PLV values corresponding to 500 Hz TB, at least at higher stimulus intensity levels,(as evident in the significant difference between y-axis intercepts of two regression lines corresponding to 250 Hz and 500 Hz TBs (figure 4)). Hence, it might be concluded that stronger phase locking and larger absolute amplitude of the ANOW are corresponding to 250 Hz TB and higher stimulus intensity levels.

One aim of this study is to establish normative data for the ANOW response recorded non-invasively from normal hearing participants. Mean hearing thresholds as well as detection percentages of the ANOW using the two test stimuli presented at multiple intensity levels are displayed in tables (2-4). Detection percentages were also computed based on the same significance criteria used for hearing thresholds. Table (4) summarizes these values. Overall, High detection percentages (>90%) are detected at stimulus intensities above 90 p-SPL for both stimuli, when 1 SD significance criteria is applied. Applying the 3 SD significance criteria, detection percentages were lower 90% across all stimulus intensity levels. In general, as the stimulus intensity decreases detection percentages decrease.

Phase locking

Phase locking value (PLV) represents the trial to trial phase variability (or relative phases) between the two signals. Small variability of differences across trials produces a PLV close to 1 (perfect synchronization between signals), whereas high variability of phase differences produce PLVs close to zero (no synchronization). In practice, the absolute PLV value is not usually of interest. Instead, we are interested in investigating whether an experimental condition induced a change in the PLV value; usually a comparison between PLVs pre and post stimulus presentation, for example Hanslmayr et al. (2007) and Melloni et al. (2007).

PLV was computed between the time series of responses related to each run and a simulated TB stimulus that mimics the evoking stimulus but has double its frequency. No offline filtration was applied to responses. However, responses are already online filtered between 100 Hz and 3000 Hz. This is different from Aydore et al. (2013) work in that we are measuring the synchrony between a single frequency signal and a narrow band signal as opposed to using two EEG narrow band signals filtered to same frequency range of interest. However, filtering the response to have

a frequency content similar to that of the response could result in a false perfect synchrony because we simply could be creating another single frequency signal similar to our stimulus. PLV values show an increase with the stimulus intensity. ANOW response recorded to 250 Hz TB showed stronger phase locking to stimulus compared to ANOW response recorded to 500 Hz TB.

PLV was also computed between the simulated TB stimuli and random noise signals created using the MATLAB software (noise-TB PLV). The noise was band-passed filtered from 100 to 3000 Hz, to allow fair comparison between noise-TB PLVs and response-TB PLVs (remember that responses were online filtered between 100 Hz and 3000 Hz). Two probability density functions of noise-TB PLVs were created for the two TB stimuli. Similar probability density functions were also created of response-TB PLVs. Noise and response PLV probability distributions were then plotted against each other and compared for each TB stimulus (figures 9-11). Means of probability density functions of response-TB PLVs are higher than 3 SD and 2 SD from the mean of the probability density function of noise –TB PLVs for 250 Hz TB and 500 Hz TB, respectively. Hence, it might be concluded that response PLVs are higher than random chance, at least for 250 Hz TB.

Reliability of the ANOW response

Within session reliability

This study investigated the within session test retest reliability of the ANOW response. Three repeated recordings were obtained from 13 participants using two low frequency TB stimuli (250 Hz and 500 Hz) presented at 7 intensity levels within the same session. Two statistical test measures (ICC and CV), three dependent variables (absolute amplitude of the ANOW response

(in μv^2), signal-to-noise ratio (SNR), and phase locking value (PLV)), and two experimental designs (within participants' and between participants' designs) were used to test the within session test retest reliability of the response (see analysis section for more details about the designs).

Between participants' design

Amplitude ICC values showed high degrees of test retest reliability (≥0.7) across all participants, except participants 1 and 11, for both TB stimuli. Participants 1 and 11 showed fair and poor test retest reliability for the 500 Hz TB stimulus, respectively. SNR and PLV ICC values, on the other hand, suggest lower test retest reliability across all participants for both 250 Hz and 500 Hz TB stimuli, with wider 95% confidence intervals, compared to amplitude ICC values. Using the logarithmic scale of data did not largely affect amplitude ICC values for most participants. I.e., the same conclusions about test retest reliability maybe drawn for most participants, using both logarithmic scale of data and using original data with no transformation. Using the logarithmic transformation of the SNR slightly improved the test retest reliability for most participants. However, same overall conclusions maybe drawn about the between participants test retest reliability of the ANOW response. PLV ICCs, on the other hand, were affected by the logarithmic transformation of data. An overall improvement (increase) in ICC values was evident with the transformation of data, indicating less variability and higher within session test retest repeatability of transformed PLVs.

Effect of stimulus intensity on test retest reliability

Within participants' design

Amplitude ICC values show dependence on the stimulus intensity level and indicate moderate to high degrees of test retest reliability of the ANOW response for the 250 Hz, and poor improving to high test retest reliability of the ANOW response as moving from 20 dB nHL to 80 dB nHL (70.22 p-SPL to 121.85 p-SPL) for the 500 Hz TB stimulus. 250 Hz TB stimulus comprises higher degrees of test retest reliability of the ANOW response than the 500 Hz TB stimulus at intensity levels below 40 dB nHL (around 87 p-SPL). However, as the intensity level increases above 40 dB nHL (around 87 p-SPL) both stimuli comprise amplitude ICC values >0.7, indicating high test retest reliability.

SNR ICCs indicate fair to moderate test retest reliability of the ANOW response for 250 Hz TB stimulus, poor to fair reliability at stimulus intensities below 50 dB nHL (95.42) for 500 Hz TB stimulus, and moderate to high reliability at stimulus intensities above 50 dB nHL for the 500 Hz TB.

Intra-class correlation coefficient (ICC) was also used to test the within session test-retest reliability of PLVs corresponding to the 3 repeated recordings of the ANOW at each stimulus presentation intensity. Fair to moderate degrees of test retest reliability were found between PLVs corresponding to the three repeated recordings of the ANOW response using 250 Hz TB. PLV ICC for 500 Hz TB stimulus fluctuates between fair, moderate, and high test retest reliability levels across the different stimulus intensities with no pattern of increase or decrease with stimulus intensity.

Overall, absolute amplitude of the ANOW response showed overall highest within session test retest reliability across all stimulus intensity levels for the 250 Hz TB stimulus and across levels higher than 30 dB nHL (78.52 p-SPL) for the 500 Hz TB stimulus. PLV ICC values are less dependent on the stimulus Intensity level compared to amplitude ICC values and SNR ICC

values. All three ICC measures are low and not statistically significant at 20 dB nHL and 30 dB nHL (at and below 78.52 p-SPL) for the 500 Hz TB (figure 13).

Based on ICC results, the absolute amplitude of the ANOW response comprises the highest within session test retest reliability degrees across different presentation levels, over SNR and PLV measures. However, reliability of ANOW's absolute amplitude is level dependent and is low at low stimulus intensity levels indicating more variability of the amplitude at low intensity levels compared to higher intensity levels. The three measures of ANOW (amplitude, SNR, and PLV) comprise poor test retest reliability at low intensity levels (below 40 dB nHL (88.42 p-SPL)) for the 500 Hz TB stimulus. For the 250 Hz, the test retest reliability for low stimulus intensity levels was fair to moderate using the absolute amplitude measure and fair using both SNR and PLV. Hence, it might be concluded that the ANOW response recorded to 250 Hz TB stimulus comprises higher test retest reliability at intensity levels below 50 dB nHL (around 95 p-SPL) compared to 500 Hz TB. However, at levels above 50 dB nHL (around 95 p-SPL), the test retest reliability of the ANOW is high (>0.8) and the 95% confidence intervals are narrower for both stimuli.

Coefficient of variation (CV) of the three repeated recordings of ANOW's absolute amplitudes, SNRs, and PLVs were computed at each stimulus intensity for each TB stimulus in each participant. Our results indicate that the within session test retest reliability of ANOW's absolute amplitude and PLV improves with stimulus intensity for both TB stimuli. Moreover, both the absolute amplitude and the PLV measures of the ANOW response show better within session repeatability compared to the SNR measure. This could be due to the fact that the SNR is subjected to the variability of the background noise as well as the variability of the amplitude, since it represents the ratio of the amplitude to the noise. Another reason could be the way

background noise was estimated, from only the bins surrounding the response bin in the power spectrum. This is not the most accurate way of estimating noise and may have added more variability to the noise. Estimating background noise before presenting the acoustic stimulus in each participant, then normalizing the amplitude by noise may have revealed less variability in the SNR values.

Between sessions test retest reliability

Recordings of the ANOW response were repeated in a second session for two participants (participants 2 and 6). Both participants showed noticeable difference between absolute amplitudes corresponding to the two sessions at each stimulus (figure 15-17). Amplitude measures show the highest variability between amplitude means corresponding to the two sessions amongst all three measures of the ANOW response.

Repeated recordings of the ANOW response of the two sessions were combined for each stimulus frequency and in each participant (a total of 6 responses at each level). CV values were then computed by taking the ratio of the SD of the combined response to their mean (for the three measurements of the ANOW). Overall, PLV measure shows lowest CV values across different intensity levels for both TB stimuli in participant 6, ranging from 0.4 to 0.2 for the 250 Hz TB and from 0.6 to 0.4 for the 500 Hz TB. For participant 2, on the other hand, the absolute amplitude measure shows lowest CV values across different stimulus intensity levels, except at levels below 40 dB nHL for the 250 Hz TB where CV values corresponding to PLV measure were lower. Overall, our results suggested that both amplitude and PLV measures are more reliable than the SNR measure. Moreover, reliability of the PLV measure is less dependent on stimulus level compared to the reliability of the amplitude measure. However, it is hard to draw

any conclusions about the between sessions reliability of the ANOW response based on results of only two participants.

A question of this research is about which measure more reliably predicts the ANOW response. To answer this question we need to look at both between sessions and within session reliabilities of the three measures (absolute amplitudes, SNRs, and PLVs). Absolute amplitude measures showed highest degrees of within-session test retest reliability between the three. However, the reliability of the absolute amplitude measures of the ANOW response depends on the stimulus intensity and is less reliable at low stimulus intensity levels. SNR and PLV measures comprised similar and at times higher reliability than the amplitude measure at low intensity levels.

Developing a technique that would more accurately measure phase synchronization between ANOW response and stimulus than the technique used in this study may reveal a more reliable measure of the ANOW response.

CLINICAL APPLICATIONS

Being able to record the sustained neural response has the potential to have many clinical applications, such as accurately assessing the perception of sustained speech sounds (vowels) in infants and customizing the hearing aid fitting accordingly. Also, these measures have potential uses in differentiating between peripheral/central auditory processing dysfunction and in more accurately assessing low frequency hearing thresholds.

LIMITATIONS AND FUTURE RESEARCH

Stimulus intensity levels higher than 65 dB SPL were used to record the ANOW response in this research project. According to Lichtenhan et al. (2014), only responses recorded at stimulus intensity levels below 65 dB SPL are purely neural. However, Lichtenhan's findings apply to invasive recordings of the ANOW response from the round window in Guinea pigs and may not necessarily apply to noninvasive recordings of the ANOW in humans.
Further research is needed to investigate the neural origin of the ANOW response. I.e., to investigate if the ANOW response is originating from nerve fibers with low characteristic frequencies as opposed to originating from low frequency tails of nerve fibers with high characteristic frequency or from the distortion in the cochlear microphonic (CM), as Lichtenhan et al. (2014) suggested. Masking techniques, such as forward masking or simultaneous masking of high frequency regions of the cochlea, maybe used to investigate the origin of the ANOW response.

PLV was computed between response and simulated tone burst stimulus that mimics the original stimulus used in the experiment but has double its frequency. Using simulation and manipulating the frequency of the original stimulus may have affected the results by adding a bias. Using the original stimulus (maybe by capturing the original stimulus using an oscilloscope) as well as computing the phase locking between the response and the stimulus using a more complex measure (for example by using higher order spectrums to compute Bi-phase locking (Darvas et al., 2009)) that could capture phase synchrony between signals of completely different frequency ranges is more accurate.

Measuring the mean background noise from the spectrum magnitude of the bins surrounding the bin of the ANOW response, in the power spectrum of the response, is not the most accurate way of measuring background biological noise. An alternative way is to estimate background noise from a test run with no stimulus presented (using the same test setting used for recording ANOW) in each participant before recording ANOW.

Finally the N of this study is relatively small given the complexity of the design. Expanding this approach to include more participants may lead to more significant results.

CONCLUSIONS

Our results showed that the ANOW response is recordable noninvasively using ECochG at the low frequency TB stimuli and is traced down to 75 to 80 p-SPL. High detection percentages of the ANOW response were achieved at high stimulus intensity levels (>90 peak SPL). Moreover, detection percentages of the ANOW response increase with stimulus intensity level. Higher absolute amplitudes and phase locking to the stimulus were revealed for 250 Hz TB stimulus and for high stimulus intensity range compared to 500 Hz TB stimulus and lower stimulus intensity levels range. Overall, high within session test retest reliability of the ANOW response were found at stimulus intensity levels higher than 90 peak SPL for both 250 Hz and 500 Hz tone burst stimuli. However, lower within session test retest reliability of the ANOW response were revealed at low stimulus intensity levels. Moreover, 500 Hz TB showed lower within session test retest reliability of the ANOW response at low stimulus intensity levels compared to 250 Hz TB stimulus. Based on all above it might be concluded that the ANOW response is more robust at lower frequency ranges of stimuli.

The within session test retest reliability of the amplitude measure of the ANOW response was the highest amongst the three measures, especially at high stimulus intensity levels. Developing a technique that would more accurately measure phase synchronization between ANOW response and stimulus as well as recruiting more participants may reveal a new more reliable measure of the ANOW response.

CHAPTER 5

REVIEW OF LITERATURE

Physiology

Human's ears transform acoustic vibrations of sound into mechanical vibrations which are then transduced into neural impulses, which are sent to and perceived by the brain. Information about the acoustic stimulus, such as the frequency and the intensity (level), are coded through neural discharges (through both the rate and the timing of neural discharges) (Johnson, 1980).

The timing of individual neural spikes can be as precise as few milliseconds or even less and varies between neurons and stimuli (Johnson, 1980). Wever et al. (1930) studied the timing of individual auditory nerve discharges in response to acoustic stimuli. They showed that peripheral auditory nerve fibers are phase locked to the stimulus, i.e., they fire in synchrony with certain phase of the acoustic stimulus. No single auditory nerve fiber is expected to fire to every single acoustic stimulus cycle, but it is the combined activity of a group of nerve fibers that encode the temporal information about the waveform through a volley of spikes. In other words, the frequency of the acoustic stimulus is encoded through the firing frequency of a group of nerve fibers, and no single nerve fiber firing at a rate equal to the frequency of the acoustic stimulus (Wever & Bray, 1930). Auditory nerve fibers show low pass characteristics of phase locking that have an upper limit of 4 to 5 KHz (R. Snyder et al., 1984). Rose et al. (1967) showed that phase locking is slowly and progressively distorted above 2500 Hz and is generally demonstrable up to 4 to 5 KHz. They also showed that peripheral auditory nerve fibers code low frequency information by discharging at intervals that are equal to the period, which is the time taken for one acoustic cycle of the stimulus to occur, or the integral multiple of the period of the

acoustic stimulus. Hence, it is not the refractory period of nerve fibers, the amount of time it takes for the excitable neuron to return back to its resting state and get ready for the next acoustic stimulus, which governs the spacing of discharges. However, the refractory period prevents the occurrence of intervals shorter than 700 to 800 microseconds.

Previous research have also shown that when both the frequency and the period of the tone are held constant, the probability of firing (within the dynamic range of the nerve fiber) change monotically as the intensity of the stimulus change. Different auditory nerve fibers have different thresholds and spontaneous rates of firing. The higher the spontaneous rate of firing, of the fiber, the lower it's threshold (i.e., the lower the input intensity needed to depolarize the fiber and start an action potential). Hence, for the same input duration and frequency, the higher the input intensity the larger number of auditory nerve fibers which fire over their spontaneous rate enough to depolarize. At moderate intensity levels of low frequency acoustic input, large population of fibers will encode input frequency in three ways: a group of fibers will transmit appropriate frequency information at a maximal rate, another group transmits same frequency information at lower rate, and a third group will transmit same frequency information at a threshold rate (minimal rate) (Rose et al., 1967).

Overview of auditory evoked potentials

Auditory evoked potentials (AEPs) can be defined as the electrophysiological activity in response to auditory stimuli. They arise from one or more sources within the peripheral or the central auditory nervous system. When measured from certain sites on the scalp, on the ear, or within the ear, AEPs appear as a waveform with positive and negative voltage deflections at successive time points after presenting auditory stimuli. The amplitude and/or timing of these peaks (or deflections) may be of interest to clinicians. AEPs can also be viewed in the frequency

domain; this is particularly when AEPs are phase locked to a repetitive pattern of stimuli (Du et al., 2011; Moller, 1992; Naatanen, 2001).

One very important issue to consider when measuring AEPs from the surface is the contaminating EEG. EEG response is the spontaneous neurophysiologic activity which is present all the time with or without any direct external stimulation. When compared to EEG activity, AEPs have amplitudes that are several times smaller. Hence, it is important to perform signal averaging, which is made possible by digital signal processing, to extract AEP small voltages from the ongoing EEG. Signal averaging sums responses to the repeatedly presented acoustic stimuli, then amplifies, filters, and converts the summed responses from analog to digital signals, and finally stores them in a computer. This whole process results in the inhibition of the random EEG activity and the amplification of AEP responses. The computer then converts the response back into analog signal and displays it as a waveform with positive and negative voltage deflections at successive time points after the onset of the auditory stimulus. The amplitude and/or timing of these peaks (or deflections) are of interest to clinicians when interpreting responses. AEPs can also be viewed in the frequency domain (mainly when AEPs are phase locked to a repetitive pattern of stimuli) (Du et al., 2011; Moller, 1992; Naatanen, 2001).

Another contaminating activity is the large amplitude myogenic (muscle) responses that can occur with and without any direct external stimulation. Common forms of unwanted myogenic responses are eye blinking, neck tension, and jaw clenching. However, myogenic responses can be reduced or eliminated by instructing the patient and/or by the proper placement of electrodes. Additional source of contamination is the 60 Hz (50 Hz in some countries) electromagnetic signal that comes from the electric outlets in the walls or from the light sources in the room. The contaminating signal can be picked up in the AEP recordings. However, the use

of notch filtering together with the good shielding against electromagnetic contamination can help eliminate such noise (Moller, 1992).

Classifications of auditory evoked potentials

AEPs can be classified according to their latencies, their anatomical origins, or their relation to the stimulus. However, the most popular classification is by latency and includes short latency potentials (<15 ms), middle latency potentials (15-80 ms), and long (or late) latency potentials (>80 ms). AEPs can also be classified as being exogenous, endogenous, or both endogenous and exogenous; exogenous potentials are sensory evoked potentials that are largely elicited and affected by the physical properties of the stimulus such as stimulus intensity, rise time, duration and frequency. They generally include all of the AEPs up to long latency potentials. Endogenous potentials, on the other hand, depend largely on the contextual features of the stimulus rather than its physical properties. They typically have very long latencies and are elicited by demanding psychological processes (such as memory and attention) to a deviant or rare event in a sequence of repetitive events. Hence, endogenous potentials are often called event-related potentials. Moreover, endogenous potentials are affected by higher cognition; a good example is the amplitude of the P300 potential, an endogenous potential, which can be made larger or smaller by simply attending or not attending to the stimulus, respectively. In general, the longer the latency of the AEP the more likely it will have endogenous features (Niedermeyer et al., 2005).

AEPs can also be classified as transient or steady state potentials. Transient potentials occur at the onset of the stimulus and have no one-to-one relation with the waveform of the stimulus; such as the compound action potential (CAP) component of the electrocochleography (ECochG), the ABR, the middle latency responses, the cortical P1/N1/P2 complexes, and the

cognitive P300. Steady state potentials, on the other hand, are elicited by repetitive or continuous stimulation where the response either follows the waveform of the stimulus or maintains a constant shift in voltage throughout the duration of the stimulus. Typical examples of the steady state responses are the summating potential (SP) of the electrocochleography (ECochG), the frequency following response (FFR) originating primarily from the brainstem, and the auditory steady-state response (ASSR) originating from multiple but segregated areas of the central auditory system. The cochlear microphonic (CM) component of the ECochG can be considered a steady state potential when measured from an area near to the cochlea (Niedermeyer et al., 2005).

Basic neural anatomy and physiology

In the cochlea, sensory cells that give rise to neuroelectric potentials are inner and outer hair cells. The outer hair cells are responsible for intensifying the basilar membrane movement through the electromotility, which sharpens auditory tuning curves. If the basilar membrane movement in response to sound is intense enough, the inner hair cells will release neurotransmitters to the auditory nerve fibers (Naatanen, 2001).

Similar to neurons, the movement of the charged ions in and out of both the inner and the outer hair calls is essential for them to function. AEPs which are elicited by the hair cells are the cochlear microphonics (CMs) and the summating potential (SP). The CM, which is a summed response of a large number of outer hair cells in the basal region, follows the waveform of the stimulus. SP, on the other hand, is the summed response of both outer and inner hair cells in the basal region with neural contribution. It reflects a constant voltage shift caused by the basilar membrane not moving equally in both directions. Both of CM and SP can be seen in ECochG recording. A third component of the ECochG, the compound action potential, represents the

summed synchronous activity of numerous auditory nerve fibers in response to abrupt acoustic stimuli. However, action potentials cannot be measured for AEPs generated at higher levels of the auditory system. Instead, AEPs at higher levels of the auditory system arise from the slow graded post-synaptic potentials, which is a synchronized extracellular activity of neuron groupings with slower membrane potential changes of 10-20 ms range and longer decay time compared to action potentials. At the cortical level of the auditory system, post-synaptic potentials are the dominant source of AEPs, which arise from the pyramidal neurons that are mostly located in layer V of the auditory cortex and interact with several other neurons (e.g., thalamocortical neurons and stellate cells) (Atcherson et al., 2012; Niedermeyer et al., 2005).

Electrocochleography (ECochG)

Electrocochleography (ECochG) is "the recording of stimulus-related potentials generated in the human cochlea, including the first-order neurons forming the auditory nerve" (Moeller, 2000). Three ECochG components are of interest to clinicians. The first component is the cochlear microphonic (CM), which is an alternating current (AC) voltage that is dominated by outer hair cells. The CM response mirrors the waveform of the acoustic stimulus at low-to-moderate stimulus levels. The second component is the summating potential (SP), which is a direct current (DC) voltage that originates from the hair cells in the cochlea. The third component is the compound action potential (CAP), which is the summed response of the synchronously firing nerve fibers in response to the onset of the acoustic stimulus (Moeller, 2000).

Clinical applications of ECochG include the diagnosis, assessment, and monitoring of Meniere's disease, Auditory Neuropathy Disorder, and tumors of the hearing nerve.

ECochG may be measured noninvasively from the skin of the ear canal or the lateral surface of the tympanic membrane (TM) (i.e., the ear drum). The process of measurement involves the use of specialized electrodes, which are approved by the FDA, made in contact with the skin surface of the ear canal or the lateral surface of the TM. It is a painless and harmless method which has been used in audiology clinics for over 25 years.

Auditory Nerve Neurophonic (ANN) Response

Auditory neurophonic responses are AC signals which occur due to the phase locked activity of local populations of neurons and can be recorded from several areas along the auditory pathway (for example: the auditory nerve, the cochlear nucleus, the superior olivary complex, and the inferior colliculus) (R. L. Snyder et al., 1984). Auditory neurophonic responses share two characteristics: their neural origin and their resemblance to the frequency characteristics of the auditory stimulus. The simplest auditory neurophonic response occurs due to the phase locked activity of the auditory nerve fibers, peripherally, and is called the auditory nerve neurophonic (ANN) response (R. L. Snyder & C. E. Schreiner, 1984). ANN is low frequency passed (Kenneth R Henry, 1997); which is expected because the phase locking of auditory nerve fibers is low passed and becomes distorted above about 2.5 KHz (Rose et al., 1967).

To better understand ANN, it is important to distinguish between two types of neural synchrony: onset synchrony and phase synchrony. Onset synchrony occurs when auditory nerve fibers fire in synchrony with the onset of the acoustic stimulus; i.e., all fibers fire at once each time the stimulus is presented. It can be seen in measures such as compound action potentials (CAP) and auditory brainstem responses (ABR), where the waveform of the measured response does not mimic that of the stimulus. Onset synchrony is poor at low frequency acoustic stimuli

and improves as the frequency of the stimulus increases (E. Laukli et al., 1988). Phase synchrony, on the other hand, is excellent at low frequencies and decreases as the frequency increases over 1000 Hz and becomes negligible by 4 KHz (Johnson, 1980). It occurs when auditory nerve fibers fire in synchrony with certain phase of the acoustic stimulus; with no single auditory nerve fiber firing to every single acoustic stimulus cycle, but the combined activity of a group of nerve fibers encodes the temporal information about the waveform. The waveform of the phase synchronized neural responses usually mimics the frequency of the stimulus (R. L. Snyder & C. E. Schreiner, 1984).

Both near field and far field recordings of auditory neurophonics have been used. Near field recordings involve recording auditory neurophonics directly from or very close to their neural sources (using intracranial electrodes). Far field recordings of auditory neurophonics, on the other hand, uses recording sites, such as the scalp surface, which are farther from the neural origins. Scalp recordings of auditory neurophonics (often referred to as the frequency following response (FFR) (R. Snyder & C. Schreiner, 1984), represent the vectorial sum of auditory neurophonics which originate from several auditory nuclei, whereas intracranial recordings of auditory neurophonics (i.e., using intracranial electrodes) are simple local responses which arise largely from single nuclei or from the auditory nerve. The Intracranially recorded ANN has been recorded mainly from animals (Kenneth R. Henry, 1995; Jeffery T. Lichtenhan et al., 2013; Lichtenhan et al., 2014; R. Snyder et al., 1984; Snyder et al., 1987), but also from humans (invasively from the round window) (Choudhury et al., 2012). Compared to intracranial recordings of ANN, surface recordings (FFR) of ANN are more prone to contaminations of CMs and of the phase locked activity from central auditory areas. However, surface recordings are noninvasive; hence, understanding the relation between FFR and ANN might be of interest in

humans. Surface recordings of auditory neurophonic responses (FFR) and the ANN response, which is directly recorded from the auditory nerve, share common properties which are different from CM response properties. Some of the similarities and differences are clear in their waveforms; CM waveform is almost linear and mimics the waveform of the stimulus, whereas ANN and FFR waveforms are more temporally and spectrally complex and nonlinear. Both ANN and FFR waveforms start with a transient response (CAP and ABR, respectively) followed by a spectrally complex AC response which slightly diminishes over time (i.e., adapts). The waveform of the CM response, on the other hand, consists almost only of an AC portion of one dominant spectral component (which matches the stimulus frequency). The fundamental component of the CM is at least 20 dB larger in amplitude than other higher frequency components, at stimulus levels less than 90 dB SPL (Johnson, 1980). The spectral decomposition of the AC portions of both ANN and FFR responses shows a fundamental component that is equal to the stimulus frequency in addition to other higher frequency harmonics. Animal studies showed that ANN response comprise at least three spectral components: the fundamental component (equals the stimulus frequency), the first harmonic (double the stimulus frequency), and the second harmonic (triple the stimulus frequency); other higher harmonics are also detectable, but only at high stimulus intensity levels. Regardless of the stimulus level, relative amplitudes of the first three components are approximately equal; i.e., the difference between the amplitude of the component with the largest amplitude (usually the fundamental or the first harmonic) and the component with the smallest amplitude (usually the second harmonic) is less than 10 dB, at any given stimulus level. Higher harmonics (higher than the third), on the other hand, have amplitudes which are 15 to 20 dB lower than the biggest component. Both CM and ANN components show increase in amplitude as the stimulus level increases. However, CM

components show linear increase up to 90 dB SPL stimulus level, while ANN components show a roughly linear increase at most stimulus frequencies and at low to mid-levels of stimulus intensity and nonlinear increase at other frequencies especially at moderate and high stimulus levels (Henry, 1995; Snyder & Schreiner, 1987). The phase of the ANN's spectral components changes as the stimulus level changes, but is relatively the same for the same stimulus level. CM spectral components, on the other hand, does not show similar phase shift in response to stimulus level.

The signal recorded at the round window in response to phase locked acoustic stimuli with non-alternating polarity would contain CM, ANN, and CAP onset responses. At near threshold stimulus levels, CMs are almost sinusoidal, while neural responses (ANN in this case) occur preferentially at one phase of the tone; this occurs because auditory nerve firing occurs preferentially at one direction of basilar membrane movement (Kenneth R Henry, 1995; Jeffery T Lichtenhan et al., 2013; Lichtenhan et al., 2014). The basilar membrane is located in the cochlea and supports the organ of Corti. The organ of Corti contains outer and inner hair cells which are connected to the auditory nerve fibers. A full cycle of acoustic stimulus hitting the ear drum results in the basilar membrane moving up then down or down then up, based on the polarity of the stimulus; polarity has to do with the initial movement direction of the speaker's diaphragm (in or out). The stimulation of auditory nerves, which innervate the organ of Corti hair cells, occurs only when the basilar membrane moves up. Hence, one would expect that reversing stimulus polarity will result in a response delayed (or advanced) by a half cycle in time. In fact, using the same tone at the same levels but reversed in polarity, results in the same neural response shifted half cycle in time. If responses to tones presented separately at opposite polarities are averaged together (i.e., summed together) they overlap and result in a neural

response that appears (in the response waveform) twice for each acoustic stimulus cycle (Henry, 1995; Lichtenhan et al., 2013; Lichtenhan et al., 2014). This response is referred to as the "residual ANN" (Kenneth R. Henry, 1995) or the auditory nerve overlapped waveform (ANOW) (Lichtenhan et al., 2013; Lichtenhan et al., 2014). ANOW is the same as the "residual ANN" described by Henry (1995). Henry's "residual ANN" or ANOW share the following characteristics: they have major energy at double the tone frequency and a negligible energy at the tone frequency, they show adaptation (amplitudes that start high and reduce over time), and they show nonlinear growth as well as phase shift as a function of stimulus intensity (level).

When compared to onset CAP thresholds at low frequencies (below 700 Hz), ANOW thresholds are 10 to 20 dB more sensitive at the same frequency range. Moreover, ANOW thresholds are 10 to 20 dB less sensitive than single auditory nerve fiber thresholds (Lichtenhan et al., 2013).

Forward masking

Forward masking occurs when the threshold of hearing of an auditory signal is elevated due to the presence of a strong enough preceding masker (Oxenham, 2000). It is believed that the preceding masker causes a neural adaptation which results in a temporary suppression of the neural activity. ANN responses recorded to a signal which is immediately preceded (but not overlapped) by an appropriate masker of varying level showed a decrease in the absolute amplitude as the level of the masker increases, but no change in the phase or the relative amplitude of the three main components (i.e., the amplitudes of f0, f1, and f2 show equal decrease with no component affected more than the other). Forward masking has been used to extract CM responses from auditory neurophonic responses in both the FFR (Snyder & Schreiner, 1984) and the direct auditory nerve recordings (Henry, 1997). The line of reasoning is

that CM responses are not affected by another signal preceding it in time (i.e., CMs are not forward masked), while ANNs do. Hence, forward masking FFR responses would eliminate neural responses (ANN) and preserve CM responses, if any. In theory, subtracting the waveform of the forward masked FFR from the waveform of the unmasked FFR (which contains both CM and ANN responses) would eliminate CM responses, if any, from the FFR and leave ANN response.

ANN measured to amplitude modulated (AM) tones

Russell L. Snyder and Christoph E. Schreiner (1987) used amplitude modulated (AM) high frequency tones (2 KHz to 30 KHz), which are modulated at rates of 400 Hz to 3000 Hz, to evoke ANN responses. ANN responses recorded to AM tones (AM-ANN) showed spectral composition, rates of adaptation, and rates of recovery from forward masking similar to those recorded to low frequency pure tones. AM-ANN responses have major frequency components that match harmonics of the modulation frequency. Forward masking revealed that AM-ANN responses arise from fibers with characteristic frequencies (CFs) that approximate the carrier frequency. Moreover, AM-ANN responses with high frequency carriers have latencies shorter than ANN responses recorded to pure tones. Hence, it can be concluded that AM-ANN responses results from the spatial summation of activity in auditory nerve fibers which are most sensitive to the carrier frequency (fibers innervating the base of the cochlea in the case of a high frequency carrier) and are phase locked to the modulation frequency of the AM stimulus.

ANN's frequency specificity

Tetrodotoxin (TTX) injections (Henry, 1997; Lichtenhan et al., 2013; Lichtenhan et al., 2014), forward masking (Kenneth R Henry, 1997; R. Snyder & C. Schreiner, 1984), and simultaneous masking techniques (Henry, 1997) have been used to study the origin of ANN

responses (including ANOW or residual ANN). Lichtenhan et al. (2014) have recorded the cochlear response to single tone bursts (both high and low frequency tone bursts) presented at moderate intensity level while slowly injecting TTX into the cochlear apex; ANOW response recorded to low frequency tone bursts declined and abolished much earlier in time than CAP responses recorded to high frequency tone bursts; suggesting that ANOW originate from auditory nerve fibers innervating low frequency (apical) regions of the cochlea. Although Lichtenhan's results suggest a contribution of the low frequency nerve fibers in the production of ANOW, it does not completely exclude high frequency nerve fibers involvement in the production of the ANOW; what if basal systematic injections of TTX were used (instead of the apical injections)? Basal injections resulting in no earlier decline in the ANOW response compared to the CAP response would confirm Lichtenhan's results.

Henry (1997) has used forward masking to create tuning curves of ANN responses recorded from the round window, to single tone burst stimuli; tuning curves were created by finding the minimum level of the forward masker, over a wide range of frequencies, which decreases the ANN's amplitude by a predetermined criterion (25% reduction). Snyder and Schreiner (1985) have also used forward masking techniques to create tuning curves of ANN responses recorded directly from auditory nerve fibers and from the surface of the scalp (FFR). Forward masking ANN tuning curves share similarities with the auditory nerve tuning curves recorded using psychophysical and physiological techniques, but also showed unusual characteristics. First, the frequency of the forward masking ANN tuning curve tip tends to shift by as much as an octave from that of the probe tone (Henry, 1997; R. Snyder et al., 1984); the frequency of the tuning curve tip tends to be higher than that of the probe tone when the probe tone is below 1400 Hz (Kenneth R. Henry, 1995; Snyder et al., 1987), and lower than the probe

tone when the probe tone is above 1400 Hz (Henry, 1997). Second, Regardless of the probe tone frequency, the threshold at the frequency of the tuning curve tip is always lower than the level of the probe tone; depending on the intensity level of the probe tone, the threshold of the tuning curve tip can be as much as 30 dBSPL below the probe tone level (Henry, 1997; Snyder et al., 1987). Third, as the intensity of the probe tone increases the frequency of the tuning curve tip tends to get higher; suggesting that as the intensity of the stimulus increases more auditory nerve fibers with characteristic frequencies above the frequency of the probe become involved in producing ANN. Fourth, the ANN response maybe enhanced by forward maskers over a limited range of frequencies which are outside the high frequency boundary of the forward masking ANN tuning curve (Henry, 1997; R. L. Snyder et al., 1984). The frequency range over which forward maskers enhanced ANN tuning curves is highly variable (0.5 to 6 octaves above the frequency of the probe tone) (Henry, 1997). Moreover, the intensity range over which forward maskers enhanced ANN tuning curves varied based on the intensity level of the probe tone; The minimum level of the forward maskers which would enhance the ANN response varied from 5 to 30 dB above the probe tone presented at intensity levels less than 45 dBSPL, and from 5 to 35 dB SPL lower than the intensity of the probe presented at an intensity level of 45 to 60 dB SPL (Henry, 1997). R. Snyder et al. (1984) have suggested a model to explain the unusual characteristics of the forward masking auditory nerve neurophonics tuning curves. The model looks at the vectorial sum of the phase locked responses of local fibers distributed along the basilar membrane as a function of their characteristic frequencies and the level of the stimulus. For low level tones (20 dBSPL), the fundamental component of the phase locked response (i.e., the component which has the same frequency as the stimulus tone) is high in amplitude, highly localized, and arise from nerve fibers of characteristic frequencies very close to the stimulus

frequency. As the stimulus level is increased, phase locked responses of the fibers with CFs very close to that of the stimulus tone are saturated and spreads to adjacent nerve fibers of characteristic frequencies further from that of the stimulus tone. As the phase locked activity spreads, the phase of the response changes as a function of fibers' CFs. For a 1 KHz stimulating tone, the plot of the response phase against the characteristic frequency of the nerve fibers is a curve of two parts: the high frequency part where the phase of the response changes at a rate of 90 degrees per octave frequency increase, and the low frequency part where the phase changes at a rate of 540 degrees per octave frequency decrease. The fibers with 1 KHz CF lies in the middle of the low frequency part. The two parts meet at a frequency that is double the stimulus frequency (i.e., 2KHz). The vectorial sum of the whole response (including the sum of the response vectors and the phases corresponding to the two parts of the curve) maybe used to explain many of the unusual characteristics of the forward masking auditory neurophonic tuning curves. For example, it explains why at very low stimulus levels the frequency of the tuning curve tip is very close to that of the stimulus, while at higher levels the tip tends to shift to higher frequencies. Low stimulus level produces a phase coherent, phase locked response that originates from highly localized fibers with characteristic frequencies very close to the stimulus frequency. Higher stimulus levels, on the other hand, stimulate wider area of the basilar membrane to include fibers with higher and lower characteristic frequencies. The spread is rapid that a 1 KHz stimulating tone presented at a level of 45 dBSPL stimulates fibers with CFs between 500 Hz and 3000 Hz, in cats. For the same tone, fibers with CFs below 2 KHz will be maximally stimulated with the response of each local population of fibers being phase locked to the stimulus. However, these local populations of fibers are expected to work out of phase to each other because of the rapid change in the response phase (remember that the rate of change is

high, 540 degrees per octave change in frequency). Hence, fibers below 2 KHz are expected to produce no recordable neurophonic response. Fibers higher than 2 KHz, on the other hand, will produce a recordable neurophonic response due to two reasons. First, the rate of phase change is slower than that of the lower frequency fibers (90 degrees per octave change in frequency). Second, the response occurs over only one octave of frequency. This model shows that when low frequency tones are presented at low intensity levels the neurophonic response arises from nerve fibers with CFs close to the stimulus frequency and therefore most efficiently masked by forward maskers of the same frequency as the stimulus frequency. Moreover, when these same tones presented at high intensity levels the neurophonic responses originates mainly from nerve fibers with CFs higher than that of the stimulus frequency by as much as an octave and is most efficiently masked by forward maskers one octave higher in frequency than the stimulus tone.

Two tones ANN

Presenting the ear with two simultaneous tones of different frequencies (f1 and f2, f2>f1), provokes a nonlinear response; i.e., a response which contains components that are not present in the stimuli. The nonlinear response of the auditory system is often called the distortion product and can occur in several forms, such as the quadratic (f2-f1) and the cubic (2f1-f2). Distortion products occur over only restricted range of combinations of frequencies and intensities of the two stimuli. Moreover, they have been depicted in otoacoustic emissions produced by the inner ear (Lonsbury-Martin et al., 1990), in the phase locked activity of the auditory nerve fibers (Kim et al., 1980), and in auditory evoked potentials recorded from the auditory nerve and the brain (R. L. Snyder et al., 1984). Henry (1996) has recorded the phase locked activity of the cochlear nerve, which corresponds to the quadratic distortion product. Two tone bursts were simultaneously presented to the ear and the response was recorded from the round window. The

two tones had different frequencies (ranging from 1 to 30 KHz), but same rise/fall times, intensity level, onset phase, onset time, and duration. The intensity levels of the tones were kept below 60 dBSPL; to avoid creating f2-f1 tone from the mixture of the two simultaneously presented tone bursts, which is above the CAP threshold of the animal (gerbil). The response was recorded both before and after the application of the TTX injection in to the cochlea. TTX injection into the cochlea affects only the neural cochlear response, but not the receptor cell potentials (such as CM response). Fourier offline analysis of the response showed a response of a frequency equal to f2-f1 which disappeared after injecting TTX, while CM responses were not affected. Hence, the difference response (f2-f1) has a neural cochlear origin. The response has been referred to as “DT-ANN”. The “DT-ANN” shows non-monotonic increase in amplitude as a response of stimulus intensity. Moreover, it is most prominent for f2-f1 values of 700 to 1100 Hz in gerbils.

“DT-ANN” frequency specificity

Simultaneously stimulating the ear with two tone burst tones which are alternating in polarity and have different frequencies (f1, f2, f2>f1), produces two responses which have frequencies equal to f2-f1 ('DT-ANN') and 2f2-2f1 ("2DT-ANN), respectively (Kenneth R Henry, 1996). The threshold of "DT-ANN" response is 10 dB more sensitive than that of the CAP response. The two responses are forward masked and show monotonic change in amplitude as a function of stimuli intensity level. However, the "2DT-ANN" response have smaller amplitude and higher threshold than the "DT-ANN" response. Forward masking tuning curves of both the "DT-ANN" and the "2DT-ANN" responses were created by finding the minimum level of the forward masker, over wide range of frequencies, which decreases the response's amplitude by a predetermined criterion. The frequency difference between the two tones (f2-f1) was kept

constant (900 Hz), f1 frequency ranged from 1.25 to 30 KHz, and only low probe tones' intensity was used (30 dBSPL). For f1 frequency range of 2 KHz to 20 KHz: the forward masking tuning curves were "V-shaped", had low tip thresholds of 20 to 30 dBSPL, and had tip frequency close to f1 and f2. Hence, it may be inferred that the two tones neurophonic responses which are recorded to low level tone bursts originate from nerve fibers with characteristic frequencies close to both f1 and f2. Moreover, high frequency nerve fibers (2 to 20 KHz in gerbils) are capable of producing sharply tuned and highly phase locked response to low level probe tones.

Extracting the Cochlear Microphonic from the FFR

Compared to the CM, the ANN response is more spectrally complex and consists of at least three components; the fundamental component which equals the stimulus frequency, the second harmonic, and the third harmonic. All components have almost the same amplitude with the largest component (usually either the fundamental or the second harmonic) being less than 10 dB larger than the smallest component (Snyder et al., 1987). The CM response, on the other hand, has a fundamental component that is at least 25 dB larger than the other components (Snyder & Schreiner, 1985).

Due to the neural nature of the auditory neurophonics, they share certain features with auditory nerve fibers. Such features have been used to distinguish neurophonics from the CM. First, ANN is a spectrally complex response which is rich in harmonics that comprise phase shift as a function of stimulus level. CM components, on the other hand, does not show similar phase shift in response to stimulus level. Hence, phase shifting in the components, especially the fundamental component, of the measured signal may suggest no significant contamination by the CM. The fundamental component is important when investigating the CM contamination; because the fundamental component is the largest component of the CM response, the

contamination is expected to be largest at the fundamental component. R. Snyder and C. Schreiner (1984) showed that the fundamental component (f0) comprise phase shifting as a function of stimulus level which parallels that of the other components (i.e., f1 and f2), up to around 80 dBSPL stimulus level and for stimulus frequencies below 3 KHz. They have also showed that because only one third of the response energy is in the fundamental component, it is unlikely that the CM response is significantly contaminating the FFR at moderate stimulus levels and at stimulus frequencies below 3 KHz. Second, unlike CMs, the amplitude of the auditory neurophonics show pronounced adaptation over time, similar to that seen in single auditory nerve fibers, which was evident in FFR and intracranial recordings of ANN (R. L. Snyder et al., 1984; Snyder et al., 1987). Third, unlike CM responses which are not affected by forward masking, neurophonics can be forward masked. Previous research have used forward masking to get rid of the CM responses; forward masked FFRs were subtracted from the unmasked traces to get a trace of ANN response only (Henry, 1996, 1997). Finally, ANN response is affected by TTX injections, while CM response is not (Kenneth R Henry, 1995; Snyder et al., 1987).

REFERENCES

Aoyagi, M., Suzuki, Y., Yokota, M., Furuse, H., Watanabe, T., & Ito, T. (1999). Reliability of 80-Hz amplitude-modulation-following response detected by phase coherence. *Audiol Neurootol, 4*(1), 28-37.

Atcherson, S. R., & Stoody, T. M. (2012). *Auditory Electrophysiology: A Clinical Guide*: Thieme.

Aydore, S., Pantazis, D., & Leahy, R. M. (2013). A note on the phase locking value and its properties. *NeuroImage, 74*, 231-244. doi: 10.1016/j.neuroimage.2013.02.008

Bartko, J. J. (1966). The intraclass correlation coefficient as a measure of reliability. *Psychological reports, 19*(1), 3-11.

Burkard, R. F., Eggermont, J. J., & Don, M. (2007). *Auditory Evoked Potentials: Basic Principles and Clinical Application*: Lippincott Williams & Wilkins.

Choudhury, B., Fitzpatrick, D. C., Buchman, C. A., Wei, B. P., Dillon, M. T., He, S., & Adunka, O. F. (2012). Intraoperative round window recordings to acoustic stimuli from cochlear implant patients. *Otology & neurotology: official publication of the American Otological Society, American Neurotology Society [and] European Academy of Otology and Neurotology, 33*(9), 1507.

Coats, A. C. (1978). Human auditory nerve action potentials and brain stem evoked responses: Latency-intensity functions in detection of cochlear and retrocochlear abnormality. *Archives of Otolaryngology, 104*(12), 709-717.

Darvas, F., Ojemann, J. G., & Sorensen, L. B. (2009). Bi-phase locking — a tool for probing non-linear interaction in the human brain. *NeuroImage, 46*(1), 123-132. doi: http://dx.doi.org/10.1016/j.neuroimage.2009.01.034

Du, Y., Kong, L., Wang, Q., Wu, X., & Li, L. (2011). Auditory frequency-following response: A neurophysiological measure for studying the "cocktail-party problem". *Neuroscience & Biobehavioral Reviews, 35*(10), 2046-2057.

Gorga, M. P., Neely, S. T., Bergman, B., Beauchaine, K. L., Kaminski, J. R., Peters, J., & Jesteadt, W. (1993). Otoacoustic emissions from normal-hearing and hearing-impaired subjects: distortion product responses. *J Acoust Soc Am, 93*(4 Pt 1), 2050-2060.

Hanslmayr, S., Aslan, A., Staudigl, T., Klimesch, W., Herrmann, C. S., & Bäuml, K.-H. (2007). Prestimulus oscillations predict visual perception performance between and within subjects. *Neuroimage, 37*(4), 1465-1473.

Henry, K. R. (1995). Auditory nerve neurophonic recorded from the round window of the Mongolian gerbil. *Hearing research, 90*(1–2), 176-184. doi: http://dx.doi.org/10.1016/0378-5955(95)00162-6

Henry, K. R. (1995). Auditory nerve neurophonic recorded from the round window of the Mongolian gerbil. *Hear Res, 90*(1), 176-184.

Henry, K. R. (1996). Tuning curves of the difference tone auditory nerve neurophonic. *Hear Res, 99*(1), 160-167.

Henry, K. R. (1997). Auditory nerve neurophonic tuning curves produced by masking of round window responses. *Hear Res, 104*(1), 167-176.

Johnson, D. H. (1980). The relationship between spike rate and synchrony in responses of auditory-nerve fibers to single tones. *J Acoust Soc Am, 68*(4), 1115-1122.

Katz, J., Chasin, M., English, K. M., Hood, L. J., & Tillery, K. L. (2014). *Handbook of Clinical Audiology*: Lippincott Williams & Wilkins.

Kim, D. O., Molnar, C. E., & Matthews, J. W. (1980). Cochlear mechanics: nonlinear behavior in two-tone responses as reflected in cochlear-nerve-fiber responses and in ear-canal sound pressure. *J Acoust Soc Am, 67*(5), 1704-1721.

Koenker, R., & Bassett Jr, G. (1982). Robust tests for heteroscedasticity based on regression quantiles. *Econometrica: Journal of the Econometric Society*, 43-61.

Lachaux, J. P., Rodriguez, E., Martinerie, J., & Varela, F. J. (1999). Measuring phase synchrony in brain signals. *Hum Brain Mapp, 8*(4), 194-208.

Laukli, E., Fjermedal, O., & Mair, I. (1988). Low-frequency auditory brainstem response threshold. *Scandinavian audiology, 17*(3), 171-178.

Laukli, E., Fjermedal, O., & Mair, I. W. S. (1988). Low-Frequency Auditory Brainstem Response Threshold. *Scandinavian audiology, 17*(3), 171-178. doi: doi:10.3109/01050398809042189

Lichtenhan, J. T., Cooper, N. P., & Guinan, J. J. (2013). A new auditory threshold estimation technique for low frequencies: proof of concept. *Ear Hear, 34*(1), 42.

Lichtenhan, J. T., Cooper, N. P., & Guinan, J. J. (2013). A new auditory threshold estimation technique for low frequencies: Proof of concept. *Ear and hearing, 34*(1), 42-51. doi: 10.1097/AUD.0b013e31825f9bd3

Lichtenhan, J. T., Hartsock, J. J., Gill, R. M., Guinan, J. J., & Salt, A. N. (2014). The Auditory Nerve Overlapped Waveform (ANOW) Originates in the Cochlear Apex. *Journal of the Association for Research in Otolaryngology, 15*(3), 395-411. doi: 10.1007/s10162-014-0447-y

Lonsbury-Martin, B. L., & Martin, G. K. (1990). The clinical utility of distortion-product otoacoustic emissions. *Ear Hear, 11*(2), 144-154.

Melloni, L., Molina, C., Pena, M., Torres, D., Singer, W., & Rodriguez, E. (2007). Synchronization of neural activity across cortical areas correlates with conscious perception. *The Journal of neuroscience, 27*(11), 2858-2865.

Moeller, M. P. (2000). Early Intervention and Language Development in Children Who Are Deaf and Hard of Hearing. *Pediatrics, 106*(3), e43. doi: 10.1542/peds.106.3.e43

Moller, A. R. (1992). Intraoperative neurophysiological monitoring. *Neurol Res, 14*(3), 216-218.

Møller, A. R. (2010). *Intraoperative neurophysiological monitoring*: Springer Science & Business Media.

Naatanen, R. (2001). The perception of speech sounds by the human brain as reflected by the mismatch negativity (MMN) and its magnetic equivalent (MMNm). *Psychophysiology, 38*(1), 1-21.

Niedermeyer, E., & da Silva, F. H. L. (2005). *Electroencephalography: Basic Principles, Clinical Applications, and Related Fields*: Lippincott Williams & Wilkins.

Oxenham, A. J. (2000). Influence of spatial and temporal coding on auditory gap detection. *J Acoust Soc Am, 107*(4), 2215-2223.

Pryce, G., & Garcia-Granero, M. (2002). Breusch-Pagan & Koenker Test Macro.

Reed, G. F., Lynn, F., & Meade, B. D. (2002). Use of coefficient of variation in assessing variability of quantitative assays. *Clinical and diagnostic laboratory immunology, 9*(6), 1235-1239.

Rogers, A. R., Burke, S. R., Kopun, J. G., Tan, H., Neely, S. T., & Gorga, M. P. (2010). Influence of calibration method on distortion-product otoacoustic emission measurements: II. threshold prediction. *Ear Hear, 31*(4), 546-554. doi: 10.1097/AUD.0b013e3181d86b59

Rose, J. E., Brugge, J. F., Anderson, D. J., & Hind, J. E. (1967). Phase-locked response to low-frequency tones in single auditory nerve fibers of the squirrel monkey. *Journal of neurophysiology, 30*(4), 769-793.

Schoonhoven, R., Prijs, V. F., & Grote, J. J. (1996). Response thresholds in electrocochleography and their relation to the pure tone audiogram. *Ear Hear, 17*(3), 266-275.

Sininger, Y. S., Abdala, C., & Cone-Wesson, B. (1997). Auditory threshold sensitivity of the human neonate as measured by the auditory brainstem response. *Hear Res, 104*(1-2), 27-38.

Snyder, R., & Schreiner, C. (1984). The auditory neurophonic: basic properties. *Hear Res, 15*(3), 261-280.

Snyder, R. L., & Schreiner, C. E. (1984). The auditory neurophonic: Basic properties. *Hear Res, 15*(3), 261-280. doi: http://dx.doi.org/10.1016/0378-5955(84)90033-9

Snyder, R. L., & Schreiner, C. E. (1987). Auditory neurophonic responses to amplitude-modulated tones: Transfer functions and forward masking. *Hear Res, 31*(1), 79-91. doi: http://dx.doi.org/10.1016/0378-5955(87)90215-2

Spoor, A., & Eggermont, J. (1976). Electrocochleography as a method for objective audiogram determination *Hearing and Davis: Essays honoring Hallowell Davis* (pp. 411-417): Washington University Press New York.

Stapells, D. R. (2000). Threshold estimation by the tone-evoked auditory brainstem response: a literature meta-analysis. *Journal of Speech Language Pathology and Audiology, 24*(2), 74-83.

Wever, E. G., & Bray, C. W. (1930). Action currents in the auditory nerve in response to acoustical stimulation. *Proceedings of the National Academy of Sciences of the United States of America, 16*(5), 344.

APPENDIX A

RESEARCH CONSENT FORM

Auditory Nerve Overlapped Waveform (ANOW) response recorded from the ear drum of normal hearing human subjects

You are being asked to participate in this study because you are an adult between the ages 18-45 years with normal hearing, and no current or previous ear illness or disorder. This study involves recording auditory nerve overlapped waveform (ANOW) responses using Electrocochleography (ECochG), which is a non-invasive, painless and routinely used procedure for recording the electrical responses of the inner ear and hearing nerve. Your participation is voluntary, and you may change your mind at any time. There will be no penalty to you if you decide not to participate, or if you start the study and decide to stop early.

This consent form explains what you will be doing if you are in the study. It also describes the possible risks and benefits. Please read the form carefully and ask as many questions as needed before deciding to participate in this research.

You can ask questions now or anytime during the study. The researchers will tell you if they receive any new information that might cause you to change your mind about participating.

This research study will take place at the University of Kansas Medical Center (KUMC) under the direction of John Ferraro, Ph.D. as the principle investigator, and Hana Almohammad, Ph.D. student, as a secondary investigator. Approximately ten subjects will participate in the study.

BACKGROUND

Two types of hearing tests are used to assess hearing: the behavioral hearing tests and the objective hearing tests. Behavioral auditory tests assess subject's hearing based on the presence or the absence of change in behavior in response to sound (such as pressing a button when hearing a sound or turning the head towards sound source), whereas objective auditory tests assess hearing based on change in physiologic activity in response to sound and no change in behavior.

Auditory evoked potentials (AEPs) are changes in the electrical activity of the brain in response to sound. They are often used in the objective evaluation of hearing function, especially in populations where behavioral hearing tests may not be feasible; such as infants and adults (e.g., adults with low mentality) who may not be able to provide behavioral responses to sounds during conventional hearing tests.

The currently used AEPs in clinic are excellent in assessing hearing thresholds at frequencies (pitches) equal to and higher than 1000 Hz, but are problematic and less accurate in assessing thresholds at lower frequencies of sound, which are very important to hearing. For example, accurate low frequency vowel amplification is important when fitting infants with hearing aids.

Recent animal research has brought attention to a new AEP response, called the auditory nerve overlapped waveform (ANOW). ANOW represents the change in electrical activity of the auditory nerve fibers innervating regions of the cochlea (which is the auditory organ located in the inner ear) that respond to low frequency (low pitch) sounds. Hence, ANOW may be able to objectively and accurately estimate hearing sensitivity at frequencies (pitches) below 1000 Hz. Thus, developing a technique for recording ANOW from humans may have important clinical applications, especially for "difficult-to-test" populations that include infants and adults who may not be able to provide behavioral responses to sounds during conventional hearing tests.

KUMC IRB # STUDY00002994 | Approval Period 8/4/2016 – 8/3/2017 | FWA# 00003411

ANOW can be recorded using Electrocochleography (ECochG) test; which is a procedure used to record electrical responses of the inner ear (cochlea) and the auditory nerve. Unfortunately, the protocol for recording ANOW to produce the most accurate and sensitive responses have yet to be fully established. This study aims to develop a technique for recording ANOW that can be used to objectively and accurately estimate low frequency thresholds from normal subjects.

Your participation in this study will help to establish a protocol for recording ANOW.

PURPOSE

By conducting this study, researchers hope to establish a non-invasive technique for recording ANOW that can be used to objectively estimate low frequency thresholds in a highly frequency specific manner from humans.

PROCEDURES

If you are eligible and decide to participate in this study, your participation will last approximately 2 hours. During the session the examiner will perform otoscopy (looking into the ear canal with an otoscope) and Electrocochleography (ECochG).

ECochG is a non-invasive and painless procedure for recording the electrical responses of the inner ear and hearing nerve. This test involves the placement of four, disposable surface electrodes: two on the forehead and one on the scalp behind each ear, and a special rubber-tipped electrode on the external surface of the ear drum. During this procedure you will be comfortably seated on a reclined chair. Skin preparation includes cleaning small areas of the forehead and scalp (behind each ear) with an alcoholsoaked swab. Self-adhesive, disposable electrodes routinely used for ECochG testing will then be attached to these areas. A conductive gel will be applied on the rubber tip of the electrode to insure proper electrical contact with the ear drum. Then, the electrode will be inserted along the ear canal and advanced until the soft, rubber tip rests against the outer surface of the ear drum. Once the electrode is placed, a small rubber plug connected via a tube to a small sound generator will be inserted into the entrance of the ear canal to hold the ECochG electrode in place and also deliver sounds to the ear. These sounds excite the inner ear and hearing nerve to send electrical responses to the brain (as all sounds do). The special electrode on the ear drum and the other electrodes on the forehead and scalp record these responses and deliver them to a special computer that stores and displays them for analysis. After ECochG recording is done, the rubber plug will be removed, and the ear drum electrode will be gently pulled out and removed from the ear canal. Also the forehead and scalp electrodes will be removed.

RISKS

Discomfort from the rubber tip of the electrode touching the ear drum may occur. If this discomfort is bothersome, the test will be terminated. Your ear drum will not be harmed or punctured and there is no risk of hearing loss. A slight red spot generally appears on the eardrum after the electrode is removed, but this condition is a temporary one that goes away in a few minutes. In addition, there may be some unexpected risks and side effects that have not been previously observed. Nevertheless, you should tell the research team about anything that is bothering you.

NEW FINDINGS STATEMENT

You will be told about anything new that might change your decision to be in this study. You may be asked to sign a new consent form if this occurs.

BENEFITS

You will not benefit directly from this study. The researchers believe that the information from this research study may be useful in the objective estimation of low frequency thresholds in a highly frequency specific manner from humans.

ALTERNATIVES

Participation in this study is voluntary. Deciding not to participate will have no effect on care or services you receive at the University of Kansas Medical Center.

COSTS

There is no cost for being in the study.

PAYMENT TO SUBJECTS

There is no payment for this study.

IN THE EVENT OF INJURY

If you have a bodily injury as a result of participating in this study, treatment will be provided for you at the usual charge. Treatment may include first aid, emergency care and follow-up care, as needed. Claims will be submitted to your health insurance policy, your government program, or other third party, but you will be billed for the costs that are not covered by insurance. You do not give up any legal rights by signing this form.

INSTITUTIONAL DISCLAIMER STATEMENT

If you think you have been harmed as a result of participating in research at the University of Kansas Medical Center (KUMC), you should contact the Director, Human Research Protection Program, Mail Stop #1032, University of Kansas Medical Center, 3901 Rainbow Blvd., Kansas City, KS 66160. Under certain conditions, Kansas state law or the Kansas Tort Claims Act may allow for payment to persons who are injured in research at KUMC.

CONFIDENTIALITY AND PRIVACY AUTHORIZATION

The researchers will protect your information, as required by law. Absolute confidentiality cannot be guaranteed because persons outside the study team may need to look at your study records. The researchers may publish the results of the study. If they do, they will only discuss group results. Your name will not be used in any publication or presentation about the study.

A federal privacy law called HIPAA protects your health information. By signing this consent form, you are giving permission for KUMC to use and share your health information. If you decide not to sign the form, you cannot be in the study.

The researchers will only use and share information that is needed for the study. To do the study, they will collect health information from the study activities. You may be identified by information such as name, address, phone, date of birth, social security number, or other identifiers. Your health information will be used at KUMC by John Ferraro, Ph.D., Hana Almohammad, Ph.D. student, members of the research team, the KUMC Human Subjects Committee, and other committees and offices that review and monitor research studies. Study records might be reviewed by government officials who oversee research,

if a regulatory review takes place. All study information that is sent outside KU Medical Center will have your name and other identifying characteristics removed, so that your identity will not be known. Because identifiers will be removed, your health information will not be re-disclosed by outside persons or groups and will not lose its federal privacy protection.

Your permission to use and share your health information will not expire unless you cancel it.

QUESTIONS

Before you sign this form, Dr. John Ferraro or other members of the study team should answer all of your questions. You can talk to the researchers if you have any more questions, suggestions, concerns, or complaints after signing this form. If you have any questions about your rights as a research subject, or if you want to talk with someone who is not involved in the study, you may call the Human Subjects Committee at (913) 588-1240. You may also write the Human Subjects Committee at Mail Stop #1032, University of Kansas Medical Center, 3901 Rainbow Blvd., Kansas City, KS 66160.

SUBJECT RIGHTS AND WITHDRAWL FROM THE STUDY

You may stop being in the study at any time. Your decision to stop will not prevent you from getting treatment or services at KUMC. The entire study may be discontinued for any reason without your consent by the investigator conducting the study.

You have the right to cancel your permission for researchers to use your health information. If you want to cancel your permission, please write to Dr. John Ferraro. The mailing address is Dr. John Ferraro, PhD., University of Kansas Medical Center, 3901 Rainbow Boulevard, Kansas City, KS 66160. If you cancel permission to use your health information, you will be withdrawn from the study. The research team will stop collecting any additional information about you. The research team may use and share information that was gathered before they received your cancellation.

CONSENT

Dr. John Ferraro or the research team has given you information about this research study. They have explained what will be done and how long it will take. They explained any inconvenience, discomfort or risks that may be experienced during this study.

By signing this form, you say that you freely and voluntarily consent to participate in this research study. You have read the information and had your questions answered.

You will be given a signed copy of the consent form to keep for your records.

_____

Print Participant's Name

_____ _____ _____

Signature of Participant Time Date

_____

Print Name of Person Obtaining Consent

_____ _____

Signature of Person Obtaining Consent Date

APPENDIX B

This appendix shows Phase Locking Value (PLV) calculations. PLV was computed between time series of ANOW's amplitudes ($x_1(t)$) and the time series of simulated TB that has double the frequency of the original TB used to evoke the ANOW response ($x_2(t)$). Simulated TBs were created using the MATLAB software. Responses were online band passed filtered between 100 Hz and 3000 Hz. Each simulated TB stimulus has single frequency.

Analytic signals ($z_i(t)$, where i={1,2}) were computed using the following equation:

$Z_i(t) = x_i(t) + jHT(x_i(t))$ ……. (1)

Where $HT(x_i(T))$ is the Hilbert transform of $x_i(t)$, i={1, 2}.

Next, the relative phase was computed as:

$$\Delta\varphi(t) = \arg\left(\frac{z1(t)*z2(t)}{|z1(t)||z2(t)|}\right) \text{……..... (2)}$$

The instantaneous PLV was computed as:

$$PLV(t) \triangleq |E\left[e^{j\Delta\varphi(t)}\right]| \text{……..… (3)}$$

Where E[.] is the expected value.

APPENDIX C

This appendix shows absolute ANOW's amplitudes and background noise for all participants across all stimulus intensity levels.

		Run 1		Run 2		Run 3	
	ID#	Amplitude1 (μV^2)	Background Noise 1 (μV^2)	Amplitude2 (μV^2)	Background Noise 2 (μV^2)	Amplitude3 (μV^2)	Background Noise 3 (μV^2)
250 Hz - 80 dB nHL	1	0.1212	0.0752	0.6929	0.0756	0.0464	0.0225
	2	2.5067	0.0551	0.7146	0.1772	1.8988	0.3157
	3	0.2956	0.0286	0.2069	0.0488	0.4950	0.0964
	4	0.2376	0.0880	0.3645	0.0191	0.1958	0.1001
	5	3.1799	0.1529	12.3610	0.1913	16.8498	0.3374
	6	0.6979	0.0330	0.4891	0.0936	0.2964	0.0603
	7	0.9078	0.0781	1.0217	0.0429	1.1278	0.0475
	8	1.5284	0.0414				
	9	0.6134	0.0858	0.5452	0.0188	0.6131	0.0688
	10	1.0824	0.1290	0.8752	0.2818	2.7221	0.1557
	11	0.8666	0.1044	1.2197	0.3090	0.7891	0.1082
	12	3.5931	0.0413	2.9737	0.1142	3.5122	0.0573
	13	1.1680	0.0508	0.6099	0.0609	0.5996	0.0652
250 Hz - 70 dB nHL	1	0.5932	0.0642	0.9750	0.1712	1.0385	0.0904
	2	1.5197	0.0359	1.4844	0.0539	1.0611	0.2208
	3	1.2691	0.0190	0.9555	0.0687	0.8531	0.0399
	4	0.4331	0.1273	0.2418	0.0620	0.5712	0.0608
	5	0.3496	0.0558	0.2930	0.0872	0.8550	0.1025
	6	1.4114	0.0627	0.4780	0.1597	1.2194	0.0514
	7	1.8726	0.1145	4.9063	0.2659	3.0813	0.1274
	8	2.2860	0.0639	2.0721	0.1576	1.8374	0.0420
	9	1.2255	0.0825	1.3951	0.0589	1.5908	0.0919
	10	1.2613	0.0609	1.8226	0.0758	1.5535	0.0921
	11	2.1318	0.2021	2.8806	0.2058	2.1874	0.1024
	12	2.4074	0.0359	2.5449	0.1228	2.0191	0.1119
	13	0.2724	0.0696	0.1638	0.0142	0.2872	0.1023
250 Hz -	1	0.7940	0.1156	0.8923	0.1904	1.0342	0.0750
	2	1.3391	0.0722	1.1787	0.1088	1.0857	0.0628
	3	0.2931	0.0976	0.3927	0.0758	0.4760	0.0838
	4	0.2018	0.0401	0.0936	0.1265	0.1220	0.0336

	5	0.6142	0.1414	1.3822	0.0737	1.1021	0.0745
	6	0.9160	0.1128	1.2488	0.0350	0.8022	0.0277
	7	2.9106	0.0810	2.1525	0.0880	4.6254	0.1170
	8	2.8712	0.0604	2.1029	0.0733	2.6283	0.1281
	9	1.6598	0.0483	1.5585	0.0693	2.6728	0.0381
	10	1.8933	0.0563	1.9505	0.0467	1.7763	0.0933
	11	0.9497	0.0836	1.1749	0.0526	0.9457	0.0215
	12	3.4035	0.0568	3.5723	0.1045	3.4430	0.0967
	13	0.1761	0.0483	0.1626	0.1047	0.2210	0.1080
250 Hz - 50 dB nHL	1	1.2671	0.1212	0.8246	0.0433	1.3500	0.0642
	2	0.2223	0.0624	0.2992	0.1392	0.4400	0.1517
	3	0.3183	0.0499	0.2558	0.0237	0.2724	0.0473
	4	0.2042	0.0860	0.3256	0.0318	0.1873	0.1013
	5	0.3210	0.0875	0.3838	0.0917	0.3025	0.0605
	6	0.8091	0.0449	0.9917	0.1365	0.8052	0.0649
	7	2.5182	0.1247	0.7984	0.0554	2.3183	0.0779
	8	2.1670	0.0623	2.5255	0.0830	1.9008	0.0465
	9	0.5939	0.0280	1.0262	0.0450	0.6318	0.0298
	10	1.0117	0.0474	1.4215	0.0535	1.1119	0.0495
	11	0.1314	0.0085	0.1246	0.0162	0.1752	0.0176
	12	2.6534	0.1179	2.2044	0.0702	2.2442	0.0641
	13	0.0867	0.1530	0.0789	0.0464	0.1513	0.0863
250 Hz - 40 dB nHL	1	0.3872	0.0753	0.6911	0.0560	0.2200	0.0322
	2	0.2718	0.0579	0.3733	0.0551	0.0786	0.0857
	3	0.2740	0.0599	0.2209	0.0350	0.2786	0.0529
	4	0.1667	0.0452	0.1006	0.0155	0.0491	0.0253
	5	0.0222	0.0608	0.0264	0.0139	0.1172	0.0406
	6	0.1906	0.0423	0.3430	0.0470	0.5313	0.0439
	7	1.2311	0.0497	0.2129	0.0395	0.7335	0.0266
	8	1.1324	0.0449	1.3117	0.0414	1.0754	0.1091
	9	0.2151	0.0173	0.0662	0.0501	0.1097	0.0122
	10	0.5324	0.0352	0.8805	0.0537	0.9150	0.0594
	11	0.0239	0.0092	0.0201	0.0107	0.0460	0.0087
	12	1.3342	0.0804	1.4996	0.0622	1.5182	0.0481
	13	0.0957	0.0595	0.1722	0.1195	0.1657	0.0997
250	1	0.0932	0.1770	0.0343	0.0556	0.1137	0.0298
	2	0.2729	0.0671	0.0512	0.0142	0.1662	0.0745

	3	0.4297	0.0632	0.2061	0.0494	0.1291	0.0371
	4	0.0874	0.0418	0.0552	0.0504	0.0655	0.0278
	5	0.1164	0.0388	0.0729	0.0312	0.0206	0.0147
	6	0.2970	0.1000	0.2679	0.0360	0.1339	0.0627
	7	0.3246	0.0326	0.0665	0.0809	0.2459	0.0319
	8	0.5613	0.0307	0.7615	0.0510	0.6736	0.0630
	9	0.0470	0.0774	0.0752	0.0912	0.0525	0.0120
	10	0.2708	0.0184	0.2833	0.2487	0.3866	0.0349
	11	0.0186	0.0030	0.0526	0.0031	0.0484	0.0203
	12	0.4250	0.0490	0.3741	0.0126	0.2275	0.0977
	13	0.0610	0.0768	0.1445	0.1057	0.2970	0.1968
250 Hz - 20 dB nHL	1	0.1171	0.0672	0.0479	0.0148	0.0277	0.0252
	2	0.2957	0.0893	0.1163	0.0271	0.2008	0.0792
	3	0.1716	0.1835	0.2695	0.0792	0.2592	0.0338
	4	0.0339	0.0452	0.0529	0.0243	0.0369	0.0245
	5	0.0381	0.0634	0.0910	0.0208	0.1354	0.0593
	6	0.0975	0.1011	0.0848	0.0500	0.1649	0.1754
	7	0.2491	0.0804	0.0399	0.0310	0.1821	0.0208
	8	0.1497	0.0222	0.2233	0.0387	0.2348	0.0164
	9	0.0135	0.1427	0.1060	0.0730	0.0664	0.1038
	10	0.1039	0.0259	0.0527	0.0165	0.1625	0.0541
	11	0.0108	0.0043	0.0039	0.0259		
	12	0.0433	0.0473	0.0464	0.0657	0.0607	0.0324
	13	0.1156	0.0245	0.1293	0.0992	0.0511	0.0773
500 Hz - 80 dB nHL	1	0.6087	0.0088	1.3488	0.0317	0.7722	0.0184
	2	0.9504	0.0125	1.0625	0.0192	0.9259	0.0203
	3	0.1157	0.0106	0.1778	0.0263	0.1542	0.0096
	4	0.0059	0.0056	0.0137	0.0020	0.0038	0.0020
	5	0.1810	0.0066	0.1031	0.0247	0.1787	0.0178
	6	0.2894	0.0104	0.5092	0.0083	0.5100	0.0138
	7	0.8646	0.0297	0.6309	0.0120	0.3739	0.0179
	8	0.2792	0.0065	0.2659	0.0125	0.3013	0.0071
	9	0.2543	0.0303	0.2590	0.0291	0.3330	0.0292
	10	0.0741	0.0018	0.0754	0.0039	0.0795	0.0069
	11	0.0149	0.0106	0.0153	0.0090		
	12	0.5424	0.0145	0.6438	0.0279	0.4382	0.0230
	13	0.5198	0.0164	0.5890	0.0223	0.4040	0.0177

500 Hz - 70 dB nHL	1	0.7299	0.0162	0.6055	0.0182	0.5911	0.0152
	2	0.5499	0.0100	1.1210	0.0256	1.0631	0.0142
	3	0.0362	0.0082	0.1045	0.0100	0.0796	0.0068
	4	0.0061	0.0016	0.0058	0.0019	0.0086	0.0027
	5	0.4936	0.0197	0.3494	0.0131	0.3906	0.0189
	6	0.1428	0.0103	0.2897	0.0136	0.3843	0.0142
	7	0.5550	0.0156	0.7529	0.0224	0.6663	0.0122
	8	0.2422	0.0065	0.1690	0.0093	0.2163	0.0048
	9	0.1606	0.0201	0.1546	0.0220	0.1975	0.0170
	10	0.0339	0.0026	0.0225	0.0027	0.0634	0.0062
	11	0.0109	0.0025	0.0112	0.0041	0.0102	0.0043
	12	0.7980	0.0366	0.7058	0.0204	0.6115	0.0213
	13	0.0236	0.0126	0.0187	0.0056	0.0441	0.0047
500 Hz - 60 dB nHL	1	0.3592	0.0148	0.3820	0.0181	0.5235	0.0159
	2	0.5106	0.0126	0.6309	0.0124	0.7481	0.0157
	3	0.0434	0.0144	0.0409	0.0109	0.0240	0.0114
	4	0.0112	0.0085	0.0049	0.0050	0.0105	0.0022
	5	0.0573	0.0042	0.0275	0.0076	0.0600	0.0053
	6	0.1358	0.0095	0.1949	0.0165	0.2123	0.0098
	7	0.4580	0.0185	0.5076	0.0233	0.3268	0.0201
	8	0.1527	0.0095	0.1577	0.0086	0.1518	0.0060
	9	0.0210	0.0072	0.0194	0.0087	0.0604	0.0072
	10	0.0250	0.0042	0.0292	0.0049	0.0249	0.0028
	11	0.0081	0.0043	0.0317	0.0028	0.0112	0.0040
	12	0.5308	0.0261	0.4932	0.0228	0.5805	0.0501
	13	0.0319	0.0036	0.0345	0.0076	0.0139	0.0047
500 Hz - 50 dB nHL	1	0.1445	0.0117	0.0637	0.0182	0.1232	0.0059
	2	0.0174	0.0027	0.0187	0.0062	0.0180	0.0037
	3	0.0429	0.0097	0.0202	0.0100	0.0195	0.0111
	4	0.0024	0.0024	0.0113	0.0052	0.0118	0.0051
	5	0.0425	0.0070	0.0422	0.0059	0.0662	0.0065
	6	0.0450	0.0173	0.0570	0.0093	0.0647	0.0069
	7	0.1785	0.0123	0.1762	0.0118	0.0995	0.0046
	8	0.0225	0.0049	0.0269	0.0038	0.0214	0.0047
	9	0.0452	0.0091	0.0324	0.0035	0.0440	0.0056
	10	0.0492	0.0035	0.0408	0.0070	0.0727	0.0043
	11	0.0093	0.0010	0.0323	0.0023	0.0054	0.0041
	12	0.2493	0.0109	0.2404	0.0188	0.3466	0.0132

	13	0.0137	0.0023	0.0097	0.0065	0.0054	0.0025
500 Hz - 40 dB nHL	1	0.0118	0.0023	0.0171	0.0025	0.0109	0.0065
	2	0.0493	0.0032	0.0287	0.0047	0.0418	0.0020
	3	0.0425	0.0048	0.0999	0.0038	0.0119	0.0111
	4	0.0030	0.0081	0.0164	0.0032	0.0068	0.0047
	5	0.0727	0.0085	0.1027	0.0120	0.0512	0.0088
	6	0.0698	0.0024	0.0450	0.0081	0.0683	0.0061
	7	0.0112	0.0057	0.0380	0.0102	0.0432	0.0045
	8	0.0239	0.0020	0.0325	0.0028	0.0565	0.0028
	9	0.0117	0.0024	0.0109	0.0021	0.0073	0.0051
	10	0.0296	0.0039	0.0142	0.0079	0.0222	0.0046
	11	0.0128	0.0080	0.0139	0.0033	0.0094	0.0059
	12	0.0607	0.0079	0.0835	0.0097	0.0689	0.0124
	13	0.0130	0.0038	0.0135	0.0048	0.0046	0.0054
500 Hz - 30 dB nHL	1	0.0107	0.0023	0.0041	0.0060	0.0117	0.0135
	2	0.0169	0.0050	0.0174	0.0026	0.0106	0.0031
	3	0.0013	0.0096	0.0194	0.0043	0.0081	0.0028
	4	0.0067	0.0028	0.0074	0.0066	0.0027	0.0029
	5	0.0115	0.0110	0.0056	0.0052	0.0119	0.0143
	6	0.0085	0.0033	0.0116	0.0049	0.0237	0.0054
	7	0.0142	0.0031	0.0116	0.0045	0.0054	0.0034
	8	0.0144	0.0037	0.0106	0.0033	0.0143	0.0023
	9	0.0067	0.0011	0.0078	0.0016	0.0180	0.0042
	10	0.0048	0.0019	0.0350	0.0013	0.0214	0.0020
	11	0.0025	0.0024	0.0084	0.0038	0.0075	0.0049
	12	0.0688	0.0053	0.0032	0.0060	0.0163	0.0068
	13	0.0064	0.0032	0.0013	0.0025	0.0084	0.0033
500 Hz - 20 dB nHL	1	0.0211	0.0030	0.0049	0.0094	0.0034	0.0031
	2	0.0065	0.0018	0.0072	0.0035	0.0099	0.0025
	3	0.0136	0.0049	0.0031	0.0043	0.0072	0.0063
	4	0.0053	0.0034	0.0039	0.0014	0.0094	0.0019
	5	0.0149	0.0043	0.0135	0.0075	0.0126	0.0053
	6	0.0078	0.0073	0.0048	0.0030	0.0431	0.0042
	7	0.0051	0.0063	0.0119	0.0041	0.0068	0.0052
	8	0.0117	0.0026	0.0065	0.0021	0.0060	0.0042
	9	0.0040	0.0041	0.0182	0.0031	0.0091	0.0032
	10	0.0027	0.0017	0.0028	0.0023	0.0019	0.0080

11	0.0036	0.0017	0.0138	0.0036	0.0080	0.0022
12	0.0162	0.0080	0.0063	0.0056	0.0196	0.0101
13	0.0091	0.0046	0.0115	0.0032	0.0049	0.0075

APPENDIX D

This appendix shows absolute ANOW's SNRs for all participants across all stimulus intensity levels.

		SNR		
	ID#	**Run 1**	**Run 2**	**Run 3**
250 Hz - 80 dB nHL	1	1.6125	9.1636	2.0625
	2	45.4765	4.0319	6.0149
	3	10.3470	4.2429	5.1338
	4	2.7000	19.0936	1.9554
	5	20.8004	17.5725	8.4455
	6	21.1607	5.2239	4.9156
	7	11.6279	23.7946	23.7280
	8	36.9406		
	9	7.1487	28.9791	8.9143
	10	8.3905	3.1062	17.4872
	11	8.3013	3.9471	7.2955
	12	86.8985	26.0384	61.3384
	13	22.9962	10.0118	9.2028
250 Hz - 70 dB nHL	1	9.2338	5.6939	11.4894
	2	42.3589	27.5534	4.8047
	3	66.8272	13.9011	21.4036
	4	3.4028	3.9011	9.3987
	5	6.2622	3.3597	8.3407
	6	22.4940	2.9934	23.7202
	7	16.3503	14.6916	24.1787
	8	35.7953	13.1455	43.7665
	9	14.8487	23.6703	17.3134
	10	20.7182	24.0596	16.8733
	11	10.5482	13.9954	21.3580
	12	66.9991	20.7298	18.0409
	13	3.9144	11.5478	2.8074
250 Hz - 60 dB nHL	1	6.8684	4.6855	13.7962
	2	18.5409	10.8340	17.2755
	3	3.0026	5.1828	5.6833
	4	5.0267	0.7400	3.6291
	5	4.3437	18.7465	14.7902
	6	8.1217	35.6376	28.9524
	7	35.9287	24.4500	30.9865

	8	47.5717	28.7028	20.5122
	9	34.3460	22.4980	70.1274
	10	33.6301	41.7602	19.0293
	11	11.3536	22.3245	43.9839
	12	59.8823	34.1846	35.5882
	13	3.6487	1.5530	2.0460
250 Hz - 50 dB nHL	1	10.4567	19.0492	21.0350
	2	3.5643	2.1500	2.9013
	3	6.3783	10.7809	5.7563
	4	2.3758	10.2540	1.8493
	5	3.6698	4.1836	4.9967
	6	18.0230	7.2630	12.4156
	7	20.1960	14.4151	29.7565
	8	34.7590	30.4248	40.8992
	9	21.2059	22.8237	21.2064
	10	21.3207	26.5569	22.4796
	11	15.4127	7.7060	9.9786
	12	22.5018	31.3935	35.0326
	13	0.5664	1.7001	1.7531
250 Hz - 40 dB nHL	1	5.1447	12.3372	6.8257
	2	4.6943	6.7717	0.9170
	3	4.5782	6.3092	5.2627
	4	3.6842	6.4762	1.9429
	5	0.3649	1.8972	2.8871
	6	4.5107	7.2983	12.1138
	7	24.7852	5.3878	27.5344
	8	25.2418	31.6975	9.8585
	9	12.4082	1.3229	9.0071
	10	15.1315	16.3839	15.4152
	11	2.6055	1.8843	5.2895
	12	16.5866	24.1055	31.5430
	13	1.6075	1.4403	1.6624
250 Hz - 30 dB nHL	1	0.5264	0.6169	3.8106
	2	4.0684	3.6019	2.2312
	3	6.8003	4.1677	3.4791
	4	2.0902	1.0960	2.3611
	5	2.9975	2.3388	1.4001
	6	2.9708	7.4473	2.1362
	7	9.9515	0.8225	7.6995

	8	18.3031	14.9218	10.6972
	9	0.6069	0.8249	4.3761
	10	14.6985	1.1391	11.0702
	11	6.3111	17.0395	2.3917
	12	8.6697	29.6887	2.3275
	13	0.7941	1.3672	1.5093
250 Hz - 20 dB nHL	1	1.7431	3.2239	1.0983
	2	3.3106	4.2962	2.5353
	3	0.9352	3.4049	7.6754
	4	0.7502	2.1773	1.5098
	5	0.6003	4.3732	2.2823
	6	0.9647	1.6955	0.9402
	7	3.0975	1.2866	8.7706
	8	6.7549	5.7721	14.3094
	9	0.0944	1.4527	0.6399
	10	4.0151	3.1872	3.0055
	11	2.5392	0.1493	
	12	0.9149	0.7066	1.8752
	13	4.7225	1.3035	0.6608
500 Hz - 80 dB nHL	1	69.2843	42.5336	41.9841
	2	75.9597	55.3302	45.5377
	3	10.8834	6.7513	16.1210
	4	1.0443	6.7110	1.8426
	5	27.3429	4.1652	10.0644
	6	27.7814	61.6792	36.9868
	7	29.0974	52.7434	20.8685
	8	42.9010	21.3243	42.2892
	9	8.3966	8.9157	11.4157
	10	41.6876	19.5735	11.5345
	11	1.4077	1.6940	
	12	37.5349	23.0679	19.0913
	13	31.6188	26.3984	22.8384
500 Hz - 70 dB nHL	1	45.0088	33.3556	38.8135
	2	55.1257	43.7639	75.0397
	3	4.4410	10.4611	11.6714
	4	3.8720	2.9959	3.1522
	5	25.0252	26.5946	20.6924
	6	13.9068	21.3544	26.9785
	7	35.5153	33.6859	54.6058

	8	37.4327	18.1404	45.2052
	9	8.0069	7.0369	11.6220
	10	13.0708	8.2282	10.2025
	11	4.2993	2.7006	2.3949
	12	21.8240	34.6262	28.7228
	13	1.8783	3.3609	9.4847
500 Hz - 60 dB nHL	1	24.2996	21.1436	32.8349
	2	40.5670	50.9228	47.6442
	3	3.0234	3.7532	2.1007
	4	1.3238	0.9797	4.7276
	5	13.6220	3.6296	11.3983
	6	14.2695	11.8426	21.6193
	7	24.7272	21.7450	16.2227
	8	16.0636	18.4286	25.4313
	9	2.9058	2.2442	8.3795
	10	5.9836	5.9966	8.9808
	11	1.8819	11.2697	2.7858
	12	20.3262	21.6412	11.5826
	13	8.7421	4.5622	2.9399
500 Hz - 50 dB nHL	1	12.3275	3.4984	21.0119
	2	6.4112	3.0246	4.8144
	3	4.4289	2.0272	1.7641
	4	0.9910	2.1590	2.2879
	5	6.0402	7.1256	10.2530
	6	2.5955	6.1037	9.4222
	7	14.5604	14.8975	21.4452
	8	4.6133	7.0999	4.5848
	9	4.9537	9.2662	7.8133
	10	13.9956	5.8250	16.8236
	11	9.6181	13.8844	1.3263
	12	22.7984	12.7581	26.2940
	13	5.8977	1.5043	2.1460
500 Hz - 40 dB nHL	1	5.1942	6.7691	1.6884
	2	15.5272	6.1007	21.3707
	3	8.8287	26.4598	1.0737
	4	0.3660	5.1633	1.4333
	5	8.5453	8.5877	5.8007
	6	28.5629	5.5705	11.1348
	7	1.9480	3.7287	9.6608

	8	11.9708	11.6494	19.9133
	9	4.8147	5.1805	1.4194
	10	7.6689	1.7845	4.8147
	11	1.6027	4.2430	1.6047
	12	7.7297	8.6116	5.5767
	13	3.3891	2.7966	0.8570
500 Hz - 30 dB nHL	1	4.6187	0.6786	0.8656
	2	3.3463	6.6270	3.4475
	3	0.1403	4.5220	2.8288
	4	2.3722	1.1189	0.9395
	5	1.0520	1.0757	0.8306
	6	2.5614	2.3551	4.4217
	7	4.5735	2.5746	1.5669
	8	3.9422	3.1987	6.1226
	9	5.8539	5.0196	4.3147
	10	2.5124	26.8054	10.6392
	11	1.0239	2.2167	1.5109
	12	13.0631	0.5235	2.4098
	13	2.0216	0.4983	2.5515
500 Hz - 20 dB nHL	1	7.1201	0.5267	1.0790
	2	3.5258	2.0897	4.0269
	3	2.8045	0.7205	1.1495
	4	1.5580	2.8355	4.9221
	5	3.5069	1.8074	2.4015
	6	1.0740	1.5828	10.2018
	7	0.8024	2.9176	1.3051
	8	4.4765	3.1883	1.4345
	9	0.9909	5.8631	2.8646
	10	1.6226	1.2561	0.2345
	11	2.0980	3.8235	3.5882
	12	2.0233	1.1202	1.9335
	13	2.0023	3.5462	0.6555

APPENDIX E

This appendix shows the SPSS macro syntax of the Koenker test used to test the statistical significance of the heteroscedasticity of data, which was developed by Martha Garcia-Granero and was published in Pryce et al. (2002) paper. Moreover, it shows Koenker test results for all three measures of the ANOW response and both TB stimuli.

MACRO:

```
* Encoding: windows-1252.
* BREUSCH-PAGAN & KOENKER TEST MACRO *
* See 'Heteroscedasticity: Testing and correcting in SPSS'
* by Gwilym Pryce, for technical details.
* Code by Marta Garcia-Granero 2002/10/28.

* The MACRO needs 3 arguments:
* the dependent, the number of predictors and the list of predictors
* (if they are consecutive, the keyword TO can be used) .

* (1) MACRO definition (select an run just ONCE).

DEFINE bpktest(!POSITIONAL !TOKENS(1) /!POSITIONAL !TOKENS(1) /!POSITIONAL !CMDEND).
* Regression to get the residuals and residual plots.
REGRESSION
/STATISTICS R ANOVA
/DEPENDENT !1
/METHOD=ENTER !3
/SCATTERPLOT=(*ZRESID,*ZPRED)
/RESIDUALS HIST(ZRESID) NORM(ZRESID)
/SAVE RESID(residual) .
do if $casenum=1.
print /"Examine the scatter plot of the residuals to detect"
/"model misspecification and/or heteroscedasticity"
/""
/"Also, check the histogram and np plot of residuals "
/"to detect non normality of residuals "
/"Skewness and kurtosis more than twice their SE indicate non-normality ".
end if.
* Checking normality of residuals.
DESCRIPTIVES
VARIABLES=residual
/STATISTICS=KURTOSIS SKEWNESS .
* New dependent variable (g) creation.
COMPUTE sq_res=residual**2.
compute constant=1.
AGGREGATE
/OUTFILE='C:\Users\user\Desktop\Bland-Altman\tempdata.sav'
/BREAK=constant
/rss = SUM(sq_res)
/N=N.
MATCH FILES /FILE=*
/FILE='C:\Users\user\Desktop\Bland-Altman\tempdata.sav'.
EXECUTE.
if missing(rss) rss=lag(rss,1).
if missing(n) n=lag(n,1).
compute g=sq_res/(rss/n).
```

```
execute.
* BP&K tests.
* Regression of g on the predictors.
REGRESSION
/STATISTICS R ANOVA
/DEPENDENT g
/METHOD=ENTER !3
/SAVE RESID(resid) .
*Final report.
do if $casenum=1.
print /" BP&K TESTS"
/" ==========".
end if.
* Routine adapted from Gwilym Pryce.
matrix.
compute p=!2.
get g /variables=g.
get resid /variables=resid.
compute sq_res2=resid&**2.
compute n=nrow(g).
compute rss=msum(sq_res2).
compute ii_1=make(n,n,1).
compute i=ident(n).
compute m0=i-((1/n)*ii_1).
compute tss=transpos(g)*m0*g.
compute regss=tss-rss.
print regss
/format="f8.4"
/title="Regression SS".
print rss
/format="f8.4"
/title="Residual SS".
print tss
/format="f8.4"
/title="Total SS".
compute r_sq=1-(rss/tss).
print r_sq
/format="f8.4"
/title="R-squared".
print n
/format="f4.0"
/title="Sample size (N)".
print p
/format="f4.0"
/title="Number of predictors (P)".
compute bp_test=0.5*regss.
print bp_test
/format="f8.3"
/title="Breusch-Pagan test for Heteroscedasticity"
+ " (CHI-SQUARE df=P)".
compute sig=1-chicdf(bp_test,p).
print sig
/format="f8.4"
/title="Significance level of Chi-square df=P (H0:"
+ "homoscedasticity)".
compute k_test=n*r_sq.
print k_test
/format="f8.3"
```

```
/title="Koenker test for Heteroscedasticity"
+ " (CHI-SQUARE df=P)".
compute sig=1-chicdf(k_test,p).
print sig
/format="f8.4"
/title="Significance level of Chi-square df=P (H0:"
+ "homoscedasticity)".
end matrix.
!ENDDEFINE.


* x1 is the dependent, x2 TO xn the predictors, n is the number of predictors.

* (3) MACRO CALL (select and run).

BPKTEST x1 n x2 TO xn
```

Test results:

Test Measure	Koenker test for Heteroscedasticity (CHI-SQUARE df=1)	Significance level of Chi-square df=1 (H0:homoscedasticity)
Amplitude	6.951	0.0084
Logarithm of amplitude	0.958	0.3277
SNR	25.538	0.0000
Logarithm of SNR	0.019	0.8891
PLV	13.489	0.0002
Lograrihtm of PLV	2.268	0.1320

Reference:

Pryce, G., & Garcia-Granero, M. (2002). Breusch-Pagan & Koenker Test Macro.

APPENDIX F

This appendix shows ANOW's absolute amplitudes and SNRs of participants 2 and 6 across all stimulus intensity levels.

		Session 2					
		Run 1		Run 2		Run 3	
	ID#	Amplitude1 (μV^2)	SNR1	Amplitude2 (μV^2)	SNR2	Amplitude3 (μV^2)	SNR3
250 Hz - 80 dB nHL	2	0.4747	5.9797	1.0249	13.5104	1.0722	25.2758
	6	4.3524	18.8303	3.8049	26.2521	3.0245	28.1726
250 Hz - 70 dB nHL	2	1.2026	28.5343	0.9685	35.4255	0.9095	22.0452
	6	3.0917	35.8421	2.1640	18.1853	3.1224	37.4098
250 Hz - 60 dB nHL	2	1.5928	26.9308	1.4292	15.4934	1.1824	25.3507
	6	1.7941	15.5183	1.7389	16.8958	2.6008	28.2459
250 Hz - 50 dB nHL	2	0.5146	5.6746	0.8389	24.6429	1.5102	51.9988
	6	1.4344	18.6417	1.0672	23.1254	1.7671	53.1167
250 Hz - 40 dB nHL	2	0.1356	5.3094	0.1489	13.9092	0.1389	4.1832

	6	0.1804	6.1648	0.2088	8.8710	0.3134	6.2247
250 Hz - 30 dB nHL	2	0.0138	5.7579	0.1335	1.9021	0.0529	2.7801
	6	0.1977	10.0800	0.0939	2.0767	0.2617	6.9676
250 Hz - 20 dB nHL	2	0.0525	2.8014	0.0201	1.7849	0.0179	1.5385
	6	0.0242	0.8889	0.3415	3.8860	0.1312	1.4988
500 Hz - 80 dB nHL	2	0.6411	43.0057	0.4352	45.1197	0.4187	30.4656
	6	0.5723	16.1399	0.5567	24.0766	0.4611	28.2319
500 Hz - 70 dB nHL	2	0.5753	76.1481	0.4581	54.6203	0.5521	35.1305
	6	0.7403	16.3102	0.6940	24.0142	0.7998	21.4988
500 Hz - 60 dB nHL	2	0.4243	64.5707	0.4033	120.6794	0.3868	32.0509
	6	0.5158	22.5908	0.6877	20.8125	0.6498	33.3342

500 Hz - 50 dB nHL	2	0.0203	4.1319	0.0187	5.2321	0.0254	5.9177
	6	0.1160	14.5576	0.1888	10.3948	0.1958	11.7833
500 Hz - 40 dB nHL	2	0.0254	8.1638	0.0220	4.5240	0.0140	4.5849
	6	0.0352	2.5540	0.0491	10.3275	0.0452	16.2950
500 Hz - 30 dB nHL	2	0.0086	2.8342	0.0054	1.8417	0.0168	7.1460
	6	0.0081	2.0872	0.0041	0.3982	0.0087	5.1249
500 Hz - 20 dB nHL	2	0.0092	4.8912	0.0122	4.0351	0.0052	5.1232
	6	0.0180	2.9986	0.0102	2.4826	0.0059	1.7258